



Lake Simcoe Region
conservation authority

The urban heat island: A review of urban climate modelling approaches with a case study in East Gwillimbury

March 2025



For more information, contact:

Watershed Plans and Strategies
Lake Simcoe Region Conservation Authority
120 Bayview Parkway, Newmarket, Ontario
Canada, L3Y 3W3
Telephone: 905-895-1281
Email: info@LSRCA.on.ca
Web: www.LSRCA.on.ca

Recommended Citation:

Lake Simcoe Region Conservation Authority. 2025. *The urban heat island: A review of climate modelling approaches with a case study in East Gwillimbury.*

Written by:

Charlotte Grieve – Climate Change Assistant, Lake Simcoe Region Conservation Authority

Edited by:

Bill Thompson – Manager, Watershed Plans and Strategies, Lake Simcoe Region Conservation Authority

Pamela Strong – Integrated Watershed Management Implementation Coordinator, Lake Simcoe Region Conservation Authority

Acknowledgements

This report could not have been completed without the advice and input of many participants, whose names are listed below.

Kaitlyn Read – Integrated Watershed Management Implementation Coordinator, Lake Simcoe Region Conservation Authority

Lauren Moretto – Climate Change Specialist, Lake Simcoe Region Conservation Authority

Laura Curran – Urban Forest Study Project Lead, Lake Simcoe Region Conservation Authority

Kathy Hillis – Senior Administrative Assistant, Lake Simcoe Region Conservation Authority

Cristina Ross – Environmental Initiatives Program Manager, Town of East Gwillimbury

Nicola Alston – GIS Technologist, Town of East Gwillimbury

We would also like to acknowledge York Region, the Toronto and Region Conservation Authority, and the authors of the Lake Simcoe Region Conservation Authority's 2018 land cover update for their land use/land cover data, which was integral to this report.



Table of Contents

Executive Summary	9
1.0 Introduction	13
1.1. Background.....	13
1.1.1 Urban Heat Mitigation Strategies.....	14
1.2. Purpose.....	15
1.3. Intended Application, Target Audience, and Scope.....	16
2.0 Urban Heat Model Selection and Rationale.....	17
2.1. Approach	17
2.2. Review of Urban Heat Models	17
2.2.1 Urban Microscale Models.....	18
2.2.2 Urban Macroscale Models.....	19
2.3. Model Selection	20
3.0 Case Study.....	23
3.1. Methods	23
3.2. Results and Discussion	28
3.2.1 Daytime Temperatures.....	28
3.2.2 Nighttime Temperatures	35
3.3. Study Limitations.....	39
4.0 Conclusion.....	41
4.1. Future Research	41
Glossary	42
A. Appendix A: Urban Climate Model Summaries.....	44
B. Appendix B: i-Tree Cool Air and InVEST Urban Cooling Literature Review	53
C. Appendix C: Detailed InVEST Methodology	55
Land Use/Land Cover Input Data.....	55
Nighttime Temperature Modelling.....	61
Climate Input Data	63
Energy Savings Valuation.....	66
Work Productivity Valuation.....	67
D. Appendix D: Land Use/Land Cover Descriptions	68
E. Appendix E: InVEST Output Maps	76
Daytime Temperatures	76
Nighttime Temperatures	78



F. Appendix F: InVEST Output Raw Data 81
 Daytime Temperatures 81
 Nighttime Temperatures 85
References 89

List of Tables

Table 2-1 – Evaluation table used to assess model capabilities for a case study in East Gwillimbury..... 20
 Table 3-1 – Description of InVEST Urban Cooling modelling scenarios with abbreviated scenario names..... 24
 Table 3-2 – Summary of InVEST daytime valuation metrics, including energy savings in dollars and percent heavy and light work productivity loss, per model scenario. Numbers displayed show energy and work productivity loss/gains in comparison to the baseline 38% canopy cover scenario. For more detailed results, see Table F-4..... 34
 Table A-1 – ENVI-met urban microclimate model summary..... 44
 Table A-2 – SOLWEIG urban microclimate model summary..... 45
 Table A-3 – RayMan urban microclimate model summary..... 47
 Table A-4 – Summary of i-Tree Cool Air model architecture, data input requirements, model outputs, and advantages and limitations. 48
 Table A-5 – Summary of InVEST Urban Cooling model architecture, data input requirements, model outputs, and advantages and limitations..... 50
 Table B-1 – Summary of i-Tree Cool Air and InVEST Urban Cooling literature. 53
 Table C-1 – Tree canopy percent cover per land use class under three canopy cover scenarios. The Green 44% canopy cover scenario is not included as its values are identical to the 44% scenario. Bolded values represent actual canopy cover conditions in East Gwillimbury as of 2018. 56
 Table C-2 – Green area classification per land use class under four canopy cover scenarios. Land use classes are given a “0” if they are not considered a green area and a “1” if they are. Bolded column represents actual 2018 conditions in East Gwillimbury. 57
 Table C-3 – Albedo values per land use class under three canopy cover scenarios. The Green 44% canopy cover scenario is not included as its values are identical to the 44% scenario. Bolded column represents actual 2018 conditions in East Gwillimbury..... 58
 Table C-4 – Crop coefficient (K_c) values per land use class under three canopy cover scenarios. The Green 44% canopy cover scenario is not included as its values are identical to the 44% scenario. Bolded column represents actual 2018 conditions in East Gwillimbury. 61



Table C-5 – Percent building cover per land use class under two East Gwillimbury development scenarios: 2018 and full buildout (projected development density given all current and future development plans). All percentages less than or equal to 0.1% are rounded down to 0%. 62

Table C-6– Building intensity per land use class under two East Gwillimbury development scenarios: 2018 and full buildout (projected development density given all current and future development plans). All values are normalized between 0 and 1. 63

Table C-7 – Maximum July air temperature (°C) values for three rural reference points around East Gwillimbury over five climate periods: current (2011-2020), SSP2-4.5 mid-century (2041-2070) and end-century (2071-2100), and SSP5-8.5 mid-century and end-century. Average air temperature for each climate period (**bold**) is the rural reference air temperature input into InVEST. Coordinates (decimal degrees) and elevation (metres) for the three rural reference points is also provided. 64

Table C-8 – Minimum July air temperature (°C) values for three rural reference points around East Gwillimbury over five climate periods: current (2011-2020), SSP2-4.5 mid-century (2041-2070) and end-century (2071-2100), and SSP5-8.5 mid-century and end-century. Average air temperature for each climate period (**bold**) is the rural reference air temperature input into InVEST. Coordinates (decimal degrees) and elevation (metres) for the three rural reference points is also provided. 65

Table C-9 – Average footprint area (m²), number of floors, and resultant total floor area (m²) for each building type in East Gwillimbury under a full buildout scenario. 66

Table C-10 – Average July percent relative humidity of 248 equally spaced reference points within the East Gwillimbury municipality, for five climate periods: current (2011-2020), SSP2-4.5 mid-century (2041-2070) and end-century (2071-2100), and SSP5-8.5 mid-century and end-century. 67

Table D-1 – Description of natural heritage land cover classes and their corresponding Ecological Land Classification (ELC) codes as found in the Lake Simcoe Region Conservation Authority 2018 land use layer. Bolded entries are the overarching Ecological Land Classification Community Classes, within which distinct communities (unbolded) belong..... 68

Table D-2 – Description of non-natural land cover classes in the Lake Simcoe Region Conservation Authority 2018 land use layer. 70

Table D-3 – Reclassification of the Lake Simcoe Region Conservation Authority’s natural heritage and non-natural land cover classes into 14 condensed land use classes for input into InVEST Urban Cooling. 71

Table D-4 – Reclassification of the Lake Simcoe Region Conservation Authority’s natural heritage land cover classes (Table D-1) into land use classes for input into InVEST Urban Cooling. 72



Table D-5 – Reclassification of the Lake Simcoe Region Conservation Authority’s non-natural land cover classes (Table D-2) into land use classes for input into InVEST Urban Cooling. 74

Table D-6 – Reclassification of East Gwillimbury (EG) development types, with their Lake Simcoe Region Conservation Authority (LSRCA) non-natural land cover class equivalents (Table D-2), into land use classes for input into InVEST Urban Cooling. 74

Table F-1 – Estimated maximum daytime July air temperatures (°C) (without air mixing) across two urban areas (Urban Core and Mount Albert) in East Gwillimbury under four canopy cover scenarios (22%, 38%, 44%, and green 44%) and five climate scenarios: current climate, SSP2-4.5 mid-century (2041-2070), SSP2-4.5 end-century (2071-2100), SSP5-8.5 mid-century, and SSP5-8.5 end-century. Displayed are mean, median, minimum, and maximum air temperatures (T), as well as standard deviation (StDev). 81

Table F-2 – Estimated maximum daytime July air temperatures (°C) (with air mixing) across two urban areas (Urban Core and Mount Albert) in East Gwillimbury under four canopy cover scenarios (22%, 38%, 44%, and green 44%) and five climate scenarios: current climate, SSP2-4.5 mid-century (2041-2070), SSP2-4.5 end-century (2071-2100), SSP5-8.5 mid-century, and SSP5-8.5 end-century. Displayed are mean, median, minimum, and maximum air temperatures (T), as well as standard deviation (StDev). 82

Table F-3 – Estimated daytime wet bulb global temperature (°C) values across two urban areas (Urban Core and Mount Albert) in East Gwillimbury under four canopy cover scenarios (22%, 38%, 44%, and green 44%) and five climate scenarios: current climate, SSP2-4.5 mid-century (2041-2070), SSP2-4.5 end-century (2071-2100), SSP5-8.5 mid-century, and SSP5-8.5 end-century. Displayed are mean, median, minimum, and maximum air temperatures (T), as well as standard deviation (StDev). 83

Table F-4 – Daytime valuation metrics for July across all of East Gwillimbury under four canopy cover scenarios (22%, 38%, 44%, and green 44%) and five climate scenarios: current climate, SSP2-4.5 mid-century (2041-2070), SSP2-4.5 end-century (2071-2100), SSP5-8.5 mid-century, and SSP5-8.5 end-century. Displayed are average air temperatures, energy savings (kWh and dollars), wet bulb global temperature (WBGT), light productivity loss, and heavy productivity loss. Energy savings represent savings compared to a theoretical scenario with no green space. 84

Table F-5 – Estimated mean July nighttime air temperatures (°C) and wet bulb global temperature (°C) values, spatially averaged across all of East Gwillimbury, under three canopy cover scenarios (22%, 38%, and 44%) and five climate scenarios: current climate, SSP2-4.5 mid-century (2041-2070), SSP2-4.5 end-century (2071-2100), SSP5-8.5 mid-century, and SSP5-8.5 end-century..... 85

Table F-6 – Estimated mean July nighttime air temperatures (°C) (without air mixing) across two urban areas (Urban Core and Mount Albert) in East Gwillimbury under three canopy cover



scenarios (22%, 38%, and 44%) and five climate scenarios: current climate, SSP2-4.5 mid-century (2041-2070), SSP2-4.5 end-century (2071-2100), SSP5-8.5 mid-century, and SSP5-8.5 end-century. Displayed are mean, median, minimum, and maximum air temperatures (T), as well as standard deviation (StDev). 86

Table F-7 – Estimated mean July nighttime air temperatures (°C) (with air mixing) across two urban areas (Urban Core and Mount Albert) in East Gwillimbury under three canopy cover scenarios (22%, 38%, and 44%) and five climate scenarios: current climate, SSP2-4.5 mid-century (2041-2070), SSP2-4.5 end-century (2071-2100), SSP5-8.5 mid-century, and SSP5-8.5 end-century. Displayed are mean, median, minimum, and maximum air temperatures (T), as well as standard deviation (StDev). 87

Table F-8 – Estimated mean nighttime wet bulb global temperature (°C) values across two urban areas (Urban Core and Mount Albert) in East Gwillimbury under three canopy cover scenarios (22%, 38%, and 44%) and five climate scenarios: current climate, SSP2-4.5 mid-century (2041-2070), SSP2-4.5 end-century (2071-2100), SSP5-8.5 mid-century, and SSP5-8.5 end-century. Displayed are mean, median, minimum, and maximum air temperatures (T), as well as standard deviation (StDev). 88

List of Figures

Figure 2-1 – Decision support tool for model selection based on fulfilment of ranked criteria, filled out with respect to the East Gwillimbury case study presented in this report..... 22

Figure 3-1 – Maps of East Gwillimbury showing estimated maximum daytime July air temperature (°C) distribution for (A) 2018 under current climate (2011-2020) conditions, and (B) a full buildout scenario under current climate (2011-2020) conditions..... 28

Figure 3-2 – Maps of East Gwillimbury showing estimated maximum daytime July air temperature (°C) distribution under a full buildout scenario and current climate (2011-2020) conditions, and four canopy cover scenarios: (A) 22%, (B) 38%, (C) 44%, and (D) green 44%. 29

Figure 3-3 – Maps of East Gwillimbury showing estimated maximum daytime July air temperature (°C) distribution by mid-century (2041-2070) under the SSP2-4.5 emissions pathway for four canopy cover scenarios: (A) 22%, (B) 38%, (C) 44%, and (D) green 44%. 30

Figure 3-4 – Maps of East Gwillimbury showing estimated maximum daytime July air temperature (°C) distribution by end-century (2071-2100) under the SSP2-4.5 emissions pathway for four canopy cover scenarios: (A) 22%, (B) 38%, (C) 44%, and (D) green 44%. 30

Figure 3-5 – Maps of East Gwillimbury showing estimated maximum daytime July air temperature (°C) distribution by mid-century (2041-2070) under the SSP5-8.5 emissions pathway for four canopy cover scenarios: (A) 22%, (B) 38%, (C) 44%, and (D) green 44%. 31



Figure 3-6 – Maps of East Gwillimbury showing estimated maximum daytime July air temperature (°C) distribution by end-century (2071-2100) under the SSP5-8.5 emissions pathway for four canopy cover scenarios: (A) 22%, (B) 38%, (C) 44%, and (D) green 44%. 31

Figure 3-7 – Maps of East Gwillimbury showing estimated average nighttime July air temperature (°C) distribution under a full buildout scenario and current climate (2011-2020) conditions, and three canopy cover scenarios: (A) 22%, (B) 38%, and (C) 44%. 37

Figure 3-8 – Maps of East Gwillimbury showing estimated average nighttime July air temperature (°C) distribution by mid-century (2041-2070) under the SSP2-4.5 emissions pathway for three canopy cover scenarios: (A) 22%, (B) 38%, and (C) 44%. 37

Figure 3-9 – Maps of East Gwillimbury showing estimated average nighttime July air temperature (°C) distribution by end-century (2071-2100) under the SSP2-4.5 emissions pathway for three canopy cover scenarios: (A) 22%, (B) 38%, and (C) 44%. 38

Figure 3-10 – Maps of East Gwillimbury showing estimated average nighttime July air temperature (°C) distribution by mid-century (2041-2070) under the SSP5-8.5 emissions pathway for three canopy cover scenarios: (A) 22%, (B) 38%, and (C) 44%. 38

Figure 3-11 – Maps of East Gwillimbury showing estimated average nighttime July air temperature (°C) distribution by end-century (2071-2100) under the SSP5-8.5 emissions pathway for three canopy cover scenarios: (A) 22%, (B) 38%, and (C) 44%. 39

Figure E-1 – Maps of East Gwillimbury showing estimated maximum daytime wet bulb global temperature (°C) distribution under a full buildout scenario and current climate (2011-2020) conditions, for four canopy cover scenarios: (A) 22%, (B) 38%, (C) 44%, and (D) green 44%. 76

Figure E-2 – Maps of East Gwillimbury showing estimated maximum daytime wet bulb global temperature (°C) distribution by mid-century (2041-2070) under the SSP2-4.5 emissions pathway for four canopy cover scenarios: (A) 22%, (B) 38%, (C) 44%, and (D) green 44%. 76

Figure E-3 – Maps of East Gwillimbury showing estimated maximum daytime wet bulb global temperature (°C) distribution by end-century (2071-2100) under the SSP2-4.5 emissions pathway for four canopy cover scenarios: (A) 22%, (B) 38%, (C) 44%, and (D) green 44%. 77

Figure E-4 – Maps of East Gwillimbury showing estimated maximum daytime wet bulb global temperature (°C) distribution by mid-century (2041-2070) under the SSP5-8.5 emissions pathway for four canopy cover scenarios: (A) 22%, (B) 38%, (C) 44%, and (D) green 44%. 77

Figure E-5 – Maps of East Gwillimbury showing estimated maximum daytime wet bulb global temperature (°C) distribution by end-century (2071-2100) under the SSP5-8.5 emissions pathway for four canopy cover scenarios: (A) 22%, (B) 38%, (C) 44%, and (D) green 44%. 78

Figure E-6 – Maps of East Gwillimbury showing estimated mean nighttime wet bulb global temperature (°C) distribution under a full buildout scenario and current climate (2011-2020) conditions, for three canopy cover scenarios: (A) 22%, (B) 38%, and (C) 44%. 78



Figure E-7 – Maps of East Gwillimbury showing estimated mean nighttime wet bulb global temperature (°C) distribution by mid-century (2041-2070) under the SSP2-4.5 emissions pathway for three canopy cover scenarios: (A) 22%, (B) 38%, and (C) 44%. 79

Figure E-8 – Maps of East Gwillimbury showing estimated mean nighttime wet bulb global temperature (°C) distribution by end-century (2071-2100) under the SSP2-4.5 emissions pathway for three canopy cover scenarios: (A) 22%, (B) 38%, and (C) 44%. 79

Figure E-9 – Maps of East Gwillimbury showing estimated mean nighttime wet bulb global temperature (°C) distribution by mid-century (2041-2070) under the SSP5-8.5 emissions pathway for three canopy cover scenarios: (A) 22%, (B) 38%, and (C) 44%. 80

Figure E-10 – Maps of East Gwillimbury showing estimated mean nighttime wet bulb global temperature (°C) distribution by end-century (2071-2100) under the SSP5-8.5 emissions pathway for three canopy cover scenarios: (A) 22%, (B) 38%, and (C) 44%. 80

Appendices

- Appendix A – Urban Climate Model Summaries
- Appendix B – i-Tree Cool Air and InVEST Urban Cooling Literature Review
- Appendix C – Detailed InVEST Methodology
- Appendix D – Land Use/Land Cover Descriptions
- Appendix E – InVEST Output Maps
- Appendix F – InVEST Output Raw Data

Executive Summary

Overview and Purpose

The urban heat island effect is the phenomenon whereby urban areas tend to be warmer than surrounding rural or peri-urban areas. Increased temperatures in urban areas are a result of high surface area of heat-trapping materials (e.g., asphalt), low surface area of permeable materials and vegetation, reduced flow of hot air out of urban areas due to building geometry, and heat inputs from anthropogenic sources such as air-conditioning units. Exposure of urban residents to increased heat has a wide range of health impacts, especially for vulnerable populations. The urban heat island effect is especially dangerous during heat waves, where it is associated with increased rates of heat-induced morbidity and mortality. The urban heat island is of growing concern worldwide due to global warming, which is expected to intensify heat in urban areas, and urbanization, which will put more people at risk of urban heat island health effects.

Considering the increased danger urban heat may pose to a growing number of urban residents worldwide, extensive research has been carried out regarding strategies to reduce heat in cities and/or increase the adaptive capacity of urban areas to the urban heat island. These mitigation strategies can be grouped into two categories: altered building practices (e.g., building with lighter-coloured materials to reflect, rather than absorb, solar radiation) and urban greening (e.g., increasing parks, planting more urban trees). Each of these strategies have been shown to reduce temperatures in cities, with a combination of multiple strategies producing the most cooling. Tree planting is a popular approach for urban cooling as it is relatively easy to carry out (compared to paving roads with lighter-coloured concrete, for example) and urban trees produce several benefits beyond cooling, including carbon sequestration, air purification, stormwater management, energy savings, and mental health benefits to urban residents.

Despite the extensive body of literature surrounding the urban heat island, the intensity of the urban heat island, as well as the efficacy of various mitigation strategies, is highly variable and depends on the specific context of each urban area. Moreover, what is currently understood about the urban heat island effect may change in the future with climate change. Place-based urban heat island research is critical to better understand and prepare for projected increases in urban heat and its associated health risks to urban residents, as well as to explore the heat mitigating effects of strategies such as urban greening. Urban climate models are promising tools to explore the urban heat island effect, as they are quick, accurate, and can be used to project urban temperatures into the future under various development, climate, and urban greening scenarios. Urban climate models are also able to simulate air temperature, which is a more accurate measure of the urban heat island effect.

This report is divided into two parts. The first is a comprehensive overview of existing urban climate models, which aims to highlight the advantages and limitations of each model, and to compare them to one another. This section gives readers a high-level understanding of current



research surrounding the urban heat island and urban climate models, which can be applied to their work in municipal planning, policy, and/or climate research. Bridging the two sections is a Decision Support Tool, which we developed, that can be used to assist with model selection for urban heat island projects. The second part of the report is a case study, where we select a model using our Decision Support Tool and apply that model to simulate air temperatures in East Gwillimbury, a municipality in the Lake Simcoe watershed. East Gwillimbury is the fastest-growing municipality in Canada, so offers a unique opportunity to explore the urban heat island effect under rapid urbanization. We use InVEST Urban Cooling, our selected model, to simulate air temperatures within East Gwillimbury under several climate and urban greening scenarios. This case study is an example of a place-based study that explores the urban heat island effect now and into the future as East Gwillimbury grows, and as temperatures increase as a result of climate change. Moreover, we directly explore the effects of urban greening (specifically, increased urban forest cover) on the urban heat island effect within East Gwillimbury.

This report, by reviewing urban heat island research and modelling approaches, and by applying a model to explore the urban heat island effect and the effectiveness of urban greening strategies now and into the future under climate change, offers important information for municipalities that can be used to directly inform municipal policies and planning decisions. Moreover, the methodology described in this report contributes novel information to a greater body of literature on the urban heat island effect.

Model Review and Selection

The urban climate models reviewed in this report can be classified as either microclimate models or macroclimate models. The three microclimate models we reviewed—ENVI-met, SOLWEIG, and RayMan—are complex, computationally expensive, and are best applied at the neighbourhood scale to reduce model run times. The two macroclimate models reviewed—i-Tree Cool Air and InVEST Urban Cooling—are simpler, less computationally expensive, and are designed to be applied at the city-wide scale.

Of the microclimate models, ENVI-met is the most comprehensive and holistic. It is highly validated and widely used across various disciplines. ENVI-met also produces the greatest number of model outputs, including information on surface, soil, and air temperatures, pollutants, water budget, and more. SOLWEIG and RayMan are slightly simpler models that focus more on human thermal comfort values. RayMan calculates a wide range of thermal comfort values that provide insight into how the urban climate affects residents. However, RayMan is unable to produce metrics across an entire area, instead calculating output data for single points in space. SOLWEIG is able to simulate the urban climate across an entire area; however, it produces fewer thermal comfort values than RayMan. SOLWEIG also resolves some of the inaccuracies of RayMan (e.g., is more accurate at higher latitudes than RayMan). Overall, ENVI-met offers a strong starting point for urban microclimate studies. Depending on project needs, data from SOLWEIG and/or RayMan can provide additional information regarding human thermal comfort.



The two macroclimate models are similar in terms of required inputs and calculated outputs. Both models rely on land use/land cover data (as opposed to the detailed urban geometry requirements of the microclimate models), which simplifies the urban landscape and allows for quicker simulations. Both models are relatively new, and thus there is a limited body of literature surrounding them. Existing research suggests that i-Tree Cool Air is more accurate in its temperature calculations than InVEST Urban Cooling; however, InVEST accuracy is still high enough to warrant its use in urban climate studies. i-Tree Cool Air requires more detailed weather input data than InVEST and thus is unable to simulate temperatures under future climate scenarios. Both models are able to compute additional metrics outside of air temperature, including water budget and runoff data for i-Tree and energy savings and work productivity loss under InVEST.

We provide a list of evaluation criteria for each of the models we reviewed to begin the process of model selection for our case study. However, selecting a model based entirely on the number of criteria met is problematic as it does not account for criteria priority (i.e., that some criteria may be more important than others) and it risks two or more models meeting the same number of criteria. We therefore developed a Decision Support Tool to assist us in model selection, but also to streamline the selection process for any urban heat project. The tool calculates model suitability for a given project based on user-defined criteria and criteria priority/importance. The tool then calculates a score for each model based on fulfilment of ranked criteria, where the model with the highest score is the most suitable model. We used the tool to identify the most suitable model for our case study. Given the scope of our case study, we ranked a model's ability to run scenarios across a wide spatial scale as high, which reduced the score of all three microclimate models. We also ranked a model's ability to simulate temperatures under future climate conditions as high priority, which reduced the score of i-Tree Cool Air. We selected InVEST Urban Cooling for our case study, as it fulfilled all our high priority (i.e., necessary) criteria and thus received the highest score.

East Gwillimbury Case Study

We used InVEST Urban Cooling to simulate daytime and nighttime July air temperatures in a fully developed East Gwillimbury. We chose to simulate maximum daytime July temperatures to better emulate heat waves. Due to data limitations, we were unable to simulate maximum nighttime temperatures, so instead ran the model for mean nighttime temperatures. We ran simulations under current climate (2010-2020) conditions, as well as two climate emissions pathways: SSP2-4.5 and SSP5-8.5, mid-century (2041-2070) and end-century (2071-2100). For each climate series, we ran three canopy cover scenarios: 22% (reduced canopy), 38% (maintenance of current East Gwillimbury canopy cover), and 44% (increased canopy) for nighttime temperatures, with an additional 44% scenario, which we named "Green 44%" for daytime temperatures. The Green 44% scenario is based on the theory that, once canopy cover reaches 40% in urban areas, the urban forest cools daytime temperatures in a way that is similar to a natural forest. Under the Green 44% scenario, the model treats developed areas with 40% canopy cover as a natural system.



Compared to East Gwillimbury as it is now, the urban heat island did not increase much in intensity after a full buildout (i.e., a projected future East Gwillimbury accounting for urbanization/development trends). However, the spatial extent of the urban heat island effect did increase substantially. Under a full buildout, current climate conditions, and 38% canopy cover, maximum July daytime temperatures across all of East Gwillimbury averaged 27.6°C. By mid-century (2041-2070), temperatures had increased by 1.8°C under SSP2-4.5 and 2.4°C under SSP5-8.5. By end-century, temperatures had increased by 2.5°C under SSP2-4.5 and 4.8°C under SSP5-8.5, compared to current climate conditions. Within urban areas, temperatures were 1-3°C warmer. Our results align with current end-century climate projections for the Lake Simcoe watershed, which predict an increase in summer temperatures by 2.8°C under RCP 4.5 and 5.0°C under RCP 8.5.

At 38% canopy cover, daytime wet bulb global temperatures across all of East Gwillimbury were 1.4-2.1°C higher than air temperatures, with the greatest difference between wet bulb temperatures and air temperatures (2.1°C) occurring by end-century under SSP5-8.5. Urban areas were 0.5-1°C warmer. Under all climate emissions scenarios and time steps, wet bulb temperatures were above 30°C, which is the point at which human thermal comfort declines rapidly. At 38% canopy, work productivity losses due to high wet bulb global temperatures were lowest under current climate conditions, with 0% light work loss and 30.7% heavy work loss. By SSP5-8.5, both light and heavy work were reduced by 75% despite any increases in canopy cover. Importantly, work productivity was lost across the entire municipality, not just within urban areas. These dramatic losses under the worst of climate change highlights the need to implement climate adaptation strategies now to prevent largescale impacts to human health and municipal functioning.

Across all climate scenarios, East Gwillimbury's current canopy cover (38%) provided 0.16-0.22°C urban cooling compared to a reduced 22% canopy. An increase from 38% to 44% produced 0.07-0.1°C cooling. The Green 44% scenario had the greatest cooling (0.7-1.1°C) compared to the 38% baseline. The cooling we observed under the 38% and 44% canopy cover scenarios was on the lower end of the range reported in the literature (0.2-5.0°C), while the Green 44% canopy cover scenario aligned well with reported median cooling values (1°C).

InVEST predicted tens of thousands of dollars of July energy savings across the municipality due to the cooling effect of the urban canopy. Increases in forest cover also reduced heat-related work productivity loss. These results clearly demonstrate the toll that the urban heat island effect can take on municipal energy demands and worker health and safety. Even relatively little cooling can have a large effect on the municipality, particularly on work productivity. It is vital that municipalities implement urban heat mitigation measures to avoid the worst impacts of urban heat on the health and well-being of their residents, as well as the municipality as a whole.

Under current climate conditions and canopy cover (38%), mean July nighttime air temperatures were 15.5°C across all of East Gwillimbury. By mid-century, nighttime temperatures had increased by 1°C under SSP2-4.5 and 1.5°C under SSP5-8.5. By end-century,



temperatures were 1.8°C higher under SSP2-4.5 and 3.7°C higher under SSP5-8.5. Notably, mean nighttime wet bulb global temperatures surpassed 20°C by end-century under SSP5-8.5. “Tropical nights,” or nights where temperatures do not drop below 20°C, are associated with increased rates of heat-related mortality. Moreover, our nighttime results reflect mean July nighttime temperatures, not maximum temperatures. It is therefore likely that, given expected increases in heat waves, the frequency of tropical nights will be higher than our results predict, and they may even occur earlier in the century under more optimistic climate pathways.

The urban heat island intensity was reduced during our nighttime temperature simulations, with mean air temperatures only 0.09-0.24°C warmer in urban areas. Building intensity is weighted heavily during InVEST’s nighttime temperature calculations, which would explain why the discrepancy between urban and rural temperatures is lower at night, given East Gwillimbury’s relatively low density. Across all climate scenarios, temperatures under current East Gwillimbury canopy cover (38%) were 0.09-0.14°C cooler than if the canopy were reduced to 22%. An increase to 44% canopy produced an additional 0.05-0.08°C cooling. These results suggest that the cooling effect of the urban canopy is reduced at night. However, it is possible that InVEST undervalues both the intensity of the urban heat island effect and the cooling effect of urban trees at night. While our results provide some insight into nighttime climate conditions within East Gwillimbury under various greening scenarios, further research is required to be able to make any conclusive recommendations.

1.0 Introduction

1.1. Background

Urbanization is on the rise globally, with over 65% of the world’s population projected to live in urban areas by 2050 (UN DESA, 2018). While there are many benefits to urban life, urban residents are also exposed to a variety of health risks due to noise, overcrowding, and air, water, and soil pollution (UN DESA, 2018; Heaviside et al., 2017). The urban heat island effect is the difference in temperature between the built and natural environment, whereby temperatures are generally higher in urban areas compared to surrounding rural or peri-urban areas (Heaviside et al., 2017; Phelan et al., 2015). On average, temperatures are around 2-4°C warmer in cities compared to surrounding areas, though in extreme cases urban centres may be up to 5-10°C warmer (Heaviside et al., 2017).

The main factors that contribute to increased temperatures in urban areas are:

- High surface area of low-albedo materials (e.g., asphalt, tar roofs), which retain heat;
- Reduced vegetation and permeable material surface area, limiting shade and evapotranspiration;



- Urban geometry, which can affect air flow and trap heat in urban areas (e.g., urban canyons, which are caused by tall buildings and narrow streets, can disrupt air flow and block the cooling effects of wind);
- Heat inputs from anthropogenic sources (e.g., car exhaust, air conditioner units). (Health Canada, 2020; Wang et al., 2016b; Phelan et al., 2015)

The urban heat island has a range of impacts, including increased energy demands in urban areas due to mechanical cooling system use, and environmental impacts such as reduced water and air quality (Phelan et al., 2015). The urban heat island may also negatively affect human health and well-being by increasing heat-related mortality and morbidity in urban areas, especially during heat waves. During the 2003 European heat wave, for example, around 50% of all heat-related deaths in the West Midlands, UK, could be attributed to the urban heat island (Heaviside et al., 2016). The elderly, children, and those with pre-existing health conditions are especially vulnerable to urban heat stress. Moreover, urban heat disproportionately affects marginalized populations and lower-income communities due to increased exposure (e.g., higher-income neighbourhoods tend to be “greener,” and therefore cooler, compared to lower-income neighbourhoods) and/or reduced capacity to cope with urban heat island health impacts (e.g., limited access to healthcare) (Anderson et al., 2022; Health Canada, 2020; Chakraborty et al., 2019).

1.1.1 Urban Heat Mitigation Strategies

Broadly speaking, urban heat island mitigation strategies can be grouped into two categories: (1) altered building practices, and (2) urban greening (Wong et al., 2021; Akbari & Kolokotsa, 2016; Phelan et al., 2015).

Altered building practices mainly involve increasing urban surface reflectivity with high-albedo materials (e.g., light-coloured concrete), though other strategies include increasing the percent cover of permeable surfaces in urban areas, as well as re-designing urban geometry to reduce heat capture (Hayes et al., 2022; Wong et al., 2021; Phelan et al., 2015). High-albedo materials reflect more solar radiation, reducing daytime air and surface temperatures (Hayes et al., 2022). In Toronto, for example, switching from low-albedo asphalt to higher-albedo concrete may reduce midday ground surface temperatures by up to 7.9°C (Wang et al., 2016b). While reflective (“cool”) materials may require additional maintenance, i.e., regular cleaning to ensure reflectivity (Hayes et al., 2022), they have the added benefit of cooling buildings, reducing overall municipal energy costs (Akbari & Kolokotsa, 2016).

Urban greening (also referred to as “green infrastructure”) strategies include urban vegetation and forestry, and green roof and wall installation (Wong et al., 2021). Green infrastructure cools urban areas through evapotranspiration, shade provision, and/or increased albedo (Anderson et al., 2022; Wong et al., 2021). Air temperature reductions vary depending on the strategy used, ranging from 2-4°C for large greenspaces (e.g., parks), 1.5-4.1°C for green roofs, and 2-4°C for green walls (Wong et al., 2021). Large greenspaces (i.e., parks) have the capacity to cool not just the spaces within the park, but also surrounding areas (Wong et al., 2021; Akbari &



Kolokotsa, 2016). Broadly speaking, urban trees may reduce peak ambient temperatures by 0.2-5°C, with a median reduction of 1°C (Balany et al., 2020); however, the cooling potential of urban trees varies with species, location, and proximity to other trees (Wong et al., 2021). Moreover, trees can drastically improve human comfort, for example, by reducing the physiological equivalent temperature by up to 14°C under tree canopies (Balany et al., 2020). In Toronto, a 2-3°C increase in temperature past the optimum can translate to a 4-7% increase in heat-induced mortality (Wang et al., 2016b). During the 2021 heat dome event in British Columbia, risk of death was higher in neighbourhoods with less green infrastructure (Henderson et al., 2022). Urban greening, by reducing urban temperatures, may thus prevent mortality caused by the urban heat island.

Beyond cooling, green infrastructure provides various ecosystem services to urban areas, including carbon sequestration, air purification, stormwater management, reduced energy and water consumption, and various physical and mental health benefits to residents (Anderson et al., 2022; Moore, 2016). Moreover, nature-based solutions such as urban greening have the added benefit of reducing urban reliance on mechanical cooling systems (i.e., air conditioning). A study performed in Los Angeles found that green infrastructure, combined with cool pavements, reduced air conditioning use in the average home by up to 50% (Rosenfeld et al., 1998), while a study in Beijing found that greenspaces can reduce cooling-related energy use by up to 60% (Zhang et al., 2014). Cooling system use may exacerbate urban heat, both directly (via heat output from air conditioning units) and indirectly (via greenhouse gas emissions) (Hayes et al., 2022; Phelan et al., 2015). The use of such systems thus forms a positive feedback loop wherein mechanical cooling contributes to urban heat, which necessitates further mechanical cooling, and so on (Hayes et al., 2022).

Importantly, combining multiple urban heat island mitigation strategies leads to more cooling (Yenneti et al., 2020), which may reduce heat-related mortality and morbidity risks in urban areas. An American study found that a combination of increased vegetation cover and reduced surface albedo in urban areas could offset 40-99% of projected increases in heat-related deaths under climate change (Stone et al., 2014). Additionally, combining mitigation strategies promotes a greater diversity of ecosystem services (Anderson et al., 2022).

1.2. Purpose

Urban heat island effects are of increasing concern given climate change, as well as global trends in urbanization and population ageing (UN DESA, 2018; Heaviside et al., 2017; Phelan et al., 2015). Simply put, urban heat island effects will intensify with global warming, and those effects will impact more people and increasingly more vulnerable populations. Moreover, heat waves are likely to become more frequent with climate change, increasing the risk of heat-induced mortality and morbidity in urban areas (Yadav et al., 2023). Higher-latitude countries such as Canada are more likely to experience pronounced warming due to climate change (Warren, 2004). Within the Lake Simcoe watershed, the number of days per year with temperatures above 30°C is projected to increase from an average of 6 per year to 27 by 2050



and 48 by 2080 under RCP 8.5 (LSRCA, 2020). More extreme heat is expected, with maximum summer temperatures projected to increase by 5.7°C by 2080 under RCP 8.5 (LSRCA, 2020). Residents of high-latitude cities are more likely to experience more dramatic urban heat island effects as they are less acclimatized to heat, and these cities tend to have less advanced cooling infrastructure (Hayes et al., 2022; Wang et al., 2016b). In Canada, the number of heat-related deaths is estimated to increase by 45-455% by 2080¹ (Health Canada, 2020; Guo et al., 2018). In Toronto, the number of heat-related deaths per year is predicted to double by 2050 and triple by 2080 (Wang et al., 2016b).

Urban heat island research is critical to better understanding and preparing for projected increases in heat risks to a growing number of urban residents. Urban heat models are especially useful tools whose spatial outputs can be used to inform urban planning (e.g., by identifying neighbourhoods most vulnerable to urban heat island effects) and address social and environmental inequity in urban areas, among other things. In this report, we provide a comprehensive review of several urban heat models. It is our hope that this review may inform and/or guide future urban heat island research and streamline decision-making processes around model selection. Additionally, we present the results of an urban heat modelling case study, wherein we selected and applied an urban heat model—InVEST Urban Cooling—to simulate potential future conditions in East Gwillimbury under different land use change, urban greening, and climate emissions scenarios. East Gwillimbury is a municipality in southern Ontario, located approximately 58 kilometres north of downtown Toronto. It is currently the fastest-growing municipality in Canada—by 2031, it is expected to have developed from a collection of smaller towns to a large urban area (Statistics Canada, 2022; Town of East Gwillimbury, 2022). East Gwillimbury thus presents a unique opportunity as a case study for urban heat modelling, as it allows us to not only explore the potential of modelling approaches, but also the impacts of rapid, large-scale urban development on heat and human health.

1.3. Intended Application, Target Audience, and Scope

By presenting a review of urban heat modelling approaches, as well as a decision support tool for selecting and running appropriate models, it is our hope that this report will assist in future urban heat modelling studies both within the Lake Simcoe watershed and beyond. Moreover, in this report we explore the effects of development and urban greening on air temperature in a municipality in southern Ontario, both presently and into the future under two climate emissions scenarios. The results of this project may thus be used by the municipality itself, as well as other local municipalities, to inform decision-making around zoning, development policies, urban forest canopy cover targets and tree protection by-laws, climate change

¹ A 45% increase is expected under a “best-case scenario” (low greenhouse gas emissions, low population growth, and implementation of mitigation measures), whereas a 455% increase is expected under a “worst-case scenario” (greenhouse gas emissions continue to increase at current rate, population growth is high, and no mitigation measures are implemented) (Guo et al., 2018).



adaptation plans, and more. This report thus represents an opportunity for us to explore ways to integrate the results of modelling into municipal policy. Beyond East Gwillimbury, our results contribute to a broader literature on the urban heat island effect, providing unique insight into the relationship between urbanization and heat, as well as urban forests and heat. To the best of our knowledge, this report is the first to use the InVEST Urban Cooling model to simulate urban air temperatures under climate emissions scenarios.

2.0 Urban Heat Model Selection and Rationale

2.1. Approach

We conducted a review of urban climate models using online academic literature databases (e.g., Google Scholar), as well as relevant urban climate modelling websites. We summarized key information on existing, validated models, including information on model methodology, inputs and outputs, and advantages and limitations (see Tables 2-1, 2-2, and Appendix A). We then developed a list of criteria to assess model suitability for our East Gwillimbury case study.

To assist with model selection, we developed a Decision Support Tool wherein criteria are ranked based on priority (High, Medium, and Low), with models given a standardized score based on fulfilment of ranked criteria. The list of criteria provided is by no means a comprehensive list; rather, it serves as a foundational starting point from which other teams may conduct future model suitability assessments for urban heat projects. The criteria list may be added to or reduced as necessary depending on specific project goals. This Decision Support Tool streamlines future decision-making by providing a clear, replicable methodology for model selection, while still allowing for flexibility around unique project goals. Moreover, it assesses model suitability based on a weighted ranking system of criteria. In this way, the Decision Support Tool resolves some challenges associated with selecting a model based on sheer number of criteria met by (a) acknowledging that some criteria may hold more importance than others, and (b) reducing the likelihood that multiple models will fulfil the same number of criteria.

2.2. Review of Urban Heat Models

The urban heat island effect can be most easily quantified using existing air temperature records and/or land surface temperature estimates. While air temperature is a direct measure of the urban heat island effect, weather stations are few and far between and it is difficult to accurately extrapolate point measurements across an entire city (Yang et al., 2013; Schwarz et al., 2012). Land surface temperature, meanwhile, can be assessed across a larger area; however, surface temperature is an indirect urban heat island measure that is not easily translated to human thermal comfort values (Yang et al., 2013; Schwarz et al., 2012). Surface temperature is also typically derived from remote sensing data and thus has limited temporal scope (i.e., data is only available at the coarse measurement intervals of satellites) (Yang et al.,



2013). As global interest in the urban heat island has increased, so has the demand for alternative methods for assessing the urban climate (Yang et al., 2013). Urban heat models are computer programs specifically designed to simulate air temperature (among other metrics) in urban areas. These models quickly calculate urban heat island data across large urban areas over several days, months, or even years. Importantly, urban heat models also allow the user to simulate the urban heat island under different scenarios, such as increased tree canopy cover, building density, and climate emissions pathways. Predictions acquired from these models may therefore not only increase our understanding of the urban heat island in cities as they are, but also how urban heat may change in the future with increased urbanization, urban greening programs, and climate change.

2.2.1 Urban Microscale Models

The models reviewed in this report can be grouped into two categories: microscale models and macroscale models. Microscale models such as ENVI-met, SOLWEIG, and RayMan are complex and therefore computationally expensive (Mutani & Beltramino, 2022) and are best suited for studies at the neighbourhood scale or smaller. ENVI-met is widely used, highly validated, and is considered the most “complete” of the urban microclimate models (Balany et al., 2020; Lin et al., 2019). It accounts not only for the complexities of vegetation (i.e., surface-plant-air interactions, types of vegetation and their spatial geometry, etc.), but also the complexities of the urban environment, including road and building materials, soil types, surface porosity, etc. (Balany et al., 2020). It provides a wide range of outputs, including surface, soil, and air temperatures, humidity, human thermal comfort values, data on pollutant dispersion, soil water balance, building physics, and more.

SOLWEIG and RayMan, while still complex in nature, are slightly simpler models in comparison to ENVI-met, especially when it comes to simulating the impacts of vegetation on the urban microclimate (Vurro & Carlucci, 2024; Balany et al., 2020; Jänicke et al., 2015). Of the three microscale models, RayMan computes the greatest range of human thermal comfort indices (Balany et al., 2020); however, model accuracy is limited by latitude (Balany et al., 2020), and calculations can only be made for specific points in space, not for an entire area (Jänicke et al., 2021; Matzarakis et al., 2015). SOLWEIG can simulate the urban microclimate over an entire study area and resolves the latitude-dependent inaccuracies of RayMan (Jänicke et al., 2021; Balany et al., 2020). Both SOLWEIG and RayMan more accurately calculate mean radiant temperature compared to ENVI-met (Chen et al., 2014).

While these models are not recommended for large study areas due to their computational requirements, spatial resolution limitations, and/or other challenges, this does not mean they are unable to perform over large spatial scales. Mutani and Beltramino (2022), for example, used SOLWEIG to simulate temperatures across all of Turin, Italy. They selected SOLWEIG over ENVI-met as it represented the best compromise between simulation time and accuracy (Mutani & Beltramino, 2022). However, to simulate temperatures during the hottest and coldest days of the year, they were required to split the city into sections due to model area

limits, and the model scenarios took approximately 27-36 hours (coldest day) and 30-33 hours (hottest day) to complete (Mutani & Beltramino, 2022). Thus, while microscale models can be used to explore the urban heat island effect at the city-wide scale, the process is time-consuming and laborious.

Urban microscale models are worthwhile to consider, even for large-scale urban heat studies, as these models can be used to investigate heat at the neighbourhood level once broad-scale temperature patterns and vulnerable areas have been identified using macroscale models. In this report, we focus on macroscale models, as we were interested in exploring urban heat across the entire East Gwillimbury municipality. For more detailed information on the three microscale models we reviewed—ENVI-met, SOLWEIG, and RayMan—see Appendix A.

2.2.2 Urban Macroscale Models

The two urban macroscale models we reviewed for this report are i-Tree Cool Air (hereafter, “Cool Air”) and InVEST Urban Cooling (hereafter, “InVEST”) (Table A-4; A-5; Appendix B²). Macroscale models tend to be much simpler and more efficient in terms of model run time compared to microscale models, which are more complex and computationally expensive (Martins et al., 2023; Lin et al., 2019). Both Cool Air and InVEST rely on land use/land cover information as input into the model (compared to ENVI-met, for example, which requires detailed three-dimensional urban geometry information). Both models are also able to compute metrics beyond temperature, such as water budget and runoff information (Cool Air) or energy savings and work productivity (InVEST).

While the i-Tree toolset as a whole is highly cited (Lin et al., 2019), the Cool Air tool is relatively new (released 2019) and not as cited as other i-Tree tools, such as i-Tree Eco. As a result, few studies have assessed Cool Air model accuracy. However, existing assessments report a high degree of accuracy. Pace et al. (2023), for example, found strong correlations for both air temperature ($r^2 \geq 0.94$) and dew point temperature ($r^2 \geq 0.89$) between the model and local weather station measurements. InVEST is also a relatively new software (released 2020), and, like Cool Air, is not as widely validated. Bosch et al. (2021a) found strong correlations between InVEST model outputs and nearby station measurements, with an r^2 value as high as 0.903. Hamel et al. (2023), meanwhile, found a moderate to strong correlation (r^2 between 0.55 and 0.85) between InVEST temperatures and temperatures simulated by other models, with InVEST performing better with nighttime temperatures ($r^2 = 0.84$; mean absolute error = 0.52°C). One possible explanation for this poorer performance (i.e., lower r^2 value) is that Hamel et al. (2023) compared InVEST’s outputs to the outputs from another model, rather than actual observed weather records, meaning the errors and/or limitations of the comparison model may have

² Appendix B contains a summary of i-Tree Cool Air and InVEST Urban Cooling literature. ENVI-met, SOLWEIG, and RayMan are older models that are widely used and highly cited, so an in-depth literature review of these three models is beyond the scope of this report. However, for high-level information on these models, as well as recommendations for further reading, see Appendix A.

contributed to a reduced r^2 value. Other explanations include data input quality and accuracy, and oversimplification of the physical processes underlying InVEST’s calculations (Hamel et al., 2023). Despite the model’s moderate performance, Hamel et al. (2013) still recommend its use as a decision support tool for urban planning and land use change.

Because both Cool Air and InVEST require land use/land cover as input data, they can efficiently simulate alternative land use scenarios such as increased or decreased canopy or impervious surface cover (for examples, see Pace et al., 2023 and Sinha et al., 2022 for Cool Air, and Keyes et al., 2022 and Bosch et al., 2021b for InVEST). While neither model can automatically run alternative land cover scenarios, it is relatively easy for the user to modify land use inputs to create scenario conditions. Of the two models, only InVEST can run alternative climate scenarios. Cool Air requires more detailed weather input data (e.g., hourly temperature, wind speed, dew point temperature) (Table A-4) that cannot easily be projected into the future. InVEST, meanwhile, requires simpler weather data inputs (Table A-5). While InVEST Urban Cooling has not yet been used to simulate future climate conditions, such simulations are possible if the rural reference temperature, urban heat island effect, and/or evapotranspiration inputs are changed to reflect a given climate pathway (Bosch et al., 2021b).

2.3. Model Selection

To assist with model selection for our East Gwillimbury case study, we developed an evaluation table (Table 2-1) to assess model suitability based on criteria fulfilment. While the spatial and temporal scope of our case study restricted our choice of model to the two macroscale models we reviewed—i-Tree Cool Air and InVEST Urban Cooling—we included the three microscale models in our evaluation table given their potential suitability for urban heat analyses. For a description of evaluation criteria, see the [Criteria Definitions](#) list below Table 2-1.

Table 2-1 – Evaluation table used to assess model capabilities for a case study in East Gwillimbury.

Evaluation Criteria	i-Tree Cool Air	InVEST Urban Cooling	ENVI-met	SOLWEIG	RayMan
Broad spatial scale	✓	✓			
Computationally inexpensive	✓	✓		✓	✓
Day and night	✓	✓	✓		
Minimal input requirements		✓	✓	✓	✓
Technical support		✓	✓	✓	✓



Evaluation Criteria	i-Tree Cool Air	InVEST Urban Cooling	ENVI-met	SOLWEIG	RayMan
Open access	✓	✓		✓	✓
Outputs easily visualized	✓	✓	✓	✓	
Scenarios: land use change	✓ ¹	✓ ¹	✓ ¹	✓ ¹	✓ ¹
Scenarios: climate projections		✓ ¹			
Scenarios: urban greening	✓ ¹	✓ ¹	✓ ¹	✓ ¹	✓ ¹
Spatially explicit	✓	✓	✓	✓	
Uncertainty assessment			✓		
Universal	✓ ²	✓	✓	✓	✓

¹ Requires user input (model is not able to automatically run scenario).

² Requires conversion of regional land cover classes to U.S. NLCD classes.

Criteria Definitions

- **Broad spatial scale:** model is capable of simulations beyond a neighbourhood scale.
- **Computationally inexpensive:** model does not require excessive computer bandwidth to run (i.e., the software does not fail on a computer with 16 GB of RAM).
- **Day and night:** model is capable of simulating both daytime and nighttime temperatures.
- **Minimal input requirements:** model inputs include data that is readily available.
- **Technical support:** there is free, accessible technical support available online for the model.
- **Open access:** model is freely available online.
- **Outputs easily visualized:** model outputs can be easily visualized with mapping software (i.e., GIS) and extracted into usable formats (e.g., JPEG, PDF).
- **Scenarios:** model can run simulations under different scenarios, including *land use change* (e.g., urban sprawl), various *climate projections* (e.g., RCP 4.5, RCP 8.5, etc.), and *urban greening* (e.g., 10% increase in forest cover) scenarios.
- **Spatially explicit:** model inputs, outputs, and/or processes vary spatially (Turner & Gardner, 2015).
- **Uncertainty assessment:** model output includes information on model uncertainty.
- **Universal:** model can be run in different regions without extensive re-calibration of parameters.

While Table 2-1 provides a useful summary of each model’s abilities, model selection based entirely on number of evaluation criteria fulfilled by each model is problematic in two main ways: (1) it ignores the relative importance of each evaluation criteria to the given project (i.e.,

does not account for the fact that some criteria might be more important than others), and (2) if two or more models fulfil the same number of criteria, the decision around which model to use for a specific project becomes completely arbitrary. Moreover, since one of the aims of this report is to assist future urban heat modelling studies, we decided to develop a [Decision Support Tool](#) (Figure 2-1) that not only resolves the two problems described above but that also streamlines future decision-making by providing a clear methodology for model selection while still allowing for flexibility around unique project goals.

A screen capture of the Decision Support Tool, filled out for this project, is shown in Figure 2-1. Prior to developing this tool, we were aware of Cool Air’s limitations with respect to our case study. First, Cool Air requires detailed weather input data that is not available for East Gwillimbury. Second, Cool Air is unable to model climate scenarios. These limitations are reflected in Figure 2-1 and contribute to Cool Air’s reduced score. Overall, InVEST Urban Cooling achieved the highest score based on fulfilment of ranked criteria. Importantly, InVEST fulfilled all our “High Priority” criteria (Figure 2-1).

Criteria list (can be added to or reduced)

Criteria ranked according to priority (3 = High, 2 = Medium, 1 = Low)

Criteria	Priority	Cool Air	InVEST Urban Cooling	ENVI-met	SOLWEIG	RayMan
Broad spatial scale	3	X	X			
Computationally inexpensive	1	X	X		X	X
Day and night simulations	3	X	X	X		
Minimal input requirements	2		X	X	X	X
Technical support available	1		X	X	X	X
Open access	3	X	X		X	X
Outputs easily visualized	2	X	X	X	X	
Scenarios: land use change	3	X	X	X	X	X
Scenarios: climate projection	3		X			
Scenarios: urban greening	3	X	X	X	X	X
Spatially explicit	3	X	X	X	X	
Uncertainty assessment	2			X	X	
Universal	2	X	X	X	X	X
MODEL SCORE		23	29	21	22	15
STANDARDIZED SCORE		0.70	0.88	0.64	0.67	0.45
BEST MODEL		InVEST Urban Cooling				

Models scored based on number of criteria fulfilled and weight (priority) of each fulfilled criterion

Decision tool automatically highlights the model with the highest standardized score and inputs model name into “BEST MODEL” cell

Figure 2-1 – Decision support tool for model selection based on fulfilment of ranked criteria, filled out with respect to the East Gwillimbury case study presented in this report.

This Decision Support Tool will ideally assist in future decision-making processes by providing a framework for model selection that reduces subjectivity and improves the transparency and replicability of model selection processes. For access to the tool, please contact the Conservation Authority (contact information found [here](#)).

3.0 Case Study

East Gwillimbury is a municipality in Southern Ontario that covers an area of approximately 238 km². A large share (70%) of that area is made up of farms and natural heritage features (forests, wetlands, etc.), with the remainder consisting of several urban areas, including Holland Landing, Queensville, Mount Albert, and Sharon (Town of East Gwillimbury, n.d.). According to 2022 Census Canada data, East Gwillimbury is the fastest-growing municipality (with at least 5,000 inhabitants) in Canada, having experienced a 44.4% increase in population between 2016 and 2021 (Statistics Canada, 2022). In 2021, East Gwillimbury had a population of 34,637 people (Statistics Canada, 2022). This number is expected to grow to 127,000 by 2051 (Town of East Gwillimbury, 2022), a further 266.7% increase in population. East Gwillimbury therefore offers a unique opportunity for urban heat modelling as it not only allows us to explore the urban heat island effect under various climate and greening scenarios within a municipality, but also to explore the direct effects of urban development on heat, *while that development is occurring*.

3.1. Methods

The goals of this case study were to explore the effect of development, tree cover, and climate on air temperature in East Gwillimbury. To do this, we came up with a list of scenarios to run using the InVEST Urban Cooling model (Table 3-1). For all scenarios, we decided to simulate maximum daytime and mean nighttime³ air temperatures for the month of July. By focusing on maximum daytime temperatures in the hottest month of the year, we are essentially simulating heat waves, which are the greatest urban heat island concern with respect to human health and well-being. We were unable to simulate maximum nighttime temperatures due to data limitations; however, mean July nighttime temperatures still provide important information on nighttime urban heat.

The climate emissions pathways we chose to incorporate into our modelling were two [Shared Socioeconomic Pathways \(SSPs\)](#), SSP2-4.5 and SSP5-8.5. SSP2-4.5 is a moderate (“middle of the road”) emissions pathway, while SSP5-8.5 represents a worst-case (“fossil-fueled development”) pathway (Government of Canada, n.d.). SSP2-4.5 has been described as the most likely pathway given current climate policy (Hausfather & Peters, 2020); however, SSP5-8.5 may also be a likely pathway considering total cumulative CO₂ emissions (Schwalm et al., 2020).

³ Due to limitations in available nighttime climate data, we used minimum daily temperatures as a proxy for mean nighttime temperatures (Seltenrich, 2023).



Table 3-1 – Description of InVEST Urban Cooling modelling scenarios with abbreviated scenario names.

Scenario	Description
Current	Simulation of current (2018) conditions within East Gwillimbury (i.e., using the most up-to-date land cover and climate data available).
Buildout_22	Simulation of potential future conditions within East Gwillimbury under a full buildout (i.e., taking all current and future development plans within East Gwillimbury into account) and reduced canopy cover to an average of 22% across the entire municipality.
Buildout_38	Simulation of potential future conditions within East Gwillimbury under a full buildout and maintenance of current canopy cover (38.1% average across the entire municipality).
Buildout_44	Simulation of potential future conditions within East Gwillimbury under a full buildout and increased canopy cover to an average of 44% across the entire municipality.
Buildout_Green44*	Identical to Buildout_44, except the urban forest is treated as a natural system by the model.
SSP245_mid_22	Simulation of potential future conditions within East Gwillimbury for the time period 2041-2070 under the SSP2-4.5 climate scenario, full buildout, and canopy reduction to 22%.
SSP245_mid_38	Simulation of potential future conditions within East Gwillimbury for the time period 2041-2070 under the SSP2-4.5 climate scenario, full buildout, and maintenance of current canopy cover (38.1%).
SSP245_mid_44	Simulation of potential future conditions within East Gwillimbury for the time period 2041-2070 under the SSP2-4.5 climate scenario, full buildout, and canopy increase to 44%.
SSP245_mid_Green44*	Identical to SSP245_mid_44, except the urban forest is treated as a natural system by the model.
SSP245_end_22	Simulation of potential future conditions within East Gwillimbury for the time period 2071-2100 under the SSP2-4.5 climate scenario, full buildout, and canopy reduction to 22%.
SSP245_end_38	Simulation of potential future conditions within East Gwillimbury for the time period 2071-2100 under the SSP2-4.5 climate scenario, full buildout, and maintenance of current canopy cover (38.1%).



Scenario	Description
SSP245_end_44	Simulation of potential future conditions within East Gwillimbury for the time period 2071-2100 under the SSP2-4.5 climate scenario, full buildout, and canopy increase to 44%.
SSP245_end_Green44*	Identical to SSP245_end_44, except the urban forest is treated as a natural system by the model.
SSP585_mid_22	Simulation of potential future conditions within East Gwillimbury for the time period 2041-2070 under the SSP5-8.5 climate scenario, full buildout, and canopy reduction to 22%.
SSP585_mid_38	Simulation of potential future conditions within East Gwillimbury for the time period 2041-2070 under the SSP5-8.5 climate scenario, full buildout, and maintenance of current canopy cover (38.1%).
SSP585_mid_44	Simulation of potential future conditions within East Gwillimbury for the time period 2041-2070 under the SSP5-8.5 climate scenario, full buildout, and canopy increase to 44%.
SSP585_mid_Green44*	Identical to SSP585_mid_44, except the urban forest is treated as a natural system by the model.
SSP585_end_22	Simulation of potential future conditions within East Gwillimbury for the time period 2071-2100 under the SSP5-8.5 climate scenario, full buildout, and canopy reduction to 22%.
SSP585_end_38	Simulation of potential future conditions within East Gwillimbury for the time period 2071-2100 under the SSP5-8.5 climate scenario, full buildout, and maintenance of current canopy cover (38.1%).
SSP585_end_44	Simulation of potential future conditions within East Gwillimbury for the time period 2071-2100 under the SSP5-8.5 climate scenario, full buildout, and canopy increase to 44%.
SSP585_end_Green44*	Identical to SSP585_end_44, except the urban forest is treated as a natural system by the model.

* Daytime only

We used the InVEST 3.14.2⁴ Urban Cooling model to explore the urban heat island and the cooling effect of urban trees within the municipality of East Gwillimbury. InVEST requires the following data inputs:

- A raster map of land use/land cover for the area of interest, with a linked table describing the following biophysical parameters for each land use class:

⁴ InVEST Urban Cooling is freely available at the Natural Capital Project's [website](#).



- [Crop coefficient \(\$K_c\$ \)](#)
- Albedo
- Shade (i.e., the proportion of coverage by tree canopy at least 2 m high)
- A true/false statement on whether the land use class is considered a [green area](#) (“0” if it is not considered a green area, “1” if it is)
- Optionally, building intensity (i.e., the ratio of building floor area to footprint area), with all values normalized between 0 and 1
- A raster map of reference evapotranspiration values (in millimetres) for a given time period in the area of interest⁵.
- A vector map outlining the area of interest.
- A maximum cooling distance value (in metres), which represents the distance over which large (> 2 hectares) greenspaces have a cooling effect.
- A reference air temperature value (in degrees Celsius) for a nearby rural area where the urban heat island effect is not observed.
- The urban heat island effect, i.e., the difference (in degrees Celsius) between the rural reference temperature and the maximum temperature observed in the urban area of interest.
- An air blending distance (in metres), which is the radius over which air temperatures are averaged to account for air mixing.

To compute additional metrics, including nighttime air temperature, energy savings, and work productivity loss, the following inputs are also required:

- A vector map of building footprints and an associated energy consumption table that provides energy consumption data—either energy consumption in kWh/°C or cost in currency/kWh—for each building type.
- Average percent relative humidity within the study area over the time period of interest.

We obtained land use/land cover information from GIS layers created by the Lake Simcoe Region Conservation Authority (LSRCA, 2022) and Toronto and Region Conservation Authority (Timmins & Sawka, 2022), as well as the municipality of East Gwillimbury⁶. We used this land use information to create two land use raster layers: one representing 2018 land cover conditions, and the other representing future conditions under a full buildout (i.e., completion of all current and future urban development plans within the municipality). We obtained development information from East Gwillimbury⁶. To fill out the biophysical parameter for each land use class, we used a Lake Simcoe Region Conservation Authority 2018 building footprint layer and a 2019 York Region land use raster layer (Timmins & Sawka, 2022), as well as

⁵ The InVEST Urban Cooling User Guide recommends using reference evapotranspiration raster data as input. However, actual evapotranspiration data may also be used so long as land use K_c values are modified accordingly.

⁶ For publicly available East Gwillimbury land use/land cover and development information, see the municipality’s [Planning and Development webpage](#), as well as their [Official Plan](#).



literature recommended by the InVEST User Guide. We added on to the Lake Simcoe building footprint layer to generate a footprint layer for our buildout scenario and consulted the literature to determine energy consumption rates for different building types.

We used values from the literature to adjust the maximum cooling distance and air blending distance values recommended in the InVEST User Guide. To obtain the urban heat island effect, we consulted the [Global Surface UHI Explorer](#), which InVEST recommends. For evapotranspiration data, we used the Lake Simcoe Region Conservation Authority's 55-year average evapotranspiration map (Earthfx, 2010) for all scenarios simulated under current climate conditions. For future climate conditions, we used the climate database ClimateNA (Mahony et al., 2022; Wang et al., 2016a) to generate reference evapotranspiration maps for our different climate emissions scenarios and timesteps. We also used ClimateNA to generate future climate reference air temperature and relative humidity values. For more detailed methodological information, see Appendix C.

Once we had obtained our input data for all scenarios, we used InVEST to compute the following outputs⁷ for each land use pixel within our study area:

- A raster of [heat mitigation index](#) and [cooling capacity](#) values⁸.
- Estimated daytime and/or nighttime air temperature values (degrees Celsius) within the study area for the time period of interest, including a raster of air temperature values with and without air mixing.
- If the work productivity loss valuation method is selected: a raster of calculated [wet bulb global temperature](#) values and data on light and heavy work productivity loss (%)⁹.
- If the energy savings valuation method is selected: a vector of building footprints that contains data on energy savings (kWh or currency) and average indoor temperatures (in degrees Celsius).

⁷ The model computes additional outputs that are not relevant to this specific project and are therefore not described in detail here. For more information on these outputs, see the [InVEST Urban Cooling User Guide](#).

⁸ We do not discuss heat mitigation index and cooling capacity in our results section, as these indices form the basis of the model's air temperature calculations and are thus reflected in the air temperature outputs. However, we list these outputs here and provide a definition of each within the [Glossary](#) so the reader can better understand the mechanisms behind InVEST.

⁹ Light and heavy work are defined according to Kjellstrom et al. (2009), where light work is work where the workers' metabolic rate is between 200 and 400 Watts, and heavy work is anything above 400 Watts.

3.2. Results and Discussion

3.2.1 Daytime Temperatures

The urban heat island impacts a larger area under the full buildout scenario compared to the current (2018) land cover scenario (Figure 3-1). After full buildout, the urban areas of Holland Landing, Queensville, Sharon, and Green Lane West merge and expand into a single urban core (Figure 3-1). However, there is not a dramatic difference in air temperature between the two scenarios. Under current land cover, average maximum July air temperature within the densest urban areas (Holland Landing, Sharon, Mount Albert) was 28.1°C without air mixing and 27.9°C with mixing (Figure 3-1). Under the full buildout scenario, air temperatures within the urban core and Mount Albert were 28.2°C without mixing and 28°C with mixing (Figure 3-1; Table F-1). Urban heat island intensity is strongly influenced by building density (Li et al., 2020a; Chapman et al., 2018). Moreover, urban heat island intensity tends to be lower in municipalities that are built “out” compared to those that are built “up” (Li et al., 2020a; Chapman et al., 2018). While East Gwillimbury is undergoing rapid development, much of this development consists of sprawling residential subdivisions. This expansion outwards of urban infrastructure without a dramatic increase in vertical density might explain the minimal change in temperature between the two scenarios. However, while overall temperature differences between the 2018 and buildout scenarios are small, the extent of the change is large.

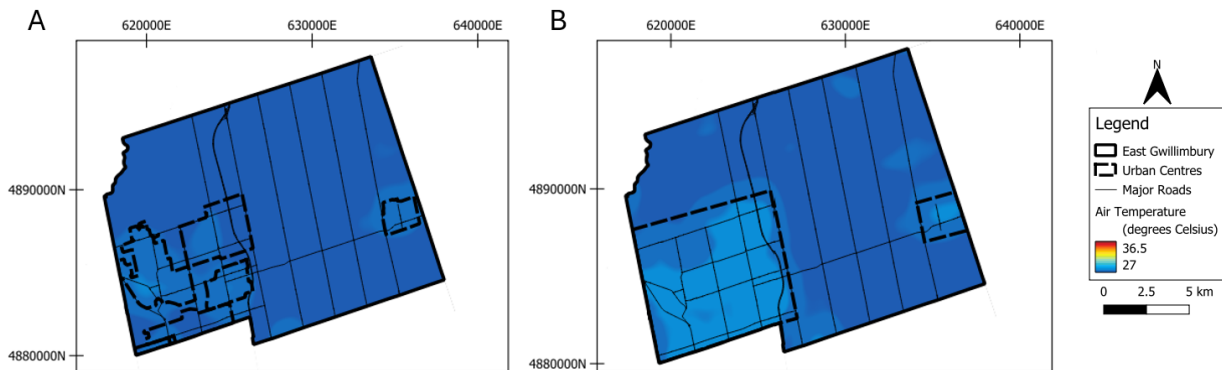


Figure 3-1 – Maps of East Gwillimbury showing estimated maximum daytime July air temperature (°C) distribution for (A) 2018 under current climate (2011-2020) conditions, and (B) a full buildout scenario under current climate (2011-2020) conditions.

Figures 3-2 to 3-6 show daytime air temperature distributions across East Gwillimbury under current climate and future climate emissions scenarios. At 38% canopy cover, spatially averaged estimated maximum July air temperatures across all of East Gwillimbury were 27.6°C under current climate conditions, and by mid-century (2041-2070) had increased to 29.4°C under SSP2-4.5 and 30.0°C under SSP5-8.5 (Table F-4). By end-century (2071-2100), temperatures had increased further to 30.1°C under SSP2-4.5 and 32.4°C under SSP5-8.5 (Table F-4). Within urban

areas, temperatures were 1-3°C warmer depending on canopy cover (Appendix E; Figures 3-2; 3-3; 3-4; Table F-3). Our results are below current climate projections for the Lake Simcoe watershed, which predict an increase in mean summer temperatures by 2.8°C (RCP 4.5) and 5°C (RCP 8.5) by end-century (LSRCA, 2020). We would expect our estimated temperatures to be higher than these projections, given that we are modelling maximum July temperatures. It is possible that this discrepancy is because we based our climate projections on Shared Socioeconomic Pathways (SSPs), rather than Representative Concentration Pathways (RCPs), which were used for the Lake Simcoe climate projections. Maximum summer temperatures in the Lake Simcoe watershed are projected to reach an average of 30.1°C by end-century under RCP 8.5. The slightly higher 32.4°C average predicted by InVEST can be explained by the urban heat island effect increasing temperatures in urban areas within East Gwillimbury, which raises average air temperatures across the entire municipality, as well as the fact that we modelled maximum temperatures for July, the hottest month of the year.

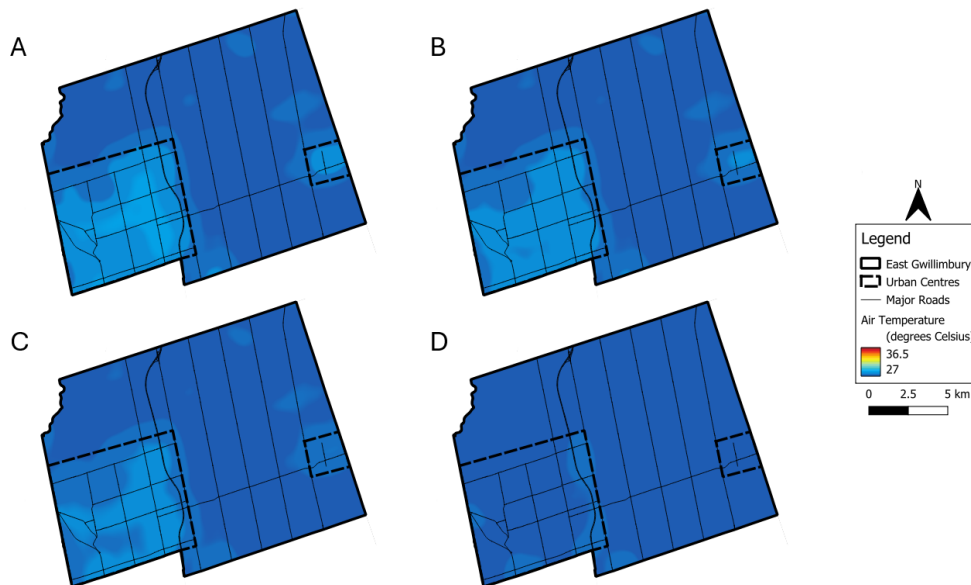


Figure 3-2 – Maps of East Gwillimbury showing estimated maximum daytime July air temperature (°C) distribution under a full buildout scenario and current climate (2011-2020) conditions, and four canopy cover scenarios: (A) 22%, (B) 38%, (C) 44%, and (D) green 44%.

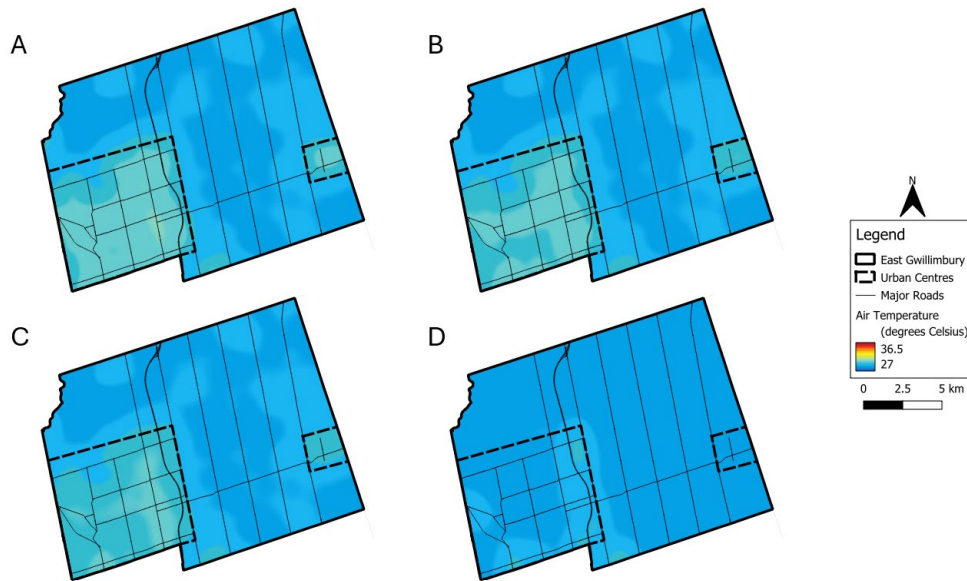


Figure 3-3 – Maps of East Gwillimbury showing estimated maximum daytime July air temperature (°C) distribution by mid-century (2041-2070) under the SSP2-4.5 emissions pathway for four canopy cover scenarios: (A) 22%, (B) 38%, (C) 44%, and (D) green 44%.

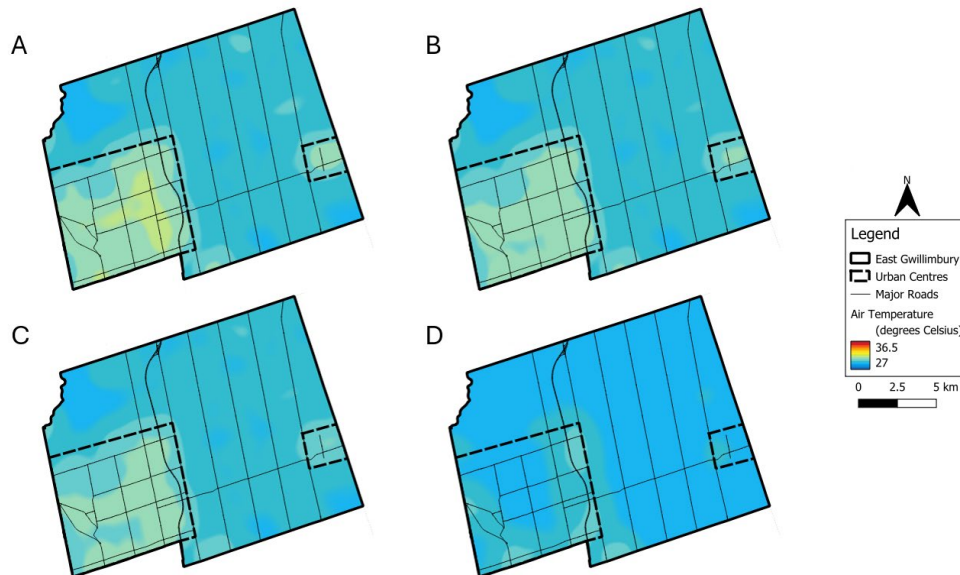


Figure 3-4 – Maps of East Gwillimbury showing estimated maximum daytime July air temperature (°C) distribution by end-century (2071-2100) under the SSP2-4.5 emissions pathway for four canopy cover scenarios: (A) 22%, (B) 38%, (C) 44%, and (D) green 44%.

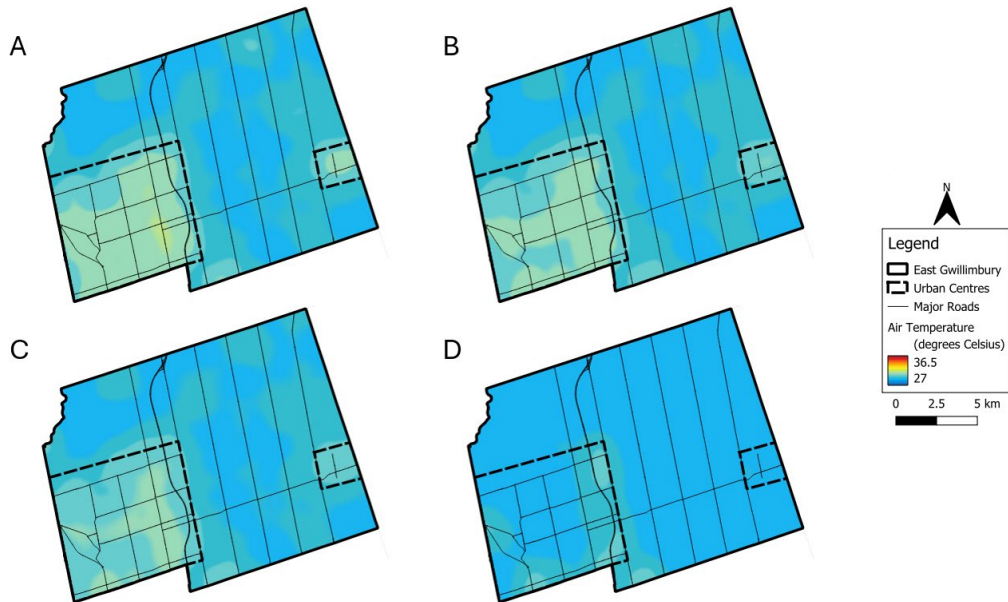


Figure 3-5 – Maps of East Gwillimbury showing estimated maximum daytime July air temperature (°C) distribution by mid-century (2041-2070) under the SSP5-8.5 emissions pathway for four canopy cover scenarios: (A) 22%, (B) 38%, (C) 44%, and (D) green 44%.

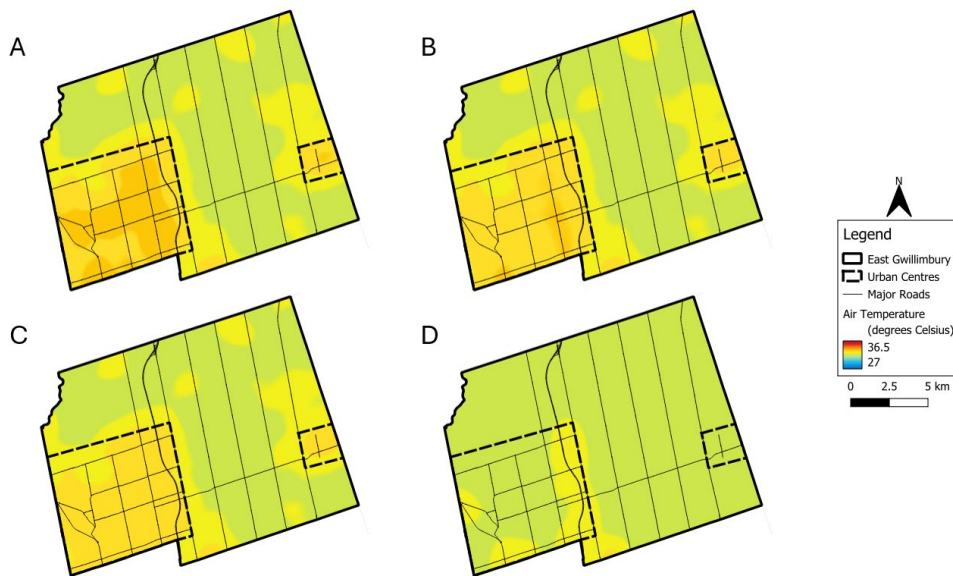


Figure 3-6 – Maps of East Gwillimbury showing estimated maximum daytime July air temperature (°C) distribution by end-century (2071-2100) under the SSP5-8.5 emissions pathway for four canopy cover scenarios: (A) 22%, (B) 38%, (C) 44%, and (D) green 44%.

When the model took humidity into account, wet bulb global temperature values across East Gwillimbury rose from 29.0°C (current climate) to 30.8°C (SSP2-4.5) and 31.5°C (SSP5-8.5) by

mid-century, and 31.7°C (SSP2-4.5) and 34.5°C (SSP5-8.5) by end-century (Table F-3). Again, wet bulb values were even higher (about 0.5-1°C) in urban areas (Appendix E; Table F-3). Figures E-1 to E-5 show wet bulb global temperature distribution across East Gwillimbury. Past a wet bulb global temperature of 26-30°C, human thermal comfort deteriorates rapidly (Kjellstrom et al., 2009). Outside heavy work losses of 30.7% are already estimated at 38% canopy cover under current climate conditions (Table F-4). Canopy increases prevented some work productivity loss under SSP2-4.5 and SSP5-8.5 (mid-century only) by lowering wet bulb temperatures; however, by end-century under SSP5-8.5, wet bulb temperatures had increased to the point where both heavy and light work productivity were reduced by 75% despite any increase in canopy cover (Table F-4). This result highlights the importance of taking measures to prevent the worst of climate change now.

Across all climate scenarios, 38% canopy (representing a “baseline,” i.e., current canopy cover in East Gwillimbury) produced approximately 0.16-0.22°C cooling within urban areas compared to a reduced (22%) canopy cover scenario (Table F-1; F-2). Cooling was less pronounced with an increase to 44% cover, at about 0.07-0.1°C cooling compared to the 38% baseline (Table F-1; F-2). There is a 16% avoided loss in canopy cover between the 22% and 38% scenarios, compared to a 6% increase between 38% and 44%, which explains the greater cooling between the 22% and 38% scenarios. Cooling is most marked under the Green 44% canopy cover scenario, with a difference in temperature of 0.77-1.2°C compared to the baseline 38% canopy cover scenario (Appendix E; Table F-1; F-2). The Green 44% scenario provides an additional 0.7-1.1°C cooling over the 44% scenario, when comparing temperatures to the baseline (Appendix E; Table F-1; F-2).

Yang et al. (2022) assessed the cooling efficiency of urban trees across 510 global cities and reported a global average of 0.063°C cooling per percent increase in tree cover. Our modelling results show a reduced cooling efficiency, with 0.01-0.2°C cooling with every percent increase in tree cover. Our results are also largely below the range provided by Balany et al. (2020), who reviewed literature on the cooling effects of urban vegetation and found that, on average, the addition of vegetation cools ambient daytime temperatures by 0.2-5.0°C, with a median cooling effect of 1°C. Yang et al. (2022) found that the cooling effect is greatest in hot and dry cities (e.g., Arizona). East Gwillimbury is in a climate zone characterized by warm, humid summers (Commission for Environmental Cooperation, 2021) and therefore might experience less summer cooling with increased canopy cover.

While the cooling effect we observed under our Green 44% scenario is less than what we would expect based on cooling efficiency values found in Yang et al. (2022), it does align with the median cooling effect reported by Balany et al. (2020). We created the Green 44% scenario to simulate the “40% threshold effect,” wherein at or above 40% canopy cover, the cooling benefits of the urban forest mimic that of a natural forest¹⁰. The “40% threshold effect” is based on research by Wang et al. (2023), Ziter et al. (2019), Zhao et al. (2017), Adams & Smith

¹⁰ See Appendix C for more details.



(2014), and others. Ziter et al. (2019), for example, found that the relationship between urban canopy cover and cooling is non-linear, with cooling increasing exponentially past the 40% mark. Their research suggests that the cooling benefits of canopy cover at or above the 40% mark is so substantial that the warming effect of impervious surfaces is essentially eliminated (Ziter et al., 2019). Under our Green 44% scenario, air temperatures over the Developed, Low Intensity land use class (which is the only urban class to have 40% canopy cover) closely resemble air temperatures over natural land use classes (Figures 3-2; 3-3; 3-4; 3-5; 3-6; Appendix F; Appendix E), which supports evidence for the urban heat-eliminating effect of the urban forest past 40% cover (Ziter et al., 2019).

According to Wang et al. (2023), at 40% canopy cover, a stable cooling system is created wherein cold air is not easily dissipated. As canopy cover increases under our four scenarios, the standard deviation of all temperature variables decreases (Appendix F). Within urban areas, standard deviation also decreased with every increase in canopy cover, which suggests that this decrease is not simply a product of increasing forest cover to an amount similar to that found in non-urban areas. Under the Green 44% scenario, standard deviation in urban areas was at its lowest. This suggests a reduction in temperature variability with increasing canopy cover in urban areas, where temperature variability is minimized under the Green 44% scenario. Increased canopy cover therefore appears to contribute to a more stable urban cooling system, which supports the findings of Wang et al. (2023).

While our results suggest that InVEST is able to simulate the “40% threshold effect,” if that effect does indeed occur, the cooling efficiency of urban trees is highly contextual and varies widely among cities (Yang et al., 2022). It is possible that, within East Gwillimbury, the 40% threshold effect would not occur to the extent that it is reported in the literature and that the cooling we observed under our 44% scenario may be more reflective of reality. We cannot therefore conclusively say which greening scenario is more accurate, but rather that a range of **0.07-1.2°C** urban cooling is possible with an increase from East Gwillimbury’s current canopy (38%) to 44% canopy cover. However, given existing evidence for the “40% threshold effect,” and that our results under the “40% threshold” scenario (i.e., Green 44%) better align with the literature, it is likely that the cooling effect of 44% canopy cover is on the higher end of that range.

Table 3 summarizes July energy and work productivity loss/gains for each canopy cover scenario compared to the 38% baseline, for each climate series. Energy savings represent the impact of tree canopy cover on overall cooling demand within East Gwillimbury. The Green 44% scenario, which cooled urban air temperatures by about 1°C, produced the greatest energy savings, approximately \$290,000 under current climate conditions and \$335,000 under both climate emissions scenarios and timesteps (Table 3; Table F-4). According to the Independent Electricity System Operator, summer air conditioning use can add an extra \$200 to the average Ontario homeowner’s energy bill (IESO, 2015). Homeowners can save up to 10% (or \$20) of this added cost by keeping their homes 2°C warmer in the summer (IESO, 2015). When we divide the maximum energy savings we observed under our Green 44% scenario (\$335,826) by the number of buildings in a fully built out East Gwillimbury (26,809 buildings, the majority of which



are residential), total energy savings can be broken down to \$12.5 saved per household. This result (\$12.5 saved per household due to 1°C cooler outdoor temperatures) aligns with the Independent Electricity System Operator’s prediction of \$20 saved per household with 2°C less cooling demand (or, \$10 with 1°C less demand).

Across all climate scenarios, productivity loss was highest under the 22% canopy cover scenario and lowest under the Green 44% scenario (Table 3; Table F-4). Changes in canopy cover had the greatest effect on light work productivity, with a maximum light work avoided loss of 18.6%, compared to a maximum heavy work avoided loss of 8.6%, both under the Green 44% scenarios and SSP2-4.5 (end-century) pathway (Table 3; Table F-4). Under current climate conditions, wet bulb temperatures were already close to the 26-30°C threshold, beyond which thermal comfort declines rapidly. Under both climate emissions pathways, temperatures surpassed this threshold, even with canopy increases. Any ability to perform heavy work under such high temperatures is therefore limited, even with additional canopy cooling. However, the work productivity savings we did observe under increased canopy cover, particularly for light work, highlights the importance of implementing heat mitigation measures. These measures may not only save workers from extreme discomfort and heat-related health risks but may also help to reduce negative impacts to essential municipal services (e.g., construction, agriculture, mail delivery). Overall, our valuation results demonstrate how a relatively small amount of cooling (less than 1.2°C) can have an impact on municipal economies and human health and well-being.

Table 3-2 – Summary of InVEST daytime valuation metrics, including energy savings in dollars and percent heavy and light work productivity loss, per model scenario. Numbers displayed show energy and work productivity loss/gains in comparison to the baseline 38% canopy cover scenario. For more detailed results, see Table F-4.

	Canopy Cover	Energy Savings (\$)	Light Work Loss (%)	Heavy Work Loss (%)
Current	22%	-74,067	-.1	+0.6
	44%	+34,050	-.1	-0.5
	Green 44%	+293,781	-.1	-5.7
SSP2 MID	22%	-77,300	+3.3	+0.7
	44%	+31,367	-0.7	-0.6
	Green 44%	+335,826	-5	-4.9
SSP2 END	22%	-77,358	+2.1	+0.4
	44%	+31,378	-1.4	-0.1
	Green 44%	+335,657	-18.6	-8.6
SSP5 MID	22%	-77,346	+3.1	+0.5
	44%	+31,376	-2.2	-0.2
	Green 44%	+335,695	-15.4	-7.4
SSP5 END	22%	-77,347	-.2	-.2
	44%	+31,376	-.2	-.2



	Canopy Cover	Energy Savings (\$)	Light Work Loss (%)	Heavy Work Loss (%)
	Green 44%	+335,689	- ²	- ²

¹ Productivity loss of 0% for all scenarios

² Productivity loss of 75% for all scenarios

3.2.2 Nighttime Temperatures

Figures 3-7 to 3-11 show nighttime air temperature distributions¹¹ across East Gwillimbury under current climate and future climate emissions scenarios. At the 38% baseline, spatially averaged nighttime air temperatures across all of East Gwillimbury were 15.5°C under current climate conditions. Under the SSP2-4.5 climate scenario, temperatures increased to 16.5°C (mid-century) and 17.3°C (end-century). Under the SSP5-8.5 scenario, temperatures increased to 17.0°C (mid-century) and 19.2°C (end-century) (Table F-5). When humidity was accounted for, wet bulb global temperatures across all of East Gwillimbury at 38% canopy cover were 17.2°C under current climate, 18.0°C (mid-century) and 18.7°C (end-century) under SSP2-4.5, and 18.4°C (mid-century) and 20.4°C (end-century) under SSP5-8.5 (Table F-5). “Tropical nights,” or nights where temperatures do not drop below 20°C, are associated with increased heat-related mortality (Seltenrich, 2023; Prairie Climate Centre, n.d.). Due to data limitations, our relative humidity values reflect average daytime humidity; however, relative humidity increases at night (Shu et al., 2022) so wet bulb temperatures may be higher than our modelling results suggest. Moreover, our nighttime temperature data reflects mean nighttime temperatures, not maximum temperatures. During heat waves, nighttime temperatures—and associated wet bulb global temperatures—would be higher than those described in this report. It is therefore likely that, during heat waves, “tropical nights” will be more common than our results suggest, with implications for human health and well-being.

Within urban areas, air temperatures were 0.09-0.24°C warmer compared to the East Gwillimbury average and wet bulb global temperatures were 0.06-0.17°C warmer, depending on canopy cover (Table F-5; F-6; F-7; F-8). This is a small difference in air temperature between urban and rural areas, especially when compared to the 1-3°C difference observed in our daytime simulation scenarios. Some studies report the urban heat island effect to be higher at night (see Chapman et al., 2018), while others report it to be lower (e.g., Shu et al., 2022; Peng et al., 2011). Our results suggest that, within East Gwillimbury, the urban heat island effect is not as pronounced at night. This may be due to the municipality’s relatively low building density, even under a full buildout. InVEST relies heavily on building intensity to calculate nighttime air temperatures (Natural Capital Project, n.d.). According to the Urban Cooling User Guide, building intensity is an important predictor of nighttime temperatures because heat stored in building surfaces is emitted at night (Natural Capital Project, n.d.). Moreover, street canyons trap heat, so urban areas with less defined street canyons (i.e., shorter buildings) may

¹¹ Note that our results show mean nighttime air temperatures, not maximum. During heat waves, nighttime air temperatures are likely to be several degrees higher than what is reported here.

trap less heat during the day, and therefore cool off more quickly at night (Coseo & Larsen, 2014; Loughner et al., 2012). Under our buildout scenario, the majority of East Gwillimbury's built infrastructure sits below three storeys. Thus, we would expect the intensity of the nighttime urban heat island effect to be reduced in a low-density, sprawling municipality like East Gwillimbury.

Several studies have suggested that building intensity has little to no effect on urban heat at night (Alhazmi et al., 2022; Ibsen et al., 2022; Coseo & Larsen, 2014), and that other factors such as tree cover, impervious surface cover, and/or surface albedo are more important predictors of nighttime air temperatures (Logan et al., 2020; Chapman et al., 2018; Coseo & Larsen, 2014; Peng et al., 2011). By not considering other urban heating factors (e.g., impervious surface cover, albedo) in its calculations, the model may have underestimated nighttime temperatures in urban areas (see [Limitations](#) section). It is therefore important to note that our results may not capture the full extent of the nighttime urban heat island within East Gwillimbury.

Across all climate scenarios, urban nighttime temperatures were 0.09-0.14°C cooler under the 38% baseline compared to the reduced 22% canopy cover scenario (Figure 3-7; 3-8; 3-9; 3-10; 3-11; Table F-6; F-7). An increase to 44% canopy cover produced 0.05-0.08°C cooling compared to the 38% baseline (Figure 3-7; 3-8; 3-9; 3-10; 3-11; Table F-6; F-7). Wet bulb global temperatures were 0.08-0.09°C cooler between the 38% and 22% scenarios, and 0.04-0.05°C cooler between the 44% and 38% scenarios (Appendix E; Table F-8). Overall, the cooling we observed was lower than the cooling ranges reported in the literature. Coseo and Larsen (2014) found that, for every 10% increase in Chicago tree canopy, nighttime temperature decreased by 0.2°C. Ibsen et al. (2022) reported 0.016°C cooling for every percent increase in canopy cover. According to their results, a reduction from 38% to 22% should produce close to 0.3°C warming, while an increase from 38% to 44% canopy cover should produce approximately 0.1°C cooling. Our results suggest that tree canopy cover has less of a cooling influence at night than it does during the day, which has been reported by other studies (e.g., Gillerot et al., 2024; Ibsen et al., 2022, Peng et al., 2011). However, given limitations and uncertainties around InVEST's calculations of nighttime temperatures (see [Limitations](#)), our results should be interpreted with caution. More research into factors influencing nighttime urban temperatures is necessary to better understand and model the urban heat island, especially given projected increases in tropical night frequency and its associated heat-related health risks (Seltenrich, 2023; Prairie Climate Centre, n.d.).

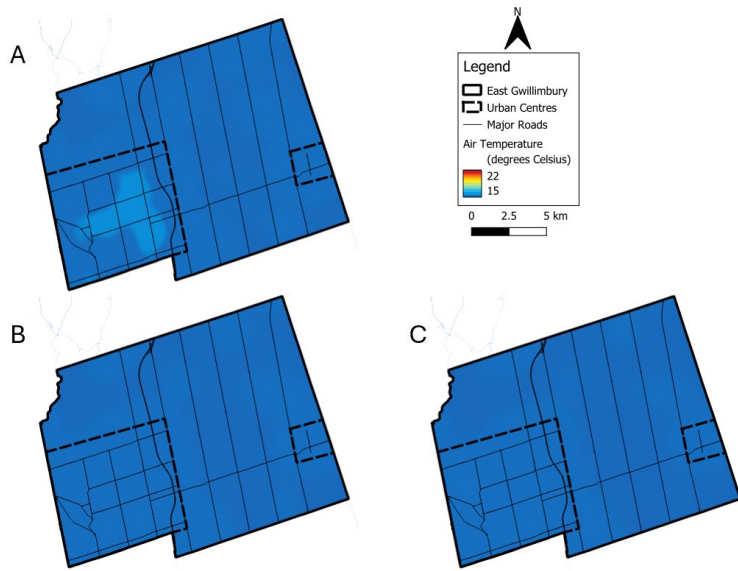


Figure 3-7 – Maps of East Gwillimbury showing estimated average nighttime July air temperature (°C) distribution under a full buildout scenario and current climate (2011-2020) conditions, and three canopy cover scenarios: (A) 22%, (B) 38%, and (C) 44%.

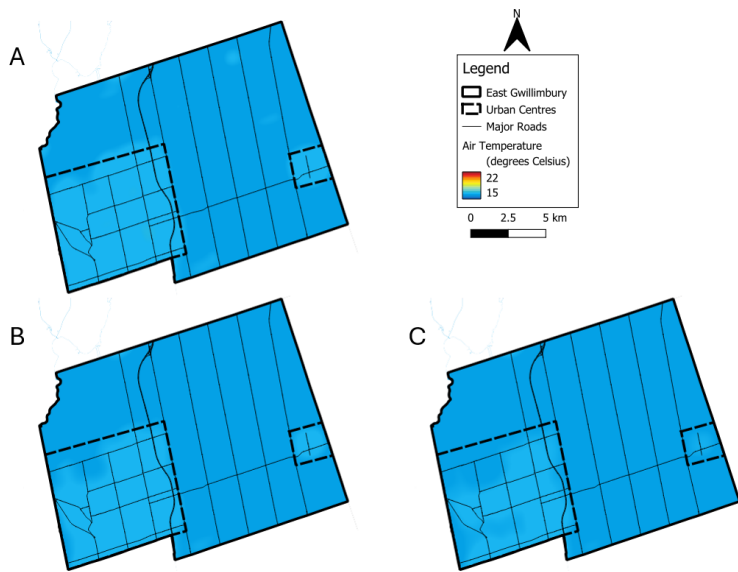


Figure 3-8 – Maps of East Gwillimbury showing estimated average nighttime July air temperature (°C) distribution by mid-century (2041-2070) under the SSP2-4.5 emissions pathway for three canopy cover scenarios: (A) 22%, (B) 38%, and (C) 44%.

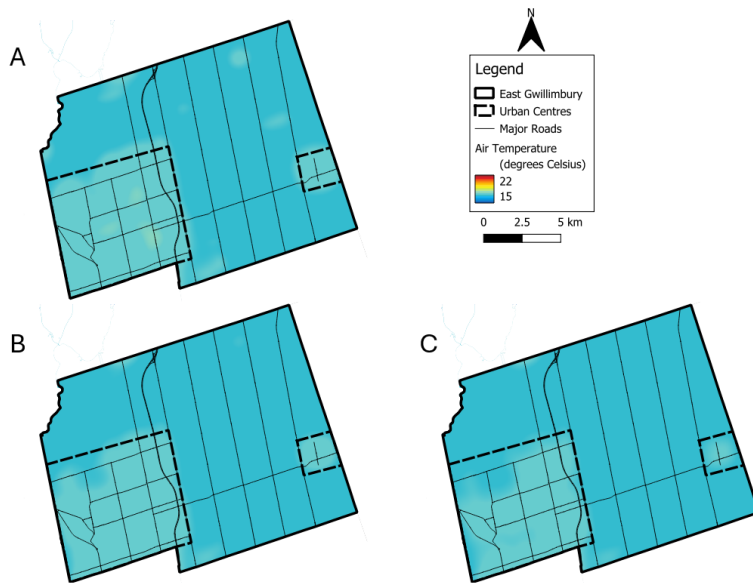


Figure 3-9 – Maps of East Gwillimbury showing estimated average nighttime July air temperature (°C) distribution by end-century (2071-2100) under the SSP2-4.5 emissions pathway for three canopy cover scenarios: (A) 22%, (B) 38%, and (C) 44%.

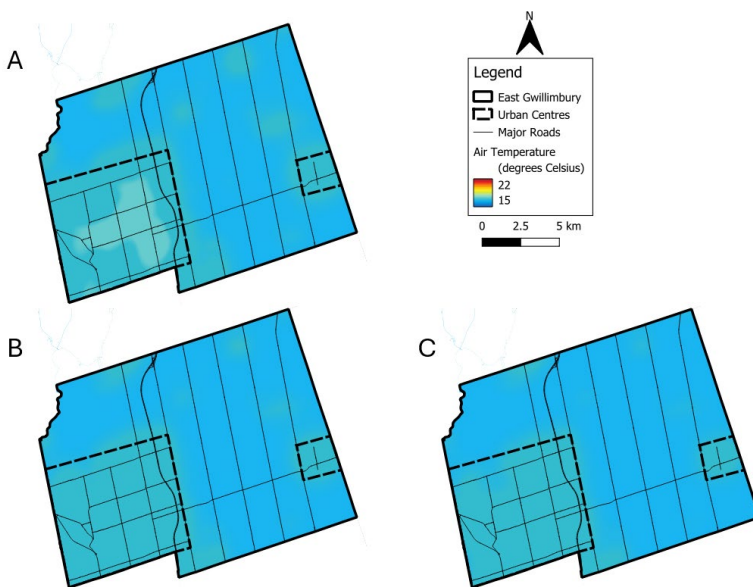


Figure 3-10 – Maps of East Gwillimbury showing estimated average nighttime July air temperature (°C) distribution by mid-century (2041-2070) under the SSP5-8.5 emissions pathway for three canopy cover scenarios: (A) 22%, (B) 38%, and (C) 44%.

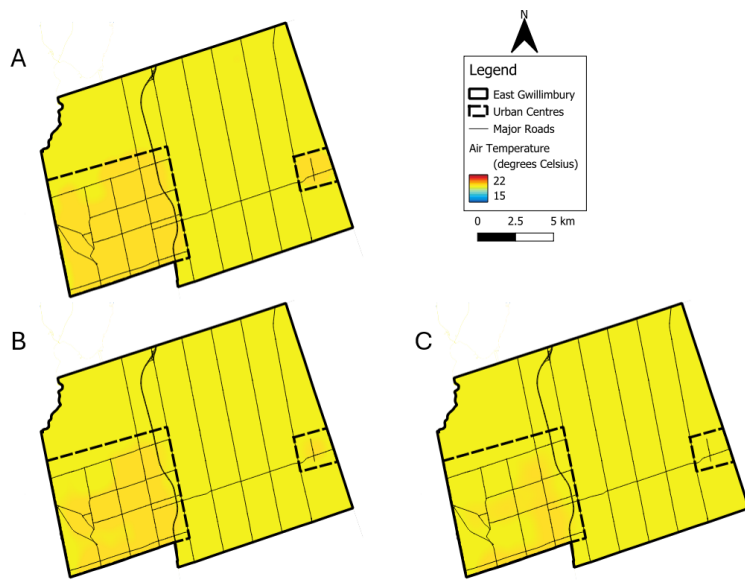


Figure 3-11 – Maps of East Gwillimbury showing estimated average nighttime July air temperature (°C) distribution by end-century (2071-2100) under the SSP5-8.5 emissions pathway for three canopy cover scenarios: (A) 22%, (B) 38%, and (C) 44%.

3.3. Study Limitations

All models are simplifications of real-world systems and thus have limitations. For a description of InVEST model limitations, refer to the [Limitations and Simplifications](#) section of the InVEST User Guide. The following are a list of model limitations that are not covered in the User Guide:

- Within the model documentation, there is some ambiguity over the definition of a “green area.” InVEST users must therefore create their own definition based on their understanding of natural systems, as well as their understanding of the literature. This introduces a degree of subjectivity into any study that uses InVEST Urban Cooling. An amendment to the User Guide that conclusively defines what a green area is may improve InVEST reliability.
- InVEST Urban Cooling uses urban intensity (defined as the ratio of building floor area to footprint area) modified by the cooling effect of nearby cooling islands (i.e., greenspaces larger than two hectares) to calculate nighttime air temperatures. It is possible that the model inaccurately calculates nighttime air temperatures by focusing solely on building intensity and neglecting other variables that affect nighttime heat (e.g., by ignoring potential nighttime heating factors such as albedo and impervious surface area, the model may minimize the intensity of the urban heat island at night; by restricting any measure of vegetative cooling to large cooling islands, the model may minimize the cooling effect of urban vegetation). Given the potentially strong influence of factors other than building intensity on nighttime heat (Alhazmi et al., 2022; Ibsen et al., 2022;

Logan et al., 2020; Chapman et al., 2018; Coseo & Larsen, 2014; Peng et al., 2011), model accuracy and overall utility may improve if additional parameters are added to nighttime temperature calculations.

Due to limitations in available data, we made some assumptions and simplifications that may have produced inaccuracies in model outputs. Some examples include:

- Our land use classes are grouped according to overall land function (i.e., residential lands, agricultural lands, etc.) rather than land cover type (i.e., tree, road, building) as we were better able to design a buildout scenario around the former. Our land use classes may therefore not fully capture future land cover (i.e., pervious and impervious surface cover) across East Gwillimbury.
- We assigned land use albedos based on the Local Climate Zone classes described in Stewart and Oke (2012). These classes, while descriptive, represent generalizations of land use classes that may not always be accurate to the specific context.
- In order to simulate future buildout, we created a new building footprint layer. This building footprint layer may not fully represent actual future conditions in East Gwillimbury given that it describes an urban layout that has yet to exist.
- When calculating K_c for our climate change scenarios, we used projected potential evapotranspiration increase rates for Eastern Canada based on trends observed over the 1979-2016 time period (Li et al., 2020b). Because we predicted future potential evapotranspiration amounts based on a 1979-2016 trendline, it is possible that we underestimated projected potential evapotranspiration increases for the SSP2-4.5 and SSP5-8.5 scenarios.
- To force the model to consider the cooling effect of urban forest cover in its nighttime air temperature calculations, we added urban tree “green area” pixels into our input data. The model then considered the cooling effects of urban trees by treating groups of treed pixels greater than two hectares as “cooling islands” (i.e., parks). While incorporating a degree of vegetative cooling into the model, this approach limits cooling to large (> 2 ha) groups of trees and does not explicitly account for the cumulative cooling effect of individual trees spread across urban areas. Model results therefore might not capture the full effect of tree cover on nighttime cooling.
- Due to a lack of up-to-date weather stations in our study area, we were unable to parameterize our inputs and validate our model outputs using actual temperature records.

Despite the limitations and simplifications described above, our results provide valuable information on the effects of cooling initiatives on urban heat island intensification under climate change. Moreover, this report is the first of its kind to use the InVEST Urban Cooling model to assess urban greening strategies under future development and climate scenarios. The methodology and results described in this report serve as a valuable tool for application of urban heat mitigation initiatives by municipalities, as well as future research into the urban heat island effect as a whole.

4.0 Conclusion

Urban climate models are a promising avenue for urban heat island research that provide place-based insight into temperatures and thermal comfort conditions within urban areas. These models allow users to compare and contrast the efficacy of various urban heat island mitigation techniques and, depending on the model, to project urban climate into the future under different climate emissions pathways. There are several urban heat models available to the public, each with their own advantages and limitations.

The results of our case study provide insight into projected summer warming within East Gwillimbury under climate change, as well as the spatial expansion of the urban heat island effect under planned development, and the efficacy of urban greening as an urban heat island mitigation approach. Overall, maximum July temperatures may increase to dangerous levels in the near future, with wet bulb global temperatures surpassing safe human thermal comfort levels by mid-century under both the SSP2-4.5 and SSP5-8.5 climate emissions scenarios. Nighttime temperatures are also expected to increase. Urban areas are an estimated 1-3°C warmer during the day, and 0.09-0.24°C warmer at night, which suggests a stronger urban heat island effect during the day. We observed 0.07-1.2°C of cooling with increased canopy cover during the day, and 0.05-0.14°C cooling at night, which suggests that urban greening has a greater cooling effect during the day. While our results point towards a small degree of overall cooling, there is still a benefit to the municipality and its residents through reduced human heat stress, particularly for outdoor workers, and decreased energy demands.

The urban heat island effect will intensify under climate change, and the results described in this report clearly outline the need for municipalities, especially rapidly growing ones, to take measures now to adapt their cities to the worst of climate change. While urban greening is a promising approach, the greatest cooling effect will result when urban vegetation is used in combination with other heat mitigation measures (e.g., using lighter-coloured building materials, increasing park size, etc.).

4.1. Future Research

Beyond what is covered in the scope of this report, InVEST can be used to explore the following urban heat island mitigation strategies¹²:

- The cooling effects of altered building practices. This can be done by increasing albedo values for developed land use classes to simulate building with lighter-coloured materials.

¹² Each of these strategies may be explored in combination, or separately. Additionally, it would be beneficial to explore the relative effects of these strategies (as well as increased urban forest cover) to each other



- Current and future savings with energy efficient building practices. This can be done by adjusting consumption rates for each building type.
- The cooling effects of increased and/or differently arranged urban greenspaces. This can be done by manually adding greenspace polygons and/or greenspace pixels to land use input maps.

InVEST outputs also offer unique opportunities for further urban heat island research, including:

- Using InVEST temperature, heat mitigation index, cooling capacity, and wet bulb global temperature maps to identify neighbourhoods with low heat resiliency. These neighbourhoods can then be targeted by municipalities for greening and other climate initiatives. Urban microclimate models are a useful tool to inform climate-smart planning in at-risk neighbourhoods.
- Overlaying InVEST temperature maps with socioeconomic and/or demographics maps to explore heat inequity in municipalities.
- Using InVEST temperature outputs to conduct a mortality analysis¹³ to assess lives saved from extreme heat by heat mitigation measures.

Glossary

Crop coefficient (K_c): An InVEST biophysical parameter. A value that describes the crop (vegetation) transpiration and soil evaporation of a given land use class (Allen et al., 1998). For non-vegetated land use classes, can be estimated based on the fraction of impervious surface area in each class.

Cooling capacity: An InVEST Urban Cooling output. An index valued on a scale of 0 to 1, that represents the capacity of each pixel to reduce air temperature, relative to all other pixels in the study area. For daytime simulations, cooling capacity is calculated using the evapotranspiration, albedo, and shade values assigned to each pixel. For nighttime simulations, cooling capacity is calculated using the building intensity value assigned to each pixel.

Green area: An InVEST biophysical parameter. In this report, defined as a natural land use class that is not subject to the urban heat island effect and/or an urban land use class with natural features that minimize the urban heat island.

Heat mitigation index: An InVEST Urban Cooling output. An index valued on a scale of 0 to 1, that represents the cooling capacity of each pixel, relative to all other pixels in the study area, when the cooling effects of nearby large (> 2 hectare) green spaces are taken into account.

¹³ For an example of a mortality analysis conducted using temperature outputs from i-Tree Cool Air, see Sinha et al. (2021).



Heat mitigation index is calculated by taking the distance-weighted average of the cooling capacity values of nearby large green spaces and the cooling capacity of the pixel of interest. If there are no nearby large green spaces, heat mitigation index is equal to the cooling capacity of the pixel of interest.

Shared Socioeconomic Pathways (SSPs): The most complex climate emissions scenarios created to date (Government of Canada, n.d.). An update to the previous Representative Concentration Pathways (RCPs) that accounts for socioeconomic factors influencing climate emissions and policy, including population and economic growth, urbanization, technological advancements, education, energy and land use change, global and regional conflicts, etc. (Government of Canada, n.d.).

Wet bulb global temperature: A measure of temperature as it affects humans, i.e., the “real-feel” temperature of a human standing in direct sunlight, taking air temperature, humidity, solar radiation, and air movement into account (National Weather Service, n.d.).



A. Appendix A: Urban Climate Model Summaries

Table A-1 – ENVI-met urban microclimate model summary.

Model	ENVI-met
Developer	ENVI-met GmbH
Year Developed / Last Updated	1998 / 2024
Description	Holistic urban microclimate model that simulates surface-plant-air interactions based on computational fluid dynamics and thermodynamics.
Access	Paid yearly license
Outputs	<p>Many outputs, grouped into the following categories:</p> <ul style="list-style-type: none"> • Atmosphere • Buildings • Pollutants • Radiation • Soil • Solar access • Surface • Vegetation
Inputs	<ul style="list-style-type: none"> • Air temperature, wind speed and direction, relative humidity • Latitude, longitude • Area input file with three-dimensional geometry • Project feature selection (pollutants, timesteps, soil, solar adjustment, etc.)
Methodology	<p>ENVI-met is a computational fluid dynamics model that provides detailed microclimate data using fluid dynamic equations to simulate heat and moisture fluxes. It captures surface-plant-air interactions by calculating short- and long-wave radiation fluxes with respect to shading, reflection, and re-radiation from vegetation (as well as buildings), as well as evapotranspiration and sensible heat flux from vegetation into the air. For more detailed methodological information, see the Model Architecture section of the ENVI-met technical documentation webpage.</p>



Model	ENVI-met
Advantages	<ul style="list-style-type: none"> • Most “complete” of the thermal comfort models, calculates radiation fluxes from shading, reflection, and re-radiation from surfaces (buildings and vegetation) • Accounts for evapotranspiration and sensible heat flux from vegetation • Allows for various material options (e.g., soils, building materials, etc.) and vegetation types (simple and three-dimensional) • Highly validated, widely used • User-friendly interface • Readily compatible with CAD/GIS • Able to simulate alternate land use scenarios (e.g., urban greening)
Limitations	<ul style="list-style-type: none"> • Paywall • Limited temporal and spatial resolution (1-10 s and 0.5-10 m, respectively), not applicable to large spatial and/or temporal scales • Computationally expensive, long run time • Requires careful/extensive calibration of parameters to avoid high model uncertainty • Potentially inaccurate measure of mean radiant temperature
Resources	<p>ENVI-met Technical Model Webpage</p> <p>ENVI-met Support Page</p>

Table A-2 – SOLWEIG urban microclimate model summary.

Model	SOLWEIG
Developer	Urban Climate Group, University of Gothenburg
Year Developed / Last Updated	2008 / 2022
Description	Radiation model that simulates spatial variation of three-dimensional radiation fluxes in six directions, as well as mean radiant temperature, in complex urban environments.
Access	Free
Outputs	<ul style="list-style-type: none"> • Mean radiant temperature (T_{mrt}) • Incoming and outgoing long-wave radiation • Incoming and outgoing short-wave radiation • Shadow patterns



Model	SOLWEIG
Inputs	<ul style="list-style-type: none">• Ground and building digital surface model• Vegetation digital surface models• Digital elevation model• Meteorological data: incoming shortwave radiation, diffuse and direct-beam shortwave radiation, air temperature, relative humidity• Environmental parameters: albedo and emissivity of ground and walls• Human exposure parameters
Methodology	<p>SOLWEIG calculates T_{mrt} using short- and long-wave radiation fluxes from six directions (upward, downward, four cardinal points). It first calculates mean radiant flux density as the sum of all short- and long-wave radiation in three dimensions, plus angular and absorption factors of an individual, which it uses to calculate T_{mrt} using the Stefan-Boltzmann law. Short-wave radiation fluxes are calculated using input data on direct, diffuse, and global radiation. Long-wave radiation fluxes are calculated using input data on air temperature and relative humidity. For more detailed methodological information, see Lindberg et al. (2008).</p>
Advantages	<ul style="list-style-type: none">• More accurately calculates mean radiant temperature compared to other thermal comfort models (e.g., RayMan, ENVI-met)• More appropriate for high elevation urban areas (see RayMan limitations, Table A-3)• User-friendly, available as a free QGIS plugin• Computationally inexpensive• Digital elevation model input improves model accuracy
Limitations	<ul style="list-style-type: none">• Does not account for wind velocity and turbulence• Does not account for surface-building-air and surface-plant-air interactions• Calculates fewer thermal indices than other thermal comfort models (e.g., RayMan)• Restricted to daytime radiation fluxes
Resources	SOLWEIG Model Introduction and User Manual



Table A-3 – RayMan urban microclimate model summary.

Model	RayMan
Developer	Chair for Environmental Meteorology, University of Freiburg
Year Developed / Last Updated	1999 / 2000
Description	Microscale bioclimate model that calculates radiation fluxes and human thermal comfort in urban environments taking complex structures (buildings, trees) into account.
Access	Free
Outputs	<ul style="list-style-type: none"> • Mean radiant temperature • Several thermal indices, including physiological equivalent temperature, standard effective temperature, universal thermal comfort index, perceived temperature, and predicted mean vote • Sunshine duration, sun path, and shadowing of obstacles
Inputs	<ul style="list-style-type: none"> • Date, time • Latitude and longitude, altitude • Air temperature, vapour pressure, wind speed, relative humidity • Biophysical data: weight, height, sex, age, clothing, activity • Geometry and position of obstacles
Methodology	RayMan is based on German VDI Guidelines 3789 and 3787, which describe short- and long-wave radiation and human biometeorology calculation methodology. The model calculates mean radiant temperature by simulating radiation flux densities, including diffuse solar radiation, reflected short-wave radiation, long-wave atmospheric radiation from the open sky, and long-wave radiation from solid surfaces. It then uses mean radiant temperature to assess other urban bioclimate and thermal indices. For more detailed methodological information, see Matzarakis et al. (2010).
Advantages	<ul style="list-style-type: none"> • Outputs include several variables related to human thermal comfort • User-friendly interface • Computationally inexpensive; short run time • Sky view factor can be estimated from fish-eye photographs, improving model accuracy



Model	RayMan
Limitations	<ul style="list-style-type: none"> • One-dimensional (all calculations performed for a single point in space) • Does not account for surface-building-air interactions • Plants are treated as obstacles that generate shade, so model does not account for interactive effects of vegetation on air temperature (e.g., evapotranspiration) • Ignores wind effects and turbulence flow • Limited application for high latitude and high-density urban areas • Restricted to daytime radiation fluxes • Accuracy of mean radiant temperature calculation depends on accuracy of wind speed input
Resources	<p>RayMan website</p> <p>RayMan Manual</p>

Table A-4 – Summary of i-Tree Cool Air model architecture, data input requirements, model outputs, and advantages and limitations.

Model	i-Tree Cool Air
Developer	Yang Yang, SUNY College of Environmental Science and Forestry (SUNY-ESF); Ted Endreny (SUNY-ESF); David J. Nowak, USDA Forest Service, Northern Research Station (USFS-NRS)
Year Developed / Last Updated	2019 / continuous (open source)
Description	Simulates the effects of land cover changes on water and energy budgets, and therefore air temperature.
Access	Free, open source
Outputs	<p>Many outputs, which can be specific to blocks (groups of cells), cells, and specific timesteps during the simulation period.</p> <ul style="list-style-type: none"> • Default: temperature, humidity, water budget and runoff (from i-Tree Hydro) • Extended: time series latent and sensible heat fluxes, net radiation, heat storage



Model	i-Tree Cool Air
Inputs	<ul style="list-style-type: none">• Land use layer (raster)• Digital elevation model (raster)• Tree canopy percent cover (raster)• Impervious surface percent cover (raster)• Time series record of meteorological measurements from a reference weather station, including:<ul style="list-style-type: none">○ Hourly air temperature○ Dew point temperature○ Wind speed○ Precipitation
Methodology	<p>i-Tree Cool Air uses the PASATH (Physically-based Analytical Spatial Air Temperature and Humidity) model developed by Yang et al. (2013), which is a land surface model that predicts heat using water balance equations from i-Tree Hydro, plus energy balance equations that balance short- and long-wave radiation with land surface latent and sensible heat emissions modulated by surface and atmospheric resistances. The model captures the heat trapping effects of buildings by their albedos. For more detailed methodological information, see Yang et al. (2013).</p>
Advantages	<ul style="list-style-type: none">• Specifically designed to simulate the urban heat island effect, including both daytime and nighttime temperature modelling• Wide range of spatial resolutions possible (10-300 m range considered “best”)• High degree of accuracy• Quick run time• Designed to be used alongside GIS for quick and effective visualization of outputs• Parameters are standardized, so do not need to be calibrated to a given location



Model	i-Tree Cool Air
Limitations	<ul style="list-style-type: none"> • Output quality and resolution largely dependent on availability of input data • Parameters and land classes based off the United States National Land Cover Database (NLCD) scheme, so land use data from outside the United States requires conversion to NCLD • Anthropogenic emissions and building materials not accounted for • Requires detailed weather input data that may not be applicable to all study areas • Limited free technical support available • Unable to simulate future climate
Resources	<p>i-Tree Research Suite webpage</p> <p>i-Tree HydroPlus Technical Manual</p>

Table A-5 – Summary of InVEST Urban Cooling model architecture, data input requirements, model outputs, and advantages and limitations.

Model	InVEST Urban Cooling
Developer	The Natural Capital Project, Stanford University
Year Developed / Last Updated	2020 / 2024
Description	Calculates daytime and nighttime air temperature as well as a heat mitigation index based on either (a) shade, evapotranspiration, albedo, and distance from cooling islands (daytime), or (b) building intensity (nighttime).
Access	Free
Outputs	<ul style="list-style-type: none"> • A copy of the input study area vector showing average air temperature, temperature anomaly, and cooling capacity, and (optionally) avoided energy consumption, average wet bulb global temperature, and light and heavy work productivity loss • Raster maps showing distribution of cooling capacity, estimated air temperature, actual evapotranspiration, wet bulb global temperature (optional) • Optionally: a copy of the input building footprint vector with energy savings values and average air temperature within buildings



Model	InVEST Urban Cooling
Inputs	<ul style="list-style-type: none"> • Land use layer (raster) with a .csv biophysical data containing the following information for each land use class: <ul style="list-style-type: none"> ○ Crop coefficient ○ Green area classification ○ Shade ○ Albedo ○ <u>Optional</u>: building intensity • Evapotranspiration layer (raster) • Study area (vector) • <u>Optional</u>: building footprints layer (vector) with a .csv table containing the energy consumption data for each building type • Maximum cooling distance (m) • Reference air temperature (°C) • Urban heat island effect (°C) • Air blending distance (m) • <u>Optional</u>: average relative humidity (%) over the time period of interest
Methodology	<p>The InVEST Urban Cooling model calculates two unique indices, cooling capacity and a heat mitigation index, for each pixel. For daytime simulations, cooling capacity is calculated as a function of shade, evapotranspiration, and albedo. For nighttime simulations, cooling capacity is calculated based on building density, which is highly correlated to heat storage capacity. Heat mitigation index is calculated by taking the distance-weighted average of the cooling capacity values of nearby large green spaces and the cooling capacity of the pixel of interest. If there are no nearby large green spaces, heat mitigation index is equal to the cooling capacity of the pixel of interest. InVEST then calculates air temperature prior to mixing (T_{nomix}) for each pixel using the user-provided rural reference temperature and urban heat island effect values, as well as model-calculated heat mitigation index. Actual air temperature (T_{air}) (i.e., air temperature once air mixing/atmospheric turbulence is accounted for) is estimated from T_{nomix} using a Gaussian function with a user-defined kernel radius. For more detailed methodological information, see the InVEST Urban Cooling User Guide.</p>



Model	InVEST Urban Cooling
Advantages	<ul style="list-style-type: none">• Able to simulate both daytime and nighttime air temperatures• Free online technical support, including a descriptive User Guide and an active online support community moderated by InVEST experts• No requirements for land cover classes—model accepts user-defined land use and infrastructure classes/parameters• Computes unique indices (i.e., cooling capacity and heat mitigation index) that provide insight into urban heat resiliency• Quick run time• Designed to be used alongside GIS for quick and effective visualization of outputs• Calculates building-related statistics (i.e., energy savings, indoor air temperature) as well as outdoor temperature metrics
Limitations	<ul style="list-style-type: none">• Like i-Tree Cool Air, output quality and resolution largely dependent on availability of land cover data• Potentially less accurate than i-Tree Cool Air; cooling capacity and air temperature calculations may require further validation• May underestimate daytime air temperatures (Hamel et al., 2023)
Resources	<p>InVEST Urban Cooling webpage</p> <p>InVEST Urban Cooling User Guide</p>

B. Appendix B: i-Tree Cool Air and InVEST Urban Cooling Literature Review

Table B-1 – Summary of i-Tree Cool Air and InVEST Urban Cooling literature.

	Authors	Study area	Major findings
i-Tree Cool Air	Pace et al. (2023)	Naples, Italy	<ul style="list-style-type: none"> • Strong correlations between modelled and observed temperatures • During warm months, forested land covers were 5°C cooler than land covers with a large proportion of impervious surface • A 10% increase or decrease in tree cover produced 0.2°C cooling or warming, respectively • Cooling limited by soil moisture, with greater cooling during wetter seasons compared to dry seasons
	Semenzato and Bortolini (2023)	Padova, Italy	<ul style="list-style-type: none"> • On a hot July day, daytime temperature differences of up to 10°C between forested land covers and open land covers with a large proportion of impervious surface • Trees have a greater cooling effect during the day
	Sinha et al. (2022)	10 U.S. cities	<ul style="list-style-type: none"> • Increasing tree cover by 10% significantly reduced heat-related mortality, with reductions varying across cities • Hot and dry cities (e.g., Phoenix) experienced the greatest benefits from tree cover increases • In cooler cities (e.g., Minneapolis), tree cover increases can help to mitigate the effects of heat waves
	Sinha et al. (2021)	Baltimore City, USA	<ul style="list-style-type: none"> • Increasing tree cover reduces annual mortality, particularly in older adults • Greatest air temperature reductions due to increased tree cover occurred in downtown Baltimore (high impervious surface cover) • Greatest mortality reductions occurred in the outskirts of Baltimore (large population of older adults)
	Nyelele et al. (2019)	The Bronx, New York City, USA	<ul style="list-style-type: none"> • 2-5% increases in tree cover had minimal effects on air temperature, with no associated reductions in heat-related mortality



	Authors	Study area	Major findings
InVEST Urban Cooling	Hamel et al. (2023)	Paris, France, and Twin Cities, USA	<ul style="list-style-type: none"> • High model performance for nighttime temperatures, medium to low performance for daytime temperatures • 50% vegetation cover resulted in less than 1°C cooling
	Hu et al. (2023)	Wuhan, China	<ul style="list-style-type: none"> • Blue and green spaces both contribute to urban heat mitigation, but in different ways • Moderate correlation between InVEST estimates and daytime surface temperatures
	Keyes et al. (2022)	Milwaukee, USA	<ul style="list-style-type: none"> • Increasing canopy cover to 40% produced the greatest change in both HMI and air temperature • Urban heat and vulnerability are unequally distributed across Milwaukee, with residents' health, race, and income emerging as key factors
	Bosch et al. (2021a)	Lausanne, Switzerland	<ul style="list-style-type: none"> • InVEST outperforms air temperature estimates based on spatial regression of satellite data • Model calibration improves InVEST performance
	Bosch et al. (2021b)	Lausanne, Switzerland	<ul style="list-style-type: none"> • Tree canopy increases can result in up to 2°C nighttime cooling, with the most cooling seen in the most urbanized areas • Scattered tree canopy configurations might produce more cooling compared to clustered configurations
	Zawadska et al. (2021)	3 towns in England	<ul style="list-style-type: none"> • Moderate correlation between InVEST heat mitigation index values and daytime land surface temperature data • A heat mitigation index change of 0.1 was associated with 0.76°C change in daytime surface temperature
	Ronchi et al. (2020)	Milan, Italy	<ul style="list-style-type: none"> • Permeable surface area, built-up footprint, and canopy cover had the greatest influence on cooling capacity

C. Appendix C: Detailed InVEST Methodology

Land Use/Land Cover Input Data

All land use/land cover data processing was conducted in QGIS 3.36.3. The Lake Simcoe Region Conservation Authority has detailed land use/land cover vector layers for the watershed, the most recent of which is based on 2018 orthoimagery (LSRCA, 2022). This 2018 layer contains information on natural heritage land cover classes (Table D-1), as well as urban land cover classes (Table D-2). For input into the InVEST model, the Lake Simcoe land cover classification scheme was simplified¹⁴ into the following 14 land use classes:

- Water
- Coniferous Forest
- Deciduous Forest
- Mixed Forest
- Woody Wetland
- Open Wetland
- Grassland
- Shrub/Scrub
- Barren Land
- Intensive Agriculture
- Non-Intensive Agriculture
- Urban Greenspace
- Developed, Low Intensity
- Developed, High Intensity

To create a land use layer representing a full buildout in East Gwillimbury, we acquired a development plan layer from the municipality¹⁵. This layer describes all current and future proposed development plans within East Gwillimbury and assigns each development polygon a land cover type (Table D-6). The East Gwillimbury land cover types were reclassified (Table D-6) into the new schema described above and each development polygon was assigned a new land use class. The East Gwillimbury development layer was merged with the Lake Simcoe 2018 land cover layer (LSRCA, 2022) to create a buildout land use layer. By now, we had two land use maps, one representing land use in East Gwillimbury as of 2018, and the other representing a future, fully developed East Gwillimbury. Both maps were rasterized for input into InVEST.

¹⁴ This simplification process is described in Appendix D.

¹⁵ For publicly available data on development applications within East Gwillimbury, see the municipality's [interactive active applications map](#).

InVEST requires a biophysical table that links biophysical parameters to each land use class. To find shade values for our land use classes under our three canopy scenarios, we used 2019 York Region land cover data (Timmins & Sawka, 2022) to determine percent impervious surface and tree canopy cover for our 14 land use classes. We then used Lake Simcoe Region Conservation Authority (LSRCA, 2016) and Toronto and Region Conservation Authority (Timmins & Sawka, 2022) documents describing the amount of impervious and pervious land cover in each land use class that is available for tree planting to inform canopy changes for our 22% and 44% canopy cover scenarios. These changes are summarized in Table C-1.

Table C-1 – Tree canopy percent cover per land use class under three canopy cover scenarios. The Green 44% canopy cover scenario is not included as its values are identical to the 44% scenario. Bolded values represent actual canopy cover conditions in East Gwillimbury as of 2018.

Land Use Class	22% Canopy	38% Canopy	44% Canopy
Water	6%	6%	6%
Coniferous Forest	70%	94%	94%
Deciduous Forest	70%	94%	94%
Mixed Forest	70%	97%	97%
Woody Wetland	60%	87%	87%
Open Wetland	10%	18%	18%
Grassland	0%	20%	30%
Shrub/Scrub	0%	47%	50%
Barren Land	0%	6%	30%
Intensive Agriculture	4%	4%	5%
Non-Intensive Agriculture	5%	14%	15%
Urban Greenspace	10%	18%	30%
Developed, Low Intensity	0%	28%	40%
Developed, High Intensity	0%	6%	20%
TOTAL	21.7%	38.5%¹	44.0%

¹ This value is influenced by rounding. Without rounding, total canopy cover is equal to 38.1%.

For the 44% canopy cover scenario, we limited most canopy increases to developed land use classes (i.e., Urban Greenspace, Developed Low Intensity, and Developed High Intensity) to emulate urban greening. We also increased canopy cover on Grassland and Barren Land, as these land use classes offer opportunities for reforestation. For our canopy cover decreases, we dramatically reduced canopy cover on the developed land use classes and several natural land

use classes to create a “worst case scenario,” wherein canopy cover in urban areas is restricted to urban parks, reforestation initiatives are minimal, and continued urban development in natural areas reduces canopy cover further. We limited canopy cover increases on agricultural lands as this would reduce farmable land area and may create conflict with farm owners. However, we did decrease Non-Intensive Agriculture canopy cover under the 22% canopy scenario to represent increased rural development and/or a shift to more intensive agriculture across the municipality to meet increased consumption demands with projected population increases.

InVEST requires the user to classify each land use class as a green area or not. When a land use class is classified as a green area, the model adds an additional cooling effect to the pixels of that land use class and incorporates that cooling into its calculation of heat mitigation index and, through that, its calculation of air temperature¹⁶. Under the 38% cover scenario, we assigned all natural land use classes as green area except for Barren Land (Table C-2). Under the 22% canopy scenario, Grassland and Shrub/Scrub were also declassified as green areas due to a complete reduction in canopy cover (Table C-2). Under the 44% scenario, all land use classes except the developed classes were classified as green areas due to canopy cover increases representing naturalization efforts (Table C-2). Across all scenarios, Water was listed as a green area (Table C-2) as it has been shown to have a cooling effect (Hu et al., 2023; Peng et al., 2020; Hathway & Sharples, 2012), and in some cases may exert stronger cooling compared to other natural land covers such as woodlands and grasslands (Zhou et al., 2019).

The Developed, Low Intensity land use class reaches 40% canopy cover under the 44% scenario (Table C-1), which partly influenced our decision to create the Green 44% scenario, wherein Developed, Low Intensity is marked as a green area (Table C-2). Many municipalities worldwide have set 40% tree canopy cover targets in an effort to combat the urban heat island effect (Metro Vancouver, 2024). Several studies have suggested that at or around 40% cover is the threshold at which urban cooling is maximized (Wang et al., 2023; Zhao et al., 2017; Adams & Smith, 2014). Research by Ziter et al. (2019) suggests that, at and above 40% canopy cover, the urban heat island effect is essentially eliminated. In other words, the urban forest, at this threshold, emulates a natural forest. We created the Green 44% scenario to simulate this “40% threshold effect” on air temperatures within East Gwillimbury.

Table C-2 – Green area classification per land use class under four canopy cover scenarios. Land use classes are given a “0” if they are not considered a green area and a “1” if they are. Bolded column represents actual 2018 conditions in East Gwillimbury.

Land Use Class	22% Canopy	38% Canopy	44% Canopy	Green 44% Canopy
Water	1	1	1	1
Coniferous Forest	1	1	1	1

¹⁶ For a more in-depth description of the effect of green area classifications on InVEST model outputs, see the Materials and Methods section of Hu et al. (2023).



Land Use Class	22% Canopy	38% Canopy	44% Canopy	Green 44% Canopy
Deciduous Forest	1	1	1	1
Mixed Forest	1	1	1	1
Woody Wetland	1	1	1	1
Open Wetland	1	1	1	1
Grassland	0	1	1	1
Shrub/Scrub	0	1	1	1
Barren Land	0	1	1	1
Intensive Agriculture	1	1	1	1
Non-Intensive Agriculture	1	1	1	1
Urban Greenspace	1	1	1	1
Developed, Low Intensity	0	0	0	1
Developed, High Intensity	0	0	0	0

To assign albedo values to each of our land use classes, we consulted Stewart and Oke (2012), which is a resource recommended by the InVEST team. Stewart and Oke (2012) present a list of albedo values for different land use/land cover types, which they call Local Climate Zones. They describe the characteristics of each Local Climate Zone, including building surface, impervious surface, and pervious surface fractions for each. They then provide a list of surface albedo values for each (Stewart & Oke, 2012). Based on our prior calculations of building, tree, and impervious surface cover percentages, we assigned a Local Climate Zone, or a combination of them, to each of our land use classes. For the different development and canopy scenarios, we adjusted our cover percentages and reclassified each land use class to different Local Climate Zones, if necessary. Stewart and Oke (2012) provide a range of albedo values for each Local Climate Zone, so we took the midpoint of that range (or the average midpoint for those land use classes assigned to multiple Local Climate Zones) as the albedo for each land use class. Final albedo values are summarized in Table C-3.

Table C-3 – Albedo values per land use class under three canopy cover scenarios. The Green 44% canopy cover scenario is not included as its values are identical to the 44% scenario. Bolded column represents actual 2018 conditions in East Gwillimbury.

Land Use Class	22% Canopy	38% Canopy	44% Canopy
Water	0.05	0.05	0.05
Coniferous Forest	0.15	0.15	0.15
Deciduous Forest	0.15	0.15	0.15
Mixed Forest	0.15	0.15	0.15
Woody Wetland	0.10	0.10	0.10
Open Wetland	0.14	0.14	0.14



Land Use Class	22% Canopy	38% Canopy	44% Canopy
Grassland	0.20	0.20	0.20
Shrub/Scrub	0.23	0.22	0.18
Barren Land	0.25	0.25	0.23
Intensive Agriculture	0.20	0.20	0.20
Non-Intensive Agriculture	0.20	0.20	0.20
Urban Greenspace	0.20	0.20	0.23
Developed, Low Intensity	0.15	0.19	0.20
Developed, High Intensity	0.20	0.20	0.20

To find evapotranspiration coefficients (K_c) for each land use class, the Natural Capital Project provides a K_c Calculator¹⁷. However, if the evapotranspiration input represents actual evapotranspiration (rather than potential evapotranspiration), all K_c values can be set to one. For our current climate InVEST scenarios, we used the Lake Simcoe Region Conservation Authority’s 55-year average July evapotranspiration map (Earthfx, 2010) as input and set all land use K_c values to one. For our future climate scenarios, we used the Natural Capital Project’s K_c Calculator. This calculator requires average monthly potential evapotranspiration values. For up-to-date monthly values, we used average 1979-2016 potential evapotranspiration for the Mixedwood Plains ecozone, found in Li et al. (2020b). We then consulted the literature for projected changes in potential evapotranspiration with climate change. Current projections report an increase in potential evapotranspiration for Eastern Canada, at 1-4 mm per year (Li et al., 2020b), with greater increase rates seen by end-century (2071-2100) (Hassanzadeh et al., 2022). Tam et al. (2023) calculated average potential evapotranspiration increases across Canada under SSP5-8.5 for 2081-2100 from a 1950-2014 baseline and found that 54% of the increase occurred in summer, 28% in spring, 14% in fall, and 4% in winter. Based on the literature, we determined future annual potential evapotranspiration values for our study area by increasing annual potential evapotranspiration values, found by adding together the monthly values from Li et al. (2020b), by 2 mm/year from 2016 to 2070 and 4 mm/year from 2071-2100. We then took the average annual potential evapotranspiration increase for the 2041-2070 period, as well as the 2071-2100 period, and distributed those annual increases across seasons using the seasonal proportions described in Tam et al. (2023). To find monthly future potential evapotranspiration, we multiplied our seasonal increases by the proportion of potential evapotranspiration occurring in each month in Li et al. (2020b). Due to local data availability limitations, we used these monthly potential

¹⁷ Downloadable from the [InVEST Downloads, User Guides, and Data Sources webpage](#).

evapotranspiration values, and the resultant K_c outputs from the K_c Calculator, for all our climate scenarios (i.e., both SSP2-4.5 and SSP5-8.5).

The Natural Capital Project's K_c Calculator also requires monthly K_c coefficients for different vegetation types. We used the K_c values described in Allen et al. (1998), which the InVEST User Guide recommends. For our Intensive Agriculture land use class, we averaged final K_c values for corn, alfalfa, and soy, as these are the three major crops in East Gwillimbury, representing approximately 70% of all croplands¹⁸. For the Water land use class, we averaged Allen et al. (1998) guidelines for shallow (< 2 m in depth) and deep (> 5 m in depth) open water and input that average into the K_c Calculator. For the Urban Greenspace land use class, we averaged the calculated (i.e., output from the K_c Calculator) K_c values for "Grassland" and "Forest." For Woody Wetlands, we averaged calculated K_c for "Wetlands" and "Forest." Following the methodology of Hamel et al. (2023), we applied the calculated "Forest" K_c to all forest land use classes (i.e., Coniferous, Deciduous, Mixed Forest), applied the "Grassland" K_c to our Grassland and Non-Intensive Agriculture land use classes, averaged "Grassland" and "Forest" K_c for our Shrub/Scrub land use class, and used the Calculator default (0.5) for Barren Land.

To find K_c for non-natural land use classes under our buildout climate scenarios, we used the following equation, which is recommended by InVEST: $K_c = f*0.1 + (1-f)*0.6$, where f is the fraction of impervious cover for that land use class. To find percent cover of impervious surface area at 38% canopy for our Developed, Low Intensity and Developed, High Intensity land use classes, we created two new polygons in QGIS: one covering a typical residential neighbourhood in East Gwillimbury in 2018, and another covering a typical industrial/commercial area. We used the 2018 York Region land cover raster map (Timmins & Sawka, 2022) to get the average impervious surface cover (excluding buildings) for residential (Developed, Low Intensity) and commercial/industrial (Developed, High Intensity) areas. We added those values to the building cover values in Table C-5 to find total impervious surface cover for the Developed, Low Intensity and Developed, High Intensity land use classes under the full buildout scenario. We then used Lake Simcoe Region Conservation Authority and Toronto and Region Conservation Authority documents (Timmins & Sawka, 2022; LSRCA, 2016) describing the amount of impervious and pervious land cover in each land use class that is available for tree planting to inform impervious surface area changes for our 22% and 44% canopy cover scenarios. Final K_c values for each land use class under different canopy cover scenarios are shown in Table C-4.

¹⁸ We used Ontario agricultural profile data for York Region (found [here](#)) to determine dominant crops in East Gwillimbury. We averaged crop amounts across all recorded years (2006, 2011, 2016, 2021) to account for crop rotations and temporal demand fluctuations.



Table C-4 – Crop coefficient (K_c) values per land use class under three canopy cover scenarios. The Green 44% canopy cover scenario is not included as its values are identical to the 44% scenario. Bolded column represents actual 2018 conditions in East Gwillimbury.

Land Use Class	22% Canopy	38% Canopy	44% Canopy
Water	0.181	0.181	0.181
Coniferous Forest	1.002	1.002	1.002
Deciduous Forest	1.002	1.002	1.002
Mixed Forest	1.002	1.002	1.002
Woody Wetland	0.922	0.922	0.922
Open Wetland	0.842	0.842	0.842
Grassland	0.929	0.929	0.929
Shrub/Scrub	0.965	0.965	0.965
Barren Land	0.444	0.472	0.522
Intensive Agriculture	0.719	0.719	0.719
Non-Intensive Agriculture	0.929	0.929	0.929
Urban Greenspace	0.965	0.965	0.965
Developed, Low Intensity	0.2252	0.3652	0.3852
Developed, High Intensity	0.2095	0.2395	0.2895

Nighttime Temperature Modelling

InVEST uses the building intensity biophysical parameter assigned to each land use class to simulate nighttime temperatures. To find building intensity values for our land use classes in 2018, we used a Lake Simcoe Region Conservation Authority building footprint layer that maps out all buildings found within the watershed based on 2018 orthoimagery. We used QGIS to calculate area in m² of each building polygon, then summed the total building cover for each land use class and divided that by total land use class area to get percent building cover. To determine percent building cover after a full buildout, we created a new building footprint layer. We first examined Google Satellite imagery and added footprint polygons to the existing Lake Simcoe building footprint layer to account for all buildings that had been constructed since 2018 (i.e., since our last building inventory). We then used the East Gwillimbury development layer (described above) to create additional building polygons. Within each development polygon, where building footprints did not already exist, we added new building footprint polygons, being careful to match the size, shape, and layout of existing infrastructure that matched the land use type described by the Town of East Gwillimbury in their layer (e.g., for a development polygon described by the Town as residential, we added building footprints that

mimicked existing residential subdivisions in East Gwillimbury). Our reasoning here was that new residential subdivisions and commercial/industrial enterprises would be built similarly to existing builds. Once we had created our new buildout footprint layer, we used QGIS to calculate the percent cover of buildings within each of our land use classes in our buildout land use layer (Table C-5).

Table C-5 – Percent building cover per land use class under two East Gwillimbury development scenarios: 2018 and full buildout (projected development density given all current and future development plans). All percentages less than or equal to 0.1% are rounded down to 0%.

Land Use Class	2018	Buildout
Water	0%	0%
Coniferous Forest	0%	0%
Deciduous Forest	0%	0%
Mixed Forest	0%	0%
Woody Wetland	0%	0%
Open Wetland	0%	0%
Grassland	0%	0%
Shrub/Scrub	0%	0%
Barren Land	0%	0%
Intensive Agriculture	0%	0%
Non-Intensive Agriculture	0.2%	0.2%
Urban Greenspace	0.4%	0.5%
Developed, Low Intensity	4%	12%
Developed, High Intensity	2%	8%

According to the InVEST User Guide and additional instructions on the Natural Capital Project’s online forum, building intensity can be calculated by multiplying the average number of floors for buildings of each land use by the average footprint area (i.e., building percent cover, Table C-5) to get the approximate building floor area for each land use class, and then dividing that number by the overall land area for each land use class. InVEST requires all building intensity

values to be normalized between 0 and 1. To do this, we used the formula $x_{norm} = \frac{x - Min}{Max - Min}$, where x is the value to be normalized, Min is the smallest of all the values to be normalized, and Max is the largest of all the values to be normalized. Building intensity values are summarized in Table C-6.

Table C-6– Building intensity per land use class under two East Gwillimbury development scenarios: 2018 and full buildout (projected development density given all current and future development plans). All values are normalized between 0 and 1.

Land Use Class	2018	Buildout
Water	0	0
Coniferous Forest	0.0002	0
Deciduous Forest	0	0
Mixed Forest	0.0007	0.0003
Woody Wetland	0.0011	0
Open Wetland	0	0
Grassland	0.0007	0.0006
Shrub/Scrub	0.0004	0.0001
Barren Land	0	0
Intensive Agriculture	0.0202	0.0067
Non-Intensive Agriculture	0.0575	0.0188
Urban Greenspace	0.0717	0.0251
Developed, Low Intensity	1	1
Developed, High Intensity	0.2717	0.4404

Because InVEST uses building intensity values to predict nighttime temperatures, all other biophysical parameters, including shade (i.e., tree canopy cover) are not accounted for. The model only includes the cooling effect of nearby “green areas.” To incorporate the impact of tree canopy into our nighttime simulations, we added a new land use class—Urban Tree—to our input land use raster maps. We used QGIS to randomly select a specific percentage of pixels of the three urban land use classes—Urban Greenspace, Developed, Low Intensity, and Developed, High Intensity—that corresponded to the canopy changes described in Table C-4, and converted those pixels to the new Urban Tree class. We then assigned these pixels as “green area” so the cooling effect of vegetation could be incorporated into nighttime modelling.

Climate Input Data

For our current climate scenarios, we used the Lake Simcoe Region Conservation Authority’s 55-year average evapotranspiration raster layer for the month of July (Earthfx, 2010). Bosch et al. (2021b) suggest altering the rural reference temperature and urban heat island effect inputs to simulate climate scenarios in InVEST. However, on top of changing these values, it is



important to also change evapotranspiration input data to reflect predicted global changes in evapotranspiration rates with climate change (Tam et al., 2023; Pan et al., 2014). We used ClimateNA v7.50 (Mahony et al., 2022; Wang et al., 2016a) to generate July reference evapotranspiration raster maps for the following climate emissions scenarios¹⁹ and timesteps:

- SSP2-4.5, mid-century (2041-2070)
- SSP2-4.5, end-century (2071-2100)
- SSP5-8.5, mid-century (2041-2070)
- SSP5-8.5, end-century (2071-2100)

InVEST requires a reference air temperature for a nearby rural area where the urban heat island effect is not observed. We used Google Maps to randomly select three rural points around East Gwillimbury. We then used ClimateNA to gather historical (2011-2020) average maximum (daytime) and minimum (nighttime) July temperature data for these coordinates, as well as future projected temperatures under the SSP2-4.5 and SSP5-8.5 emissions scenarios. For current temperatures, we chose to extract data for the 2011-2020 period to better simulate heat waves as the ten warmest years have occurred in the past decade (2014-2023) (NOAA, 2024). To generate point data, ClimateNA requires elevation information for each set of coordinates. We used the [Ontario Provincial Digital Elevation Model](#) to acquire elevation in metres for each point. Geographical and weather data for the three reference points is described in Table C-7 (daytime) and Table C-8 (nighttime). We took the average temperature of all three points for input into InVEST.

Table C-7 – Maximum July air temperature (°C) values for three rural reference points around East Gwillimbury over five climate periods: current (2011-2020), SSP2-4.5 mid-century (2041-2070) and end-century (2071-2100), and SSP5-8.5 mid-century and end-century. Average air temperature for each climate period (bold) is the rural reference air temperature input into InVEST. Coordinates (decimal degrees) and elevation (metres) for the three rural reference points is also provided.

Coordinates	Elevation	Current	SSP2-4.5, Mid-Century	SSP2-4.5, End-Century	SSP5-8.5, Mid-Century	SSP5-8.5, End-Century
44.21206, -79.3525	230	27.0	28.8	29.5	29.4	31.9
44.05993, -79.3185	316	26.8	28.6	29.3	29.2	31.6
44.13123, -79.5311	219	27.3	29.0	29.7	29.6	32.1

¹⁹ We used the 8-model ensemble mean available on ClimateNA. For more information on the general circulation models used by ClimateNA to generate climate emissions projections, see [this report](#).



Coordinates	Elevation	Current	SSP2-4.5, Mid-Century	SSP2-4.5, End-Century	SSP5-8.5, Mid-Century	SSP5-8.5, End-Century
AVERAGE		27.0	28.8	29.5	29.4	31.9

Table C-8 – Minimum July air temperature (°C) values for three rural reference points around East Gwillimbury over five climate periods: current (2011-2020), SSP2-4.5 mid-century (2041-2070) and end-century (2071-2100), and SSP5-8.5 mid-century and end-century. Average air temperature for each climate period (**bold**) is the rural reference air temperature input into InVEST. Coordinates (decimal degrees) and elevation (metres) for the three rural reference points is also provided.

Coordinates	Elevation	Current	SSP2-4.5, Mid-Century	SSP2-4.5, End-Century	SSP5-8.5, Mid-Century	SSP5-8.5, End-Century
44.21206, -79.3525	230	15.3	16.3	17.1	16.8	19.0
44.05993, -79.3185	316	15.5	16.6	17.3	17.1	19.2
44.13123, -79.5311	219	15.4	16.4	17.1	16.9	19.0
AVERAGE		15.4	16.4	17.2	16.9	19.1

To get the urban heat island effect, we used the recommended [Global Surface UHI Explorer](#), which was developed by researchers at Yale University. For East Gwillimbury, the UHI Explorer provides an urban heat island effect for a broader region that includes East Gwillimbury, Newmarket, and Aurora. This is beneficial to our study, as Newmarket and Aurora are more developed than East Gwillimbury, so this urban heat island value better reflects a total buildout scenario. According to the UHI Explorer, the summer daytime urban heat island effect for this region is 2.27°C, and the summer nighttime effect is 0.65°C. For detailed information on the methodology behind the Global Surface UHI Explorer, see [their webpage](#) at the Yale Center for Geospatial Solutions.

To account for air mixing due to atmospheric turbulence, InVEST applies a Gaussian function with kernel radius equal to a user-defined air blending distance. The User Guide recommends an air blending distance of 500-600 metres. To reduce model runtime, and to align with the literature suggesting that InVEST accuracy may be improved with a shorter air blending distance (Bosch et al., 2021a), we used an air blending distance of 500 metres. InVEST also requires a maximum cooling distance over which large greenspaces have a cooling effect. Zawadzka et al. (2021) used 100 m, 200 m, and 300 m in their InVEST study, and found that InVEST model accuracy was highest for developed (buildings, paved) land use classes with 200 m cooling distance. We therefore chose to use 200 metres as the cooling distance. In their comprehensive

review of urban greening, Wong et al. (2021) provide a park cooling distance of 40-440 metres depending on the shape and size of the park. A 200 m cooling distance aligns with this range.

Energy Savings Valuation

To run the energy savings valuation in InVEST, the model requires an energy consumption table that provides energy consumption values and (optionally) energy costs²⁰ for each building type within the building footprint input layer. We were only interested in running the energy savings valuation for our buildout simulations, as we were less interested in evaluating energy savings between the pre-buildout vs. buildout infrastructure and more interested in evaluating energy savings across the climate and greening scenarios. For the buildout building footprint layer (described above), we assigned each building polygon a building type by overlaying the layer with our buildout land use map and extracting the corresponding land use class for each building polygon. The majority of buildings were located within the Developed, Low Intensity and Developed, High Intensity land use classes, and we reclassified these buildings as “residential” and “commercial/industrial,” respectively. Several buildings were located in other land use polygons; however, the majority of these buildings were similar in shape and size and likely had a similar function to urban residential buildings (e.g., farmhouses, rural households, etc.), so we assigned these as “residential” as well. Our building footprint layer therefore had buildings grouped into two types: commercial/industrial and residential. We used QGIS to calculate the area (m²) of each footprint polygon, which we then used to find the average total floor area per building type (Table C-9).

Table C-9 – Average footprint area (m²), number of floors, and resultant total floor area (m²) for each building type in East Gwillimbury under a full buildout scenario.

Building Type	Footprint Area	Number of Floors	Total Area (All Floors)
Residential	189.65	3	568.95
Commercial/Industrial	2910.18	2	5820.36

The InVEST Urban Cooling User Guide suggests referring to Santamouris et al. (2015) for information on energy consumption per °C for specific regions. Santamouris et al. (2015) report a 1.5% increase in the base electricity load per degree temperature increase in Ontario. In 2019, the average annual energy use intensity for commercial and institutional buildings across Canada was 336.1 kWh/m² (Statistics Canada, 2019), while average annual energy use for a single detached home in Ontario was 147.2 kWh/m² (Natural Resources Canada, 2019). Given

²⁰ Because energy costs vary with time, we did not input energy costs into the energy consumption table to evaluate cooling in dollars, choosing instead to evaluate cooling in kWh. We then calculated energy costs based on kWh saved using Ontario mid-peak time-of-use pricing at the time of report preparation, which was 12.2 cents per kWh.



this information and the areas presented in Table C-9, we calculated annual energy consumption per building type in kWh/m²/°C as follows:

Residential

$$147.2 \times 0.015 = 2.208 \text{ kWh/m}^2/\text{°C} \text{ (increase in energy per °C)}$$

$$\frac{2.208 \times 568.95}{189.65} = \mathbf{6.619 \text{ kWh/m}^2/\text{°C}} \text{ (consumption adjusted for total floor area}^{21}\text{)}$$

Commercial/Industrial

$$336.1 \times 0.015 = 5.0415 \text{ kWh/m}^2/\text{°C} \text{ (increase in energy per °C)}$$

$$\frac{5.0415 \times 5820.36}{2910.18} = \mathbf{10.083 \text{ kWh/m}^2/\text{°C}} \text{ (consumption adjusted for total floor area}^{21}\text{)}$$

We then divided the annual consumption values calculated above by 12 to get an average monthly value, which we used as an estimate of July energy consumption per building type. Final July energy consumption values were 0.55 kWh/m²/°C for residential buildings, and 0.84 kWh/m²/°C for commercial/industrial buildings.

Work Productivity Valuation

InVEST is able to calculate work productivity loss (%) for light work (defined as when workers’ metabolic rates sit between 200 and 400 Watts) and heavy work (metabolic rates above 400 Watts) (Kjellstrom et al., 2009). InVEST does this by converting air temperature into wet bulb global temperature. For this conversion, the model requires average relative humidity for the study area over the time period of interest. We used QGIS to create a grid of points, equally spaced one kilometre apart, within our study area. We then extracted coordinates and elevation for each point and used ClimateNA to generate July relative humidity for all points, under all climate scenarios. Average relative humidity of all points for each scenario, which we used for input into InVEST, is provided in Table C-10.

Table C-10 – Average July percent relative humidity of 248 equally spaced reference points within the East Gwillimbury municipality, for five climate periods: current (2011-2020), SSP2-4.5 mid-century (2041-2070) and end-century (2071-2100), and SSP5-8.5 mid-century and end-century.

Current	SSP2-4.5, Mid-Century	SSP2-4.5, End-Century	SSP5-8.5, Mid-Century	SSP5-8.5, End-Century
65.7	64.0	64.1	63.9	63.6

²¹ The InVEST User Guide recommends adjusting energy consumption values for the average number of stories for buildings of this type.



D. Appendix D: Land Use/Land Cover Descriptions

Table D-1 – Description of natural heritage land cover classes and their corresponding Ecological Land Classification (ELC) codes as found in the Lake Simcoe Region Conservation Authority 2018 land use layer. Bolded entries are the overarching Ecological Land Classification Community Classes, within which distinct communities (unbolded) belong.

ELC Code	Land Cover	Description
FO	Forest	Tree cover > 60%
FOC	Coniferous Forest	Conifers > 75% of canopy cover
FOD	Deciduous Forest	Deciduous species > 75% of canopy cover
FOM	Mixed Forest	Conifers > 25%; deciduous trees > 25% of canopy cover
FE	Fen	Tree cover <= 25% (trees > 2 m high); sedges, grasses, and low (< 2 m) shrubs dominate; organic substrate; minerotrophic peatland
FEO	Open Fen	Tree cover <= 10%; shrub cover <= 25%
FES	Shrub Fen	Tree cover <= 10%; shrub cover > 25%
FET	Treed Fen	Tree cover between 10-25%
MA	Marsh	Tree and shrub cover <= 25%; dominated by emergent hydrophytic macrophytes; variable flooding regime; water depth < 2 m
MAM	Meadow Marsh	Species less tolerant of prolonged flooding; seasonal flooding (soils flooded in spring, moist-dry by summer); wetland-terrestrial interface
MAS	Shallow Marsh	Water up to 2 m deep; standing or flowing water for much or all of growing season
SW	Swamp	Tree or shrub cover > 25%; dominated by hydrophytic shrub and tree species; standing water or vernal pooling > 20% of ground coverage
SWC	Coniferous Swamp	Tree cover > 25% with conifers > 75% of that cover; trees > 5m in height; typically more northern species (e.g., bunchberry, dwarf raspberry, bluebead lily)



ELC Code	Land Cover	Description
SWD	Deciduous Swamp	Tree cover > 25% with deciduous species > 75% of that cover; trees > 5m in height; typically fern and sedge rich
SWM	Mixed Swamp	Tree cover > 25% (trees > 5 m in height) with deciduous > 25% and coniferous > 25% of canopy cover; vegetation a mix of typical conifer and deciduous swamp species; typically fern rich
SWT	Thicket Swamp	Tree cover <= 25%; hydrophytic shrubs > 25%
BO	Bog	Tree cover <= 25% (trees > 2 m high); organic substrate, > 40 cm of <i>Sphagnum</i> peat; acidic; ombotrophic peatland
BOS	Shrub Bog	Tree cover <= 10%; shrub cover > 25%; continuous <i>Sphagnum</i> spp. cover
BOT	Treed Bog	Tree cover between 10-25%; continuous <i>Sphagnum</i> cover
SA	Shallow Water	Submerged or floating-leaved macrophytes; emergent vegetation may be present but never dominant; no tree or shrub cover; water <= 2 m in depth; standing water always present
SAF	Floating-leaved Shallow Aquatic	Dominated (> 25% by floating-leaved macrophytes)
SAM	Mixed Shallow Aquatic	Dominated (> 25%) by a mixture of submerged and floating-leaved macrophytes
SAS	Submerged Shallow Aquatic	Dominated (> 25%) by submerged macrophytes
OAD	Open Aquatic	No macrophyte vegetation (no trees or shrub cover); water > 2 m depth
CU	Cultural	Community resulting from, or maintained by, cultural or anthropogenic-based disturbances
CUM	Cultural Meadow	Tree cover <= 25%; shrub cover <= 25%
CUP	Cultural Plantation	Tree cover > 60%
CUS	Cultural Savannah	Tree cover 25-35%
CUT	Cultural Thicket	Tree cover <= 25%; shrub cover > 25%
CUW	Cultural Woodland	Tree cover 35-60%



ELC Code	Land Cover	Description
	<u>Grasslands</u>	
AL	Alvar	Vegetation cover varies from patchy and barren to more closed and treed; tree cover \leq 60%; patchy mosaic of bare rock pavement and shallow (< 15 cm) substrate over bedrock
ALO	Open Alvar	Tree cover \leq 25%; shrub cover \leq 25%; plant cover varies from patchy and barren to continuous herbaceous meadow
ALS	Shrub Alvar	Tree cover \leq 25%; shrub cover > 25%; patchy to continuous cover of shrubs; on very shallow substrates or in fractures (grykes)
SB	Sand Barren	Vegetation cover varies from patchy and barren to more closed and treed; tree cover \leq 60%
SBO	Open Sand Barren and Dune	Tree cover < 25%; shrub cover < 25%
TP	Tallgrass Prairie, Savannah, and Woodland	Ground layer dominated by prairie graminoids (e.g., big & little bluestem, Indian grass); variable cover of open-grown trees; tree cover \leq 60%
TPO	Open Tallgrass Prairie	Tree cover \leq 25%; shrub cover \leq 25%

Table D-2 – Description of non-natural land cover classes in the Lake Simcoe Region Conservation Authority 2018 land use layer.

Land Cover	Description
Aggregate	Resource extraction pits and quarries.
Commercial (Urban)	Impervious properties containing a building and adjacent parking lot (e.g., shopping malls, scrap yards, other less impervious areas).
Estate Residential (Urban)	A home within a natural heritage feature (but excluding that feature) including the manicured area around the home and driveway.
Industrial (Urban)	Larger impervious areas than commercial (e.g., large factories, etc.).
Institutional (Urban)	Includes schools and other institutional structures and adjacent fields, sometimes stormwater management ponds.



Land Cover	Description
Intensive Agriculture (Rural)	Cultivated fields producing crops in varying degrees.
Manicured Open Space (Urban)	Dominated by gardens, parkland, and lawn areas. Minimum size of two hectares. Low tree density.
Non-Intensive Agriculture (Rural)	Fields dominated with herbaceous vegetation and grasses. Weedy hay and/or pasture covers more than 50% of area. Associated with extensive or unconfined grazing of livestock. Minimal evidence of recent cultivation.
Rural Development (Rural)	Lands with residential, commercial, or other buildings not directly associated with farming or manicured open space. Lands are heavily impacted and still under intensive use. Canopy cover < 60%.
Urban (Urban)	Heavily impacted areas of gravel or pavement with buildings and structures that are developed or under construction, and may be industrial, residential, or commercial. Minimal ecological function with little opportunity for restoration.

Table D-3 – Reclassification of the Lake Simcoe Region Conservation Authority’s natural heritage and non-natural land cover classes into 14 condensed land use classes for input into InVEST Urban Cooling.

InVEST Land Use Class	Description
Coniferous Forest	Includes the FOC and CUP land use types. See FOC and CUP (Table D-1) for descriptions.
Deciduous Forest	Includes the FOD land use type. See FOD (Table D-1) for description.
Mixed Forest	Includes the FOM and CUW land use types. See Table D-1 for descriptions.
Woody Wetland	Includes all SW land use types. See SW (Table D-1) for descriptions.
Open Wetland	Includes all FE, MA, and BO land use types. See Table D-1 for descriptions.
Shrub/Scrub	Includes the CUT and ALS land use types. See Table D-1 for descriptions.
Grassland	Includes the CUM, CUS, ALO, and TPO land use types. See Table D-1 for descriptions.



InVEST Land Use Class	Description
Water	Includes OAO and all SA land use types. See Table D-1 for descriptions.
Barren Land	Includes non-natural (Active Aggregate) and natural (SBO) barren land types. See Table D-1 and D-2 for descriptions.
Intensive Agriculture	Cultivated crops. Includes Intensive Agriculture (see Table D-2 for description)
Non-intensive Agriculture	Hay/pasture lands. Includes Non-Intensive Agriculture (see Table D-2 for description).
Urban Greenspace	Includes Manicured Open Areas (e.g., lawns, parks, golf courses). See Table D-2 for description.
Developed, Low Intensity	Urban classes with more pervious surface cover (e.g., grass, tree canopy, etc.). Includes the Urban ²² , Estate Residential, Institutional, and Rural Development non-natural land cover types. See Table D-2 for descriptions.
Developed, High Intensity	Urban classes with a high degree of impervious surface cover. Includes the Commercial/Industrial, Rail, and Road non-natural land cover types. See Table D-2 for descriptions.

Table D-4 – Reclassification of the Lake Simcoe Region Conservation Authority’s natural heritage land cover classes (Table D-1) into land use classes for input into InVEST Urban Cooling.

InVEST Land Use Class	ELC Code	Name
Coniferous Forest	FOC	Coniferous Forest
Deciduous Forest	FOD	Deciduous Forest
Mixed Forest	FOM	Mixed Forest
Open Wetland	FEO	Open Fen

²² The Conservation Authority describes the Urban land cover type as “heavily impacted” with “minimal ecological function” (Table D-2). However, the majority of Urban polygons fall on residential areas within East Gwillimbury, which is why we included it in the “Developed, High Intensity” InVEST land use class.



InVEST Land Use Class	ELC Code	Name
Open Wetland	FES	Shrub Fen
Open Wetland	FET	Treed Fen
Open Wetland	MAM	Meadow Marsh
Open Wetland	MAS	Shallow Marsh
Woody Wetland	SWC	Coniferous Swamp
Woody Wetland	SWD	Deciduous Swamp
Woody Wetland	SWM	Mixed Swamp
Woody Wetland	SWT	Thicket Swamp
Open Wetland	BOS	Shrub Bog
Open Wetland	BOT	Treed Bog
Water	SAF	Floating-leaved Shallow Aquatic
Water	SAM	Mixed Shallow Aquatic
Water	SAS	Submerged Shallow Aquatic
Water	OAD	Open Aquatic
Grassland	CUM	Cultural Meadow
Coniferous Forest	CUP	Cultural Plantation
Grassland	CUS	Cultural Savannah
Shrub/Scrub	CUT	Cultural Thicket
Mixed Forest	CUW	Cultural Woodland
Grassland	ALO	Open Alvar
Shrub/Scrub	ALS	Shrub Alvar
Barren Land	SBO	Open Sand Barren and Dune
Grassland	TPO	Open Tallgrass Prairie



Table D-5 – Reclassification of the Lake Simcoe Region Conservation Authority’s non-natural land cover classes (Table D-2) into land use classes for input into InVEST Urban Cooling.

InVEST Land Use Class	Non-Natural Land Cover
Barren Land	Active Aggregate
Developed, High Intensity	Commercial
Developed, Low Intensity	Estate Residential
Developed, High Intensity	Industrial
Developed, Low Intensity	Institutional
Intensive Agriculture	Intensive Agriculture
Urban Greenspace	Manicured Open Space
Non-intensive Agriculture	Non-Intensive Agriculture
Developed, High Intensity	Rail
Developed, High Intensity	Road
Developed, Low Intensity	Rural Development
Developed, Low Intensity	Urban

Table D-6 – Reclassification of East Gwillimbury (EG) development types, with their Lake Simcoe Region Conservation Authority (LSRCA) non-natural land cover class equivalents (Table D-2), into land use classes for input into InVEST Urban Cooling.

InVEST Land Use Class	EG Development Type	LSRCA Equivalent
Developed, High Intensity	Commercial	Commercial (Urban)
Developed, High Intensity	General Employment	Commercial (Urban); Industrial (Urban)
Developed, High Intensity	Industrial	Industrial (Urban)
Developed, Low Intensity	Institutional	Institutional (Urban)



InVEST Land Use Class	EG Development Type	LSRCA Equivalent
Urban Greenspace	Manicured Open Space	Manicured Open Space (Urban)
Developed, High Intensity	Mixed Use	Commercial (Urban); Residential (Urban) ²³
Non-intensive Agriculture	Non-intensive Ag	Non-Intensive Agriculture (Rural)
Developed, Low Intensity	Residential	Urban (Urban)
Developed, Low Intensity	Rural Development	Rural Development (Rural)
Developed, High Intensity	Village Core	N/A ²⁴

²³ While the East Gwillimbury “Mixed Use” development type can be considered a combination of the Lake Simcoe “Commercial (Urban)” (which is considered “Developed, High Intensity”) and “Residential (Urban)” (which is considered “Developed, Low Intensity”) types, we chose to classify this type as “Developed, High Intensity” given the type of infrastructure (e.g., condominiums with retail space at ground level).

²⁴ This East Gwillimbury land type has no Lake Simcoe equivalent. We classified it as “Developed, High Intensity” as urban centres tend to combine high-density housing (e.g., condominiums) with commercial infrastructure.

E. Appendix E: InVEST Output Maps

Daytime Temperatures

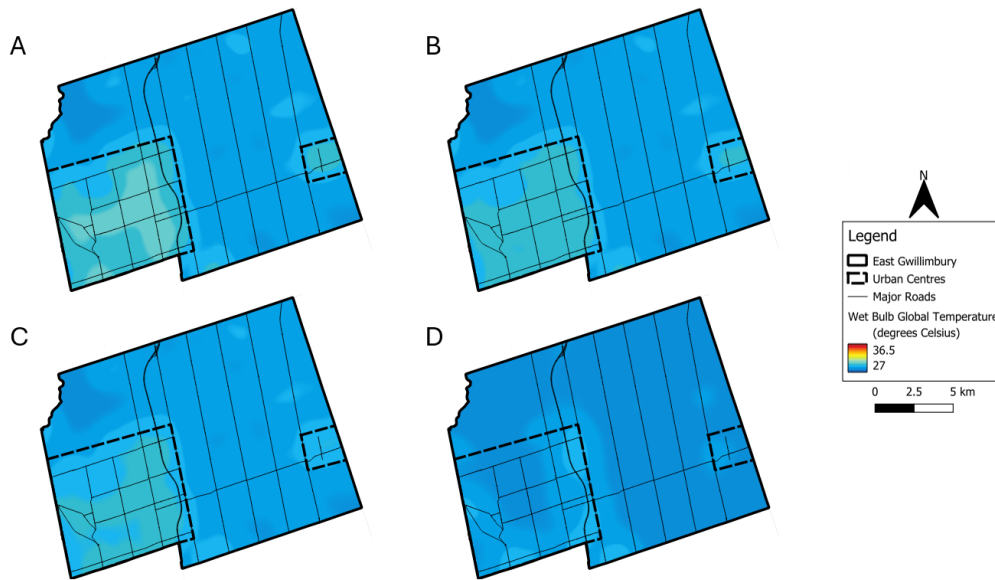


Figure E-1 – Maps of East Gwillimbury showing estimated maximum daytime wet bulb global temperature (°C) distribution under a full buildout scenario and current climate (2011-2020) conditions, for four canopy cover scenarios: (A) 22%, (B) 38%, (C) 44%, and (D) green 44%.

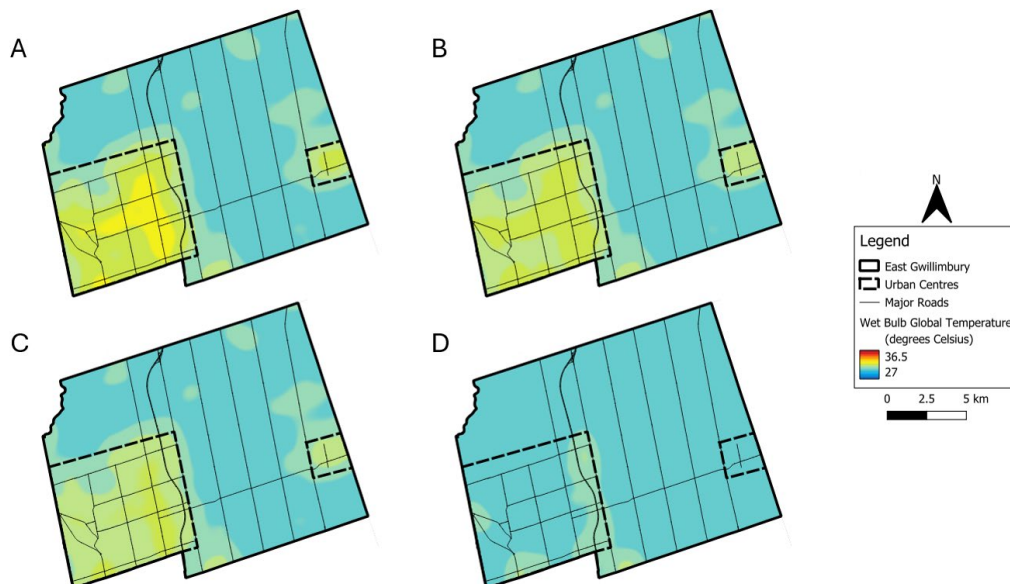


Figure E-2 – Maps of East Gwillimbury showing estimated maximum daytime wet bulb global temperature (°C) distribution by mid-century (2041-2070) under the SSP2-4.5 emissions pathway for four canopy cover scenarios: (A) 22%, (B) 38%, (C) 44%, and (D) green 44%.

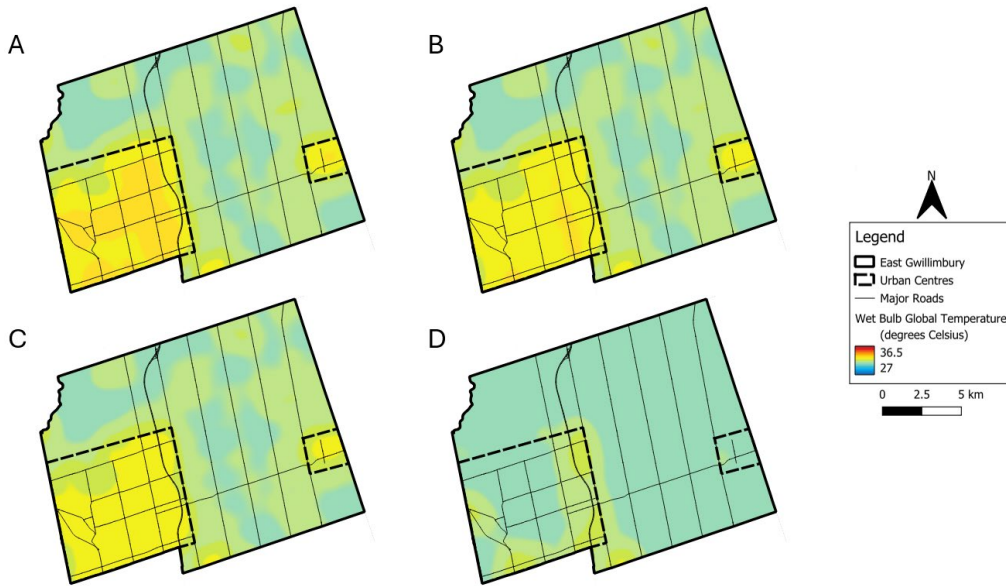


Figure E-3 – Maps of East Gwillimbury showing estimated maximum daytime wet bulb global temperature (°C) distribution by end-century (2071-2100) under the SSP2-4.5 emissions pathway for four canopy cover scenarios: (A) 22%, (B) 38%, (C) 44%, and (D) green 44%.

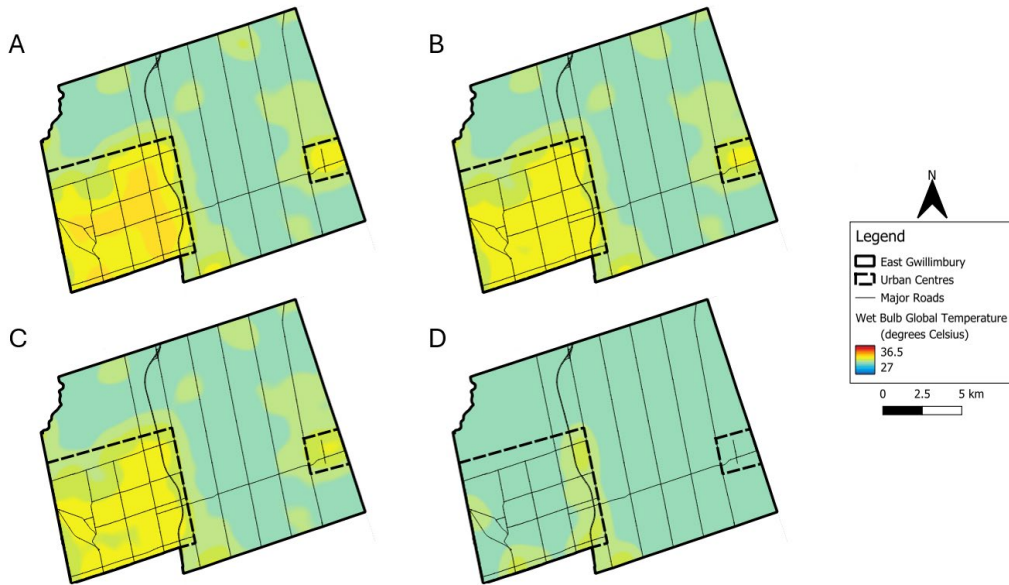


Figure E-4 – Maps of East Gwillimbury showing estimated maximum daytime wet bulb global temperature (°C) distribution by mid-century (2041-2070) under the SSP5-8.5 emissions pathway for four canopy cover scenarios: (A) 22%, (B) 38%, (C) 44%, and (D) green 44%.

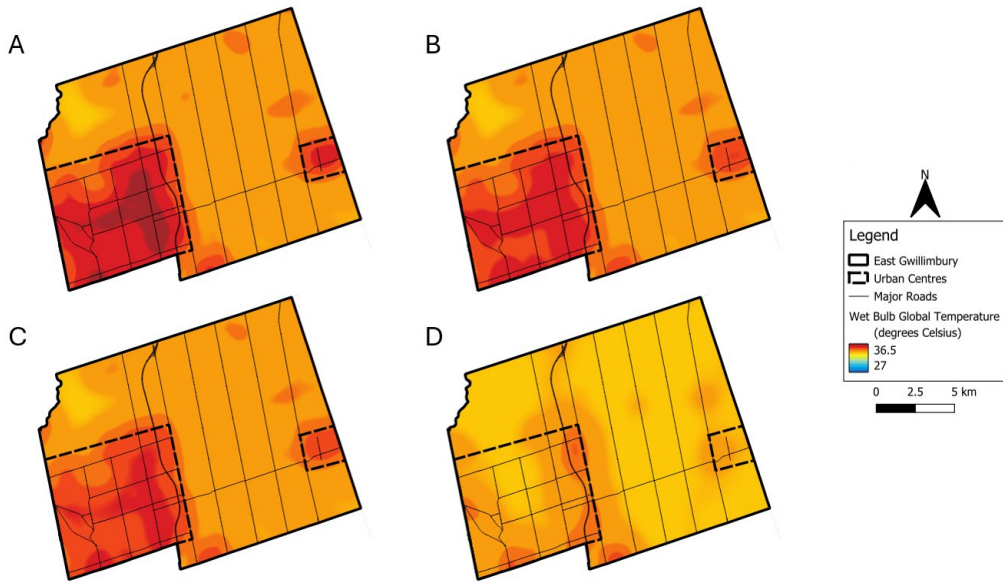


Figure E-5 – Maps of East Gwillimbury showing estimated maximum daytime wet bulb global temperature (°C) distribution by end-century (2071-2100) under the SSP5-8.5 emissions pathway for four canopy cover scenarios: (A) 22%, (B) 38%, (C) 44%, and (D) green 44%.

Nighttime Temperatures

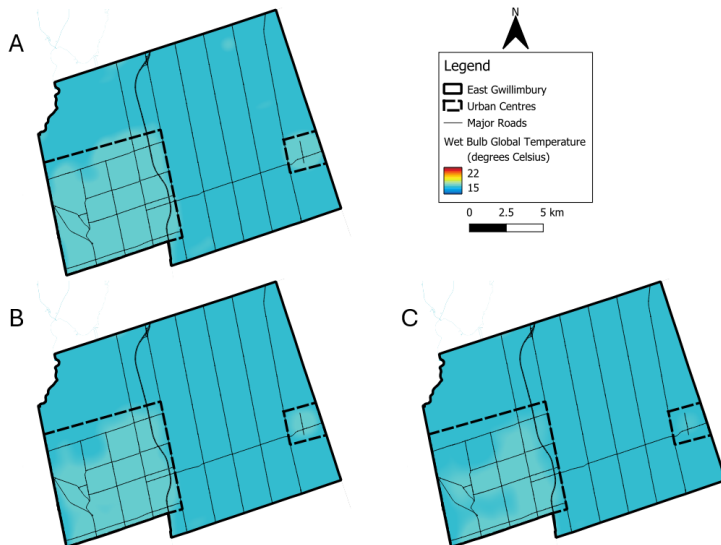


Figure E-6 – Maps of East Gwillimbury showing estimated mean nighttime wet bulb global temperature (°C) distribution under a full buildout scenario and current climate (2011-2020) conditions, for three canopy cover scenarios: (A) 22%, (B) 38%, and (C) 44%.

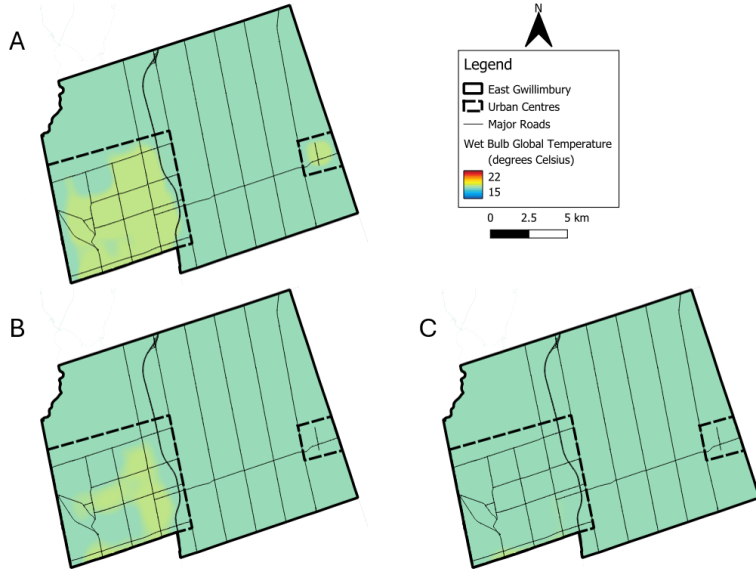


Figure E-7 – Maps of East Gwillimbury showing estimated mean nighttime wet bulb global temperature (°C) distribution by mid-century (2041-2070) under the SSP2-4.5 emissions pathway for three canopy cover scenarios: (A) 22%, (B) 38%, and (C) 44%.

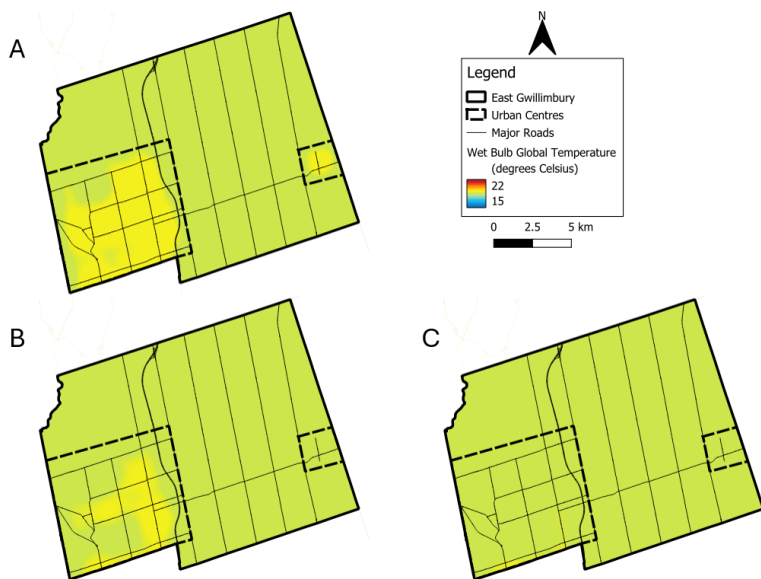


Figure E-8 – Maps of East Gwillimbury showing estimated mean nighttime wet bulb global temperature (°C) distribution by end-century (2071-2100) under the SSP2-4.5 emissions pathway for three canopy cover scenarios: (A) 22%, (B) 38%, and (C) 44%.

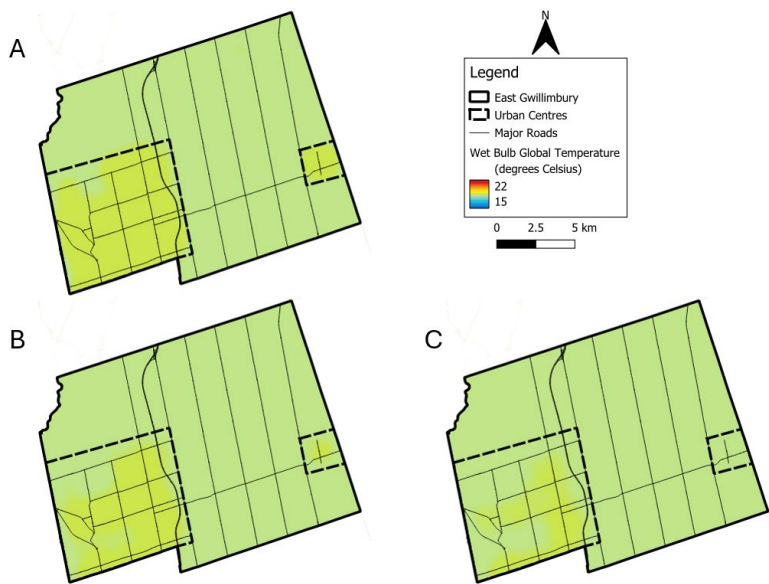


Figure E-9 – Maps of East Gwillimbury showing estimated mean nighttime wet bulb global temperature (°C) distribution by mid-century (2041-2070) under the SSP5-8.5 emissions pathway for three canopy cover scenarios: (A) 22%, (B) 38%, and (C) 44%.

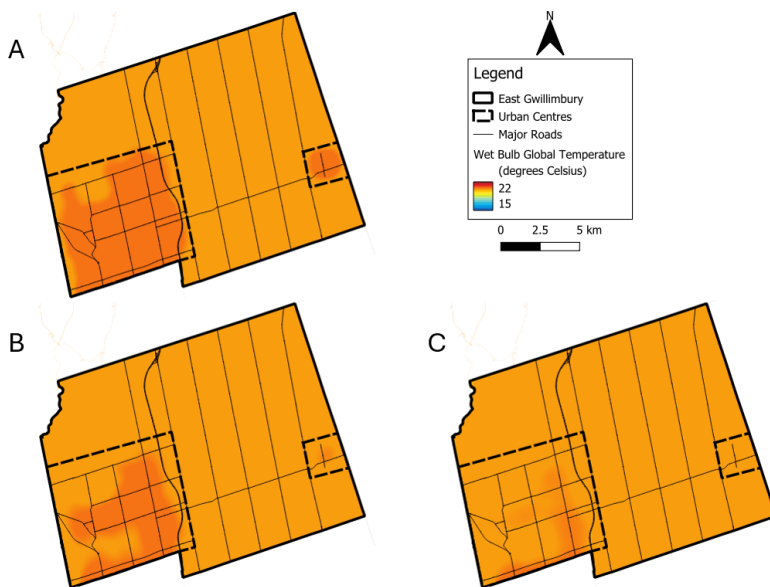


Figure E-10 – Maps of East Gwillimbury showing estimated mean nighttime wet bulb global temperature (°C) distribution by end-century (2071-2100) under the SSP5-8.5 emissions pathway for three canopy cover scenarios: (A) 22%, (B) 38%, and (C) 44%.

F. Appendix F: InVEST Output Raw Data

Daytime Temperatures

Table F-1 – Estimated maximum daytime July air temperatures (°C) (without air mixing) across two urban areas (Urban Core and Mount Albert) in East Gwillimbury under four canopy cover scenarios (22%, 38%, 44%, and green 44%) and five climate scenarios: current climate, SSP2-4.5 mid-century (2041-2070), SSP2-4.5 end-century (2071-2100), SSP5-8.5 mid-century, and SSP5-8.5 end-century. Displayed are mean, median, minimum, and maximum air temperatures (T), as well as standard deviation (StDev).

		URBAN CORE					MOUNT ALBERT				
		Mean T	Median T	StDev T	Min T	Max T	Mean T	Median T	StDev T	Min T	Max T
Current Climate	22%	28.29	28.46	0.53	27.03	28.78	28.43	28.62	0.43	27.19	28.78
	38%	28.11	28.38	0.44	27.03	28.75	28.22	28.38	0.32	27.19	28.71
	44%	28.03	28.22	0.38	27.03	28.75	28.11	28.22	0.27	27.19	28.69
	Green 44%	27.30	27.22	0.22	27.04	27.90	27.14	27.13	0.05	27.08	27.27
SSP2-4.5 mid	22%	30.18	30.23	0.64	28.80	30.88	30.33	30.41	0.55	28.96	30.88
	38%	30.00	30.22	0.53	28.80	30.78	30.11	30.36	0.41	28.96	30.78
	44%	29.92	30.20	0.47	28.80	30.67	30.02	30.22	0.35	28.96	30.59
	Green 44%	29.11	28.90	0.45	28.80	30.59	28.94	28.88	0.16	28.81	29.54
SSP2-4.5 end	22%	30.88	30.93	0.64	29.50	31.58	31.03	31.11	0.55	29.66	31.58
	38%	30.70	30.92	0.53	29.50	31.48	30.81	31.06	0.40	29.66	31.48
	44%	30.62	30.90	0.47	29.50	31.37	30.72	30.92	0.34	29.66	31.29
	Green 44%	29.81	29.60	0.45	29.50	31.29	29.64	29.58	0.16	29.51	30.24
SSP5-8.5 mid	22%	30.78	30.83	0.64	29.40	31.48	30.93	31.01	0.55	29.56	31.48
	38%	30.60	30.82	0.53	29.40	31.38	30.71	30.96	0.40	29.56	31.38
	44%	30.52	30.80	0.47	29.40	31.27	30.62	30.82	0.34	29.56	31.19
	Green 44%	29.71	29.50	0.45	29.40	31.19	29.54	29.48	0.16	29.41	30.14
SSP5-8.5 end	22%	33.25	33.30	0.64	31.87	33.95	33.40	33.48	0.55	32.03	33.95
	38%	33.07	33.29	0.53	31.87	33.85	33.18	33.43	0.40	32.03	33.85
	44%	32.99	33.27	0.47	31.87	33.74	33.09	33.29	0.34	32.03	33.66
	Green 44%	32.18	31.97	0.45	31.87	33.66	32.01	31.95	0.16	31.88	32.61

Table F-2 – Estimated maximum daytime July air temperatures (°C) (with air mixing) across two urban areas (Urban Core and Mount Albert) in East Gwillimbury under four canopy cover scenarios (22%, 38%, 44%, and green 44%) and five climate scenarios: current climate, SSP2-4.5 mid-century (2041-2070), SSP2-4.5 end-century (2071-2100), SSP5-8.5 mid-century, and SSP5-8.5 end-century. Displayed are mean, median, minimum, and maximum air temperatures (T), as well as standard deviation (StDev).

		URBAN CORE					MOUNT ALBERT				
		Mean T	Median T	StDev T	Min T	Max T	Mean T	Median T	StDev T	Min T	Max T
Current Climate	22%	28.25	28.35	0.36	27.16	28.70	28.15	28.18	0.19	27.60	28.42
	38%	28.07	28.17	0.27	27.15	28.43	27.99	28.02	0.15	27.55	28.18
	44%	27.99	28.08	0.24	27.15	28.29	27.92	27.94	0.13	27.52	28.07
	Green 44%	27.30	27.22	0.22	27.04	27.90	27.14	27.13	0.05	27.08	27.27
SSP2-4.5 mid	22%	30.13	30.23	0.42	28.94	30.71	30.01	30.05	0.22	29.41	30.35
	38%	29.95	30.05	0.33	28.93	30.43	29.85	29.88	0.18	29.35	30.09
	44%	29.88	29.97	0.29	28.93	30.29	29.79	29.82	0.16	29.32	29.99
	Green 44%	29.08	29.00	0.24	28.81	29.78	28.91	28.90	0.05	28.85	29.04
SSP2-4.5 end	22%	30.83	30.93	0.42	29.64	31.41	30.71	30.75	0.22	30.10	31.05
	38%	30.65	30.75	0.33	29.63	31.13	30.55	30.58	0.18	30.05	30.79
	44%	30.58	30.67	0.29	29.63	30.99	30.48	30.52	0.16	30.02	30.69
	Green 44%	29.78	29.70	0.24	29.51	30.48	29.61	29.60	0.05	29.55	29.74
SSP5-8.5 mid	22%	30.73	30.83	0.42	29.54	31.31	30.61	30.65	0.22	30.01	30.95
	38%	30.55	30.65	0.33	29.53	31.03	30.45	30.48	0.18	29.95	30.69
	44%	30.48	30.57	0.29	29.53	30.89	30.39	30.42	0.16	29.92	30.59
	Green 44%	29.68	29.60	0.24	29.41	30.38	29.51	29.50	0.05	29.45	29.64
SSP5-8.5 end	22%	33.20	33.30	0.42	32.01	33.78	33.08	33.12	0.22	32.48	33.42
	38%	33.02	33.12	0.33	32.00	33.50	32.92	32.95	0.18	32.42	33.16
	44%	32.95	33.04	0.29	32.00	33.35	32.86	32.89	0.16	32.39	33.06
	Green 44%	32.15	32.07	0.24	31.88	32.85	31.98	31.97	0.05	31.92	32.11

Table F-3 – Estimated daytime wet bulb global temperature (°C) values across two urban areas (Urban Core and Mount Albert) in East Gwillimbury under four canopy cover scenarios (22%, 38%, 44%, and green 44%) and five climate scenarios: current climate, SSP2-4.5 mid-century (2041-2070), SSP2-4.5 end-century (2071-2100), SSP5-8.5 mid-century, and SSP5-8.5 end-century. Displayed are mean, median, minimum, and maximum air temperatures (T), as well as standard deviation (StDev).

		URBAN CORE					MOUNT ALBERT				
		Mean T	Median T	StDev T	Min T	Max T	Mean T	Median T	StDev T	Min T	Max T
Current Climate	22%	29.83	29.95	0.40	28.60	30.34	29.71	29.75	0.22	29.10	30.02
	38%	29.63	29.73	0.31	28.60	30.04	29.53	29.57	0.17	29.04	29.75
	44%	29.53	29.63	0.27	28.59	29.87	29.45	29.48	0.14	29.01	29.62
	Green 44%	28.76	28.67	0.25	28.47	29.44	28.59	28.57	0.06	28.52	28.72
SSP2-4.5 mid	22%	31.75	31.86	0.49	30.35	32.43	31.60	31.64	0.26	30.89	32.00
	38%	31.53	31.64	0.38	30.34	32.09	31.41	31.45	0.21	30.82	31.70
	44%	31.45	31.55	0.34	30.34	31.92	31.33	31.37	0.18	30.80	31.58
	Green 44%	30.52	30.42	0.28	30.21	31.32	30.33	30.31	0.06	30.26	30.47
SSP2-4.5 end	22%	32.60	32.71	0.50	31.18	33.30	32.45	32.49	0.27	31.73	32.85
	38%	32.38	32.49	0.39	31.17	32.95	32.26	32.29	0.21	31.66	32.55
	44%	32.29	32.40	0.35	31.17	32.78	32.18	32.21	0.18	31.63	32.42
	Green 44%	31.35	31.25	0.28	31.03	32.17	31.15	31.13	0.06	31.08	31.29
SSP5-8.5 mid	22%	32.44	32.56	0.50	31.03	33.14	32.30	32.33	0.27	31.58	32.70
	38%	32.22	32.34	0.39	31.02	32.79	32.10	32.14	0.21	31.51	32.39
	44%	32.14	32.25	0.34	31.02	32.62	32.02	32.06	0.18	31.48	32.27
	Green 44%	31.20	31.10	0.28	30.88	32.01	31.00	30.98	0.06	30.93	31.14
SSP5-8.5 end	22%	35.44	35.56	0.53	33.93	36.18	35.29	35.32	0.28	34.52	35.71
	38%	35.21	35.33	0.41	33.93	35.81	35.08	35.12	0.22	34.44	35.39
	44%	35.11	35.23	0.37	33.92	35.63	35.00	35.03	0.20	34.42	35.26
	Green 44%	34.11	34.01	0.30	33.78	34.98	33.91	33.89	0.06	33.83	34.06

Table F-4 – Daytime valuation metrics for July across all of East Gwillimbury under four canopy cover scenarios (22%, 38%, 44%, and green 44%) and five climate scenarios: current climate, SSP2-4.5 mid-century (2041-2070), SSP2-4.5 end-century (2071-2100), SSP5-8.5 mid-century, and SSP5-8.5 end-century. Displayed are average air temperatures, energy savings (kWh and dollars), wet bulb global temperature (WBGT), light productivity loss, and heavy productivity loss. Energy savings represent savings compared to a theoretical scenario with no green space.

		Avg T	Energy Savings (kWh)	Energy Savings (\$)	Avg WBGT	Avg L Work Loss (%)	Avg H Work Loss (%)
Current Climate	22%	27.6	2332182.4	284526.3	29.1	0.0	31.3
	38%	27.6	2939289.7	358593.3	29.0	0.0	30.7
	44%	27.5	3218390.2	392643.6	29.0	0.0	30.2
	Green 44%	27.2	5347333.6	652374.7	28.6	0.0	25.0
SSP2-4.5 mid	22%	29.4	1928632.8	235293.2	30.9	8.3	55.6
	38%	29.4	2562236.0	312592.8	30.8	5.0	54.9
	44%	29.3	2819343.5	343959.9	30.8	4.3	54.3
	Green 44%	28.9	5314910.5	648419.1	30.3	0.0	50.0
SSP2-4.5 end	22%	30.1	1929582.8	235409.1	31.8	23.6	61.6
	38%	30.1	2563665.5	312767.2	31.7	21.5	61.2
	44%	30.0	2820858.6	344144.8	31.6	20.1	61.1
	Green 44%	29.6	5314952.4	648424.2	31.2	2.9	52.6
SSP5-8.5 mid	22%	30.0	1929366.9	235382.8	31.6	20.1	59.5
	38%	30.0	2563346.5	312728.3	31.5	17.0	59.0
	44%	29.9	2820517.2	344103.5	31.5	14.8	58.8
	Green 44%	29.5	5314941.4	648422.9	31.0	1.6	51.6
SSP5-8.5 end	22%	32.5	1929413.8	235388.5	34.6	75.0	75.0
	38%	32.4	2563402.3	312735.1	34.5	75.0	75.0
	44%	32.4	2820582.0	344111.0	34.4	75.0	75.0
	Green 44%	32.0	5314950.9	648424.0	33.9	75.0	75.0

Nighttime Temperatures

Table F-5 – Estimated mean July nighttime air temperatures (°C) and wet bulb global temperature (°C) values, spatially averaged across all of East Gwillimbury, under three canopy cover scenarios (22%, 38%, and 44%) and five climate scenarios: current climate, SSP2-4.5 mid-century (2041-2070), SSP2-4.5 end-century (2071-2100), SSP5-8.5 mid-century, and SSP5-8.5 end-century.

		Air Temperature	Wet Bulb Temperature
Current Climate	22%	15.50	17.28
	38%	15.47	17.24
	44%	15.45	17.22
SSP2-4.5 mid	22%	16.50	18.00
	38%	16.47	17.98
	44%	16.45	17.96
SSP2-4.5 end	22%	17.30	18.70
	38%	17.27	18.69
	44%	17.25	18.67
SSP5-8.5 mid	22%	17.01	18.44
	38%	16.97	18.40
	44%	16.95	18.39
SSP5-8.5 end	22%	19.21	20.38
	38%	19.17	20.35
	44%	19.15	20.33

Table F-6 – Estimated mean July nighttime air temperatures (°C) (without air mixing) across two urban areas (Urban Core and Mount Albert) in East Gwillimbury under three canopy cover scenarios (22%, 38%, and 44%) and five climate scenarios: current climate, SSP2-4.5 mid-century (2041-2070), SSP2-4.5 end-century (2071-2100), SSP5-8.5 mid-century, and SSP5-8.5 end-century. Displayed are mean, median, minimum, and maximum air temperatures (T), as well as standard deviation (StDev).

	URBAN CORE					MOUNT ALBERT					
		Mean T	Median T	StDev T	Min T	Max T	Mean T	Median T	StDev T	Min T	Max T
Current Climate	22%	15.73	15.69	0.27	15.40	16.05	15.76	15.79	0.28	15.40	16.05
	38%	15.61	15.69	0.20	15.40	16.05	15.61	15.68	0.20	15.40	16.05
	44%	15.55	15.40	0.17	15.40	16.05	15.54	15.40	0.16	15.40	15.80
SSP2-4.5 mid	22%	16.73	16.69	0.27	16.40	17.05	16.76	16.79	0.28	16.40	17.05
	38%	16.61	16.69	0.20	16.40	17.05	16.61	16.68	0.20	16.40	17.05
	44%	16.55	16.40	0.17	16.40	17.05	16.54	16.40	0.16	16.40	16.80
SSP2-4.5 end	22%	17.53	17.49	0.27	17.20	17.85	17.56	17.59	0.28	17.20	17.85
	38%	17.41	17.49	0.20	17.20	17.85	17.41	17.48	0.20	17.20	17.85
	44%	17.35	17.20	0.17	17.20	17.85	17.34	17.20	0.16	17.20	17.60
SSP5-8.5 mid	22%	17.23	17.19	0.27	16.90	17.55	17.26	17.29	0.28	16.90	17.55
	38%	17.11	17.19	0.20	16.90	17.55	17.11	17.18	0.20	16.90	17.55
	44%	17.05	16.90	0.17	16.90	17.55	17.04	16.90	0.16	16.90	17.30
SSP5-8.5 end	22%	19.43	19.39	0.27	19.10	19.75	19.46	19.49	0.28	19.10	19.75
	38%	19.31	19.39	0.20	19.10	19.75	19.31	19.38	0.20	19.10	19.75
	44%	19.25	19.10	0.17	19.10	19.75	19.24	19.10	0.16	19.10	19.50

Table F-7 – Estimated mean July nighttime air temperatures (°C) (with air mixing) across two urban areas (Urban Core and Mount Albert) in East Gwillimbury under three canopy cover scenarios (22%, 38%, and 44%) and five climate scenarios: current climate, SSP2-4.5 mid-century (2041-2070), SSP2-4.5 end-century (2071-2100), SSP5-8.5 mid-century, and SSP5-8.5 end-century. Displayed are mean, median, minimum, and maximum air temperatures (T), as well as standard deviation (StDev).

		URBAN CORE					MOUNT ALBERT				
		Mean T	Median T	StDev T	Min T	Max T	Mean T	Median T	StDev T	Min T	Max T
Current Climate	22%	15.72	15.71	0.12	15.45	15.93	15.64	15.63	0.07	15.47	15.77
	38%	15.61	15.61	0.08	15.43	15.77	15.54	15.54	0.04	15.44	15.62
	44%	15.55	15.55	0.06	15.42	15.74	15.49	15.49	0.03	15.43	15.54
SSP2-4.5 mid	22%	16.72	16.71	0.12	16.45	16.93	16.64	16.63	0.07	16.47	16.77
	38%	16.61	16.61	0.08	16.43	16.77	16.54	16.54	0.04	16.44	16.62
	44%	16.55	16.55	0.03	16.43	16.54	16.49	16.49	0.03	16.43	16.54
SSP2-4.5 end	22%	17.52	17.51	0.12	17.25	17.73	17.44	17.43	0.07	17.27	17.57
	38%	17.41	17.41	0.08	17.23	17.57	17.34	17.34	0.04	17.24	17.42
	44%	17.35	17.35	0.06	17.22	17.53	17.29	17.29	0.03	17.23	17.34
SSP5-8.5 mid	22%	17.22	17.21	0.12	16.95	17.43	17.14	17.13	0.07	16.97	17.27
	38%	17.11	17.11	0.08	16.93	17.27	17.04	17.04	0.04	16.94	17.12
	44%	17.05	17.05	0.06	16.92	17.23	16.99	16.99	0.03	16.93	17.04
SSP5-8.5 end	22%	19.42	19.41	0.12	19.15	19.63	19.34	19.33	0.07	19.17	19.47
	38%	19.31	19.31	0.08	19.13	19.47	19.24	19.24	0.04	19.14	19.32
	44%	19.25	19.25	0.06	19.12	19.43	19.19	19.19	0.03	19.13	19.24

Table F-8 – Estimated mean nighttime wet bulb global temperature (°C) values across two urban areas (Urban Core and Mount Albert) in East Gwillimbury under three canopy cover scenarios (22%, 38%, and 44%) and five climate scenarios: current climate, SSP2-4.5 mid-century (2041-2070), SSP2-4.5 end-century (2071-2100), SSP5-8.5 mid-century, and SSP5-8.5 end-century. Displayed are mean, median, minimum, and maximum air temperatures (T), as well as standard deviation (StDev).

	URBAN CORE					MOUNT ALBERT					
	Mean T	Median T	StDev T	Min T	Max T	Mean T	Median T	StDev T	Min T	Max T	
Current Climate	22%	17.45	17.45	0.10	17.22	17.64	17.38	17.38	0.06	17.24	17.49
	38%	17.36	17.36	0.07	17.20	17.50	17.30	17.30	0.04	17.21	17.37
	44%	17.30	17.30	0.05	17.20	17.47	17.26	17.26	0.02	17.20	17.30
SSP2-4.5 mid	22%	18.19	18.19	0.10	17.96	18.38	18.13	18.12	0.06	17.98	18.24
	38%	18.10	18.10	0.07	17.95	18.24	18.04	18.04	0.04	17.95	18.11
	44%	18.05	18.05	0.05	17.94	18.21	18.00	18.00	0.02	17.94	18.04
SSP2-4.5 end	22%	18.90	18.90	0.11	18.67	19.10	18.83	18.83	0.06	18.68	18.95
	38%	18.81	18.81	0.07	18.65	18.95	18.75	18.75	0.04	18.66	18.82
	44%	18.75	18.75	0.05	18.64	18.92	18.71	18.71	0.02	18.65	18.75
SSP5-8.5 mid	22%	18.62	18.62	0.11	18.39	18.82	18.55	18.55	0.06	18.40	18.67
	38%	18.53	18.53	0.07	18.37	18.67	18.47	18.47	0.04	18.38	18.54
	44%	18.47	18.47	0.05	18.36	18.64	18.43	18.43	0.02	18.37	18.47
SSP5-8.5 end	22%	20.57	20.57	0.11	20.33	20.77	20.50	20.50	0.07	20.34	20.62
	38%	20.47	20.47	0.07	20.31	20.62	20.41	20.41	0.04	20.32	20.48
	44%	20.42	20.42	0.05	20.30	20.59	20.37	20.37	0.02	20.31	20.41



References

- Adams, M. P., & Smith, P. L. (2014). A systematic approach to model the influence of the type and density of vegetation cover on urban heat using remote sensing. *Landscape and Urban Planning*, 132, 47-54. <https://doi.org/10.1016/j.landurbplan.2014.08.008>
- Akbari, H., & Kolokotsa, D. (2016). Three decades of urban heat islands and mitigation technologies research. *Energy and Buildings*, 133, 834-842. <https://doi.org/10.1016/j.enbuild.2016.09.067>
- Alhazmi, M., Sailor, D. J., & Anand, J. (2022). A new perspective for understanding the actual anthropogenic heat emissions from buildings. *Energy and Buildings*, 258, Article e111860. <https://doi.org/10.1016/j.enbuild.2022.111860>
- Allen, R. G., Pereira, L. S., Raes, D., & Smith, M. (1998). *Crop evapotranspiration – Guidelines for computing crop water requirements* (Report No. M-56). Food and Agricultural Organization of the United Nations. <https://www.fao.org/4/x0490e/x0490e00.htm>
- Anderson, V., Gough, W. A., Zgela, M., Milosevic, D., & Dunjic, J. (2022). Lowering the temperature to increase heat equity: A multi-scale evaluation of nature-based solutions in Toronto, Ontario, Canada. *Atmosphere*, 13(7), Article e1027. <https://doi.org/10.3390/atmos13071027>
- Balany, F., Ng, A. W. M., Muttill, N., Muthukumaran, S., & Wong, M. S. (2020). Green infrastructure as an urban heat island mitigation strategy—A review. *Water*, 12(12), Article e3577. <https://doi.org/10.3390/w12123577>
- Bosch, M., Locatelli, M., Hamel, P., Remme, R. P., Chenal, J., & Joost, S. (2021a). A spatially explicit approach to simulate urban heat mitigation with InVEST (v3.8.0). *Geoscientific Model Development*, 14(6), 3521-3537. <https://doi.org/10.5194/gmd-14-3521-2021>
- Bosch, M., Locatelli, M., Hamel, P., Remme, R. P., Jaligot, R., Chenal, J., & Joost, S. (2021b). Evaluating urban greening scenarios for urban heat mitigation: A spatially explicit approach. *Royal Society Open Science*, 8(12), Article e202174. <https://doi.org/10.1098/rsos.202174>
- Chakraborty, T., Hsu, A., Manya, D., & Sheriff, G. (2019). Disproportionately higher exposure to urban heat in lower-income neighbourhoods: A multi-city perspective. *Environmental Research Letters*, 14, Article e105003. <https://doi.org/10.1088/1748-9326/ab3b99>
- Chapman, S., Thatcher, M., Salazar, A., Watson, J. E. M., & McAlpine, C. A. (2018). The effect of urban density and vegetation cover on the heat island of a subtropical city. *Journal of Applied Meteorology and Climatology*, 57(11), 2531-2550. <https://doi.org/10.1175/JAMC-D-17-0316.1>



- Chen, Y. C., Lin, T. P., & Matzarakis, A. (2014). Comparison of mean radiant temperature from field experiment and modelling: A case study in Freiburg, Germany. *Theoretical and Applied Climatology*, 118, 535-551. <https://doi.org/10.1007/s00704-013-1081-z>
- Commission for Environmental Cooperation. (2021). *Guide to drought indices and indicators used in North America*. <http://www.cec.org/files/documents/publications/11872-guide-drought-indices-and-indicators-used-in-north-america-en.pdf>
- Coseo, P., & Larsen, L. (2014). How factors of land use/land cover building configuration, and adjacent heat sources and sinks explain urban heat islands in Chicago. *Landscape and Urban Planning*, 125, 117-129. <https://doi.org/10.1016/j.landurbplan.2014.02.019>
- Earthfx. (2010). *Water balance analysis of the Lake Simcoe Basin using the Precipitation-Runoff Modelling System (PRMS)*.
- Gillerot, L., Landuyt, D., De Frenne, P., Muys, B., & Verheyen, K. (2024). Urban tree canopies drive human heat stress mitigation. *Urban Forestry & Urban Greening*, 92, Article e128192. <https://doi.org/10.1016/j.ufug.2023.128192>
- Government of Canada. (n.d.). *CMIP6 and Shared Socio-economic Pathways overview*. Canadian Climate Data and Scenarios. <https://climate-scenarios.canada.ca/?page=cmip6-overview-notes>
- Guo, Y., Gasparrini, A., Li, S., Sera, F., Vicedo-Cabrera, A., de Sousa Zanotti Stagliorio Coelho, M., Hilario, P., Saldiva, N., Lavigne, E., Tawatsupa, B., Punnasiri, K., Overcenco, A., Correa, P. M., Ortega, N. V., Kan, H., Osorio, S., Jaakkola, J. J. K., Rytty, N. R. I., Goodman, P. G., ... Tong, S. (2018). Quantifying excess deaths related to heatwaves under climate change scenarios: A multicountry time series modelling study. *PLoS Medicine*, 15(7), Article e1002629. <https://doi.org/10.1371/journal.pmed.1002629>
- Hamel, P., Bosch, M., Tardieu, L., Lemonsu, A., de Munck, C., Nootenboom, C., Viguié, V., Lonsdorf, E., Douglass, J. A., & Sharp, R. A. (2023). Calibrating and validating the InVEST urban cooling model: Case studies in France and the United States. *EGU sphere*. <https://doi.org/10.5194/egusphere-2023-928>
- Hassanzadeh, E., Bordeau-Goulet, S. C., & Nazemi, A. (2022, December). *Canada's potential evapotranspiration increases under climate change* [Conference abstract]. AGU 2022 Fall Meeting, Chicago, IL, USA. <https://ui.adsabs.harvard.edu/abs/2022AGUFMGC25H0767H/abstract>
- Hathway, E. A., & Sharples, S. (2012). The interaction of rivers and urban form in mitigating the urban heat island effect: A UK case study. *Building and Environment*, 58, 14-22. <https://doi.org/10.1016/j.buildenv.2012.06.013>



- Hausfather, Z., & Peters, G. P. (2020). Emissions – The ‘business as usual’ story is misleading. *Nature*, 577, 618-620. <https://doi.org/10.1038/d41586-020-00177-3>
- Hayes, A. T., Jandaghian, Z., Lacasse, M. A., Gaur, A., Lu, H., Laouadi, A., Ge, H., & Wang, L. (2022). Nature-based solutions (NBSs) to mitigate urban heat island (UHI) effects in Canadian cities. *Buildings*, 12(7), Article e925. <https://doi.org/10.3390/buildings12070925>
- Health Canada. (2020). *Reducing urban heat islands to protect health in Canada: An introduction for public health professionals*. <https://www.canada.ca/en/services/health/publications/healthy-living/reducing-urban-heat-islands-protect-health-canada.html>
- Heaviside, C., Macintyre, H., & Vardoulakis, S. (2017). The urban heat island: Implications for health in a changing environment. *Current Environmental Health Reports*, 4, 296-305. <https://doi.org/10.1007/s40572-017-0150-3>
- Heaviside, C., Vardoulakis, S., & Cai, X.-M. (2016). Attribution of mortality to the urban heat island during heatwaves in the West Midlands, UK. *Environmental Health*, 15, 49-59. <https://doi.org/10.1186/s12940-016-0100-9>
- Henderson, S. B., McLean, K. E., Lee, M. J., & Kosatsky, T. (2022). Analysis of community deaths during the catastrophic 2021 heat dome: Early evidence to inform the public health response during subsequent events in greater Vancouver, Canada. *Environmental Epidemiology*, 6(1), Article e189.
- Hu, Y., Wang, C., & Li, J. (2023). Assessment of heat mitigation services provided by blue and green spaces: An application of the InVEST Urban Cooling model with scenario analysis in Wuhan, China. *Land*, 12(5), 963. <https://doi.org/10.3390/land12050963>
- Ibsen, P. C., Jenerette, G. D., Dell, T., Bagstad, K. J., & Diffendorfer, J. E. (2022). Landcover differentially drives day and nighttime air temperature across a semi-arid city. *Science of the Total Environment*, 829, Article e154589. <https://doi.org/10.1016/j.scitotenv.2022.154589>
- Independent Electricity System Operator [IESO]. (2015, July 16). *On hot summer days, air conditioning accounts for roughly one-third of Ontario’s electricity use. Beat the heat and conserve energy this summer* [Press release]. <https://www.ieso.ca/corporate-ieso/media/news-releases/2015/07/on-hot-summer-days-air-conditioning-accounts-for-roughly-one-third-of-ontarios-electricity-use>
- Jänicke, B., Meier, F., Hoelscher, M.-T., Scherer, D. (2015). Evaluating the effects of façade greening on human bioclimate in a complex urban environment. *Advances in Meteorology*, 2015, Article e747259. <https://doi.org/10.1155/2015/747259>



- Jänicke, B., Milošević, D., & Manavvi, S. (2021). Review of user-friendly models to improve the urban micro-climate. *Atmosphere*, 12(10), Article e1291. <https://doi.org/10.3390/atmos12101291>
- Keyes, N., McLaren, C., Phan, N., & Vazques, D. (2022). *Milwaukee urban development: Assessing climate vulnerability through the InVEST model on urban cooling in Milwaukee using NASA Earth observations*. National Aeronautics and Space Administration. <https://ntrs.nasa.gov/api/citations/20220018647/downloads/20220018647.pdf>
- Kjellstrom, T., Holmer, I., & Lemke, B. (2009). Workplace heat stress, health and productivity – An increasing challenge for low and middle-income countries during climate change. *Global Health Action*, 2(1), Article e2047. <https://doi.org/10.3402/gha.v2i0.2047>
- Lake Simcoe Region Conservation Authority [LSRCA]. (2022). *Lake Simcoe watershed land cover update: 2018*. <https://lsrca.on.ca/wp-content/uploads/2023/07/Lake-Simcoe-Watershed-Land-Cover-Update-2018.pdf>
- Lake Simcoe Region Conservation Authority [LSRCA]. (2020). *Climate change adaptation strategy for the Lake Simcoe Region Conservation Authority*. <https://lsrca.on.ca/wp-content/uploads/2023/10/Climate-Change-Adaptation-Strategy-opt.pdf>
- Lake Simcoe Region Conservation Authority [LSRCA]. (2016). *Upper York Region urban forest study: Technical report*.
- Leahy, I. (2017, January 12). Why we no longer recommend a 40 percent urban tree canopy goal. *American Forests*. <https://www.americanforests.org/article/why-we-no-longer-recommend-a-40-percent-urban-tree-canopy-goal/>
- Li, Y., Schubert, S., Kropp, J. P., & Rybski, D. (2020a). On the influence of density and morphology on the urban heat island intensity. *Nature Communications*, 11, Article e2647. <https://doi.org/10.1038/s41467-020-16461-9>
- Li, Z., Wang, S., & Li, J. (2020b). Spatial variations and long-term trends of potential evaporation in Canada. *Scientific Reports*, 10, Article e22089. <https://doi.org/10.1038/s41598-020-78994-9>
- Lin, J., Kroll, C. N., Nowak, D. J., & Greenfield, E. J. (2019). A review of urban forest modeling: Implications for management and future research. *Urban Forestry & Urban Greening*, 43, Article e126366. <https://doi.org/10.1016/j.ufug.2019.126366>
- Lindberg, F., Holmer, B., & Thorsson, S. (2008). SOLWEIG 1.0 – Modelling spatial variations of 3D radiant fluxes and mean radiant temperature in complex urban settings. *International Journal of Biometeorology*, 52, 697-713. <https://doi.org/10.1007/s00484-008-0162-7>



- Logan, T. M., Zaitchik, B., Guikema, S., & Nisbet, A. (2020). Night and day: The influence and relative importance of urban characteristics on remotely sensed land surface temperature. *Remote Sensing of Environment*, 247, Article e111861. <https://doi.org/10.1016/j.rse.2020.111861>
- Loughner, C. P., Allen, D. J., Zhang, D.-L., Pickering, K. E., Dickerson, R. R., & Landry, L. (2012). Roles of urban tree canopy and buildings in urban heat island effects: Parameterization and preliminary results. *Journal of Applied Meteorology and Climatology*, 51(10), 1775-1793. <https://doi.org/10.1175/JAMC-D-11-0228.1>
- Mahony, C. R., Wang, T., Hamann, A., & Cannon, A. J. (2022). A CMIP6 ensemble for downscaled monthly climate normal over North America. *International Journal of Climatology*, 42(11), 5871-5891. <https://doi.org/10.1002/joc.7566>
- Martins, R., Feliciano, M., Brianezi, D., & Gonçalves, A. (2023). Analysis of the influence of Nature-Based Solutions (NBS) on air quality in industrial areas – Case study in Bragança (Portugal). *ES3 Web of Conferences*, 436, Article e10011. <https://doi.org/10.1051/e3sconf/202343610011>
- Matzarakis, A., Fröhlich, D., Gangwisch, M., Ketterer, C., & Peer, A. (2015). Developments and applications of thermal indices in urban structures by RayMan and SkyHelios model. *Proceedings of the 9th International Conference on Urban Climate*, 23. http://www.meteo.fr/icuc9/LongAbstracts/bph1-2-2941295_a.pdf
- Matzarakis, A., Rutz, F., & Mayer, H. (2010). Modelling radiation fluxes in simple and complex environments: Basics of the RayMan model. *International Journal of Biometeorology*, 54, 131-139. <https://doi.org/10.1007/s00484-009-0261-0>
- Metro Vancouver. (2024, March). *2020 regional tree canopy cover and impervious surface*. <https://metrovancover.org/services/regional-planning/Documents/regional-tree-canopy-cover-impervious-surface-2020.pdf>
- Moore, G. M. (2016). The economic value of trees in the urban forest as climate changes. *Acta Horticulturae*, 1108, 1-12. <https://doi.org/10.17660/ActaHortic.2016.1108.1>
- Mutani, G., & Beltramino, S. (2022). Geospatial assessment and modeling of outdoor thermal comfort at urban scale. *International Journal of Heat and Technology*, 40(4), 871-878. <https://doi.org/10.18280/ijht.400402>
- National Weather Service. (n.d.). *Wet bulb global temperature: How and when to use it*. National Oceanic and Atmospheric Administration. <https://www.weather.gov/news/211009-WBGT>
- Natural Capital Project. (n.d.). *Urban cooling*. http://releases.naturalcapitalproject.org/invest-userguide/latest/en/urban_cooling_model.html



- Natural Resources Canada. (2019). *Table 3.3a – Energy intensity per heated area (excluding garage) by region* [Data table].
<https://oee.nrcan.gc.ca/corporate/statistics/neud/dpa/showTable.cfm?type=SH§or=aaa&juris=ca&year=2019&rn=11&page=1>
- NOAA National Centers for Environmental Information. (2024, January 17). 2023 was the warmest year in the modern temperature record. *Climate.gov*.
<https://www.climate.gov/news-features/featured-images/2023-was-warmest-year-modern-temperature-record>
- Nyelele, C., Kroll, C. N., & Nowak, D. J. (2019). Present and future ecosystem services of trees in the Bronx, NY. *Urban Forestry & Urban Greening*, 42, 10-20.
<https://doi.org/10.1016/j.ufug.2019.04.018>
- Pace, R., Chiochini, F., Sarti, M., Endreny, T. A., Calfapietra, C., & Ciolfi, M. (2023). Integrating Copernicus land cover data into the i-Tree Cool Air model to evaluate and map urban heat mitigation by tree cover. *European Journal of Remote Sensing*, 56(1), Article e2125833. <https://doi.org/10.1080/22797254.2022.2125833>
- Pan, S., Tian, H., Dangal, S. R. S., Yang, Q., Yang, J., Lu, C., Tao, B., Ren, W., & Ouyang, Z. (2014). Responses of global terrestrial evapotranspiration to climate change and increasing atmospheric CO₂ in the 21st century. *Earth's Future*, 3(1), 15-35.
<https://doi.org/10.1002/2014EF000263>
- Peng, J., Liu, Q., Xu, Z., Lyu, D., Du, Y., Qiao, R., & Wu, J. (2020). How to effectively mitigate the urban heat island effect? A perspective of waterbody patch size threshold. *Landscape and Urban Planning*, 202, Article e103873.
<https://doi.org/10.1016/j.landurbplan.2020.103873>
- Peng, S., Piao, S., Ciais, P., Friedlingstein, P., Ottle, C., Bréon, F.-M., Nan, H., Zhou, L., & Myneni, R. B. (2011). Surface urban heat island across 419 global big cities. *Environmental Science & Technology*, 46(2), 696-703. <https://doi.org/10.1021/es2030438>
- Phelan, P. E., Kaloush, K., Miner, M., Golden, J., Phelan, B., Silva, H., III, & Taylor, R. A. (2015). Urban heat island: Mechanisms, implications, and possible remedies. *Annual Review of Environment and Resources*, 40, 285-307. <https://doi.org/10.1146/annurev-environ-102014-021155>
- Prairie Climate Centre. (n.d.). *Tropical nights*. Climate Atlas of Canada.
https://climateatlas.ca/map/canada/tropicalnights_2060_85#
- Ronchi, S., Salata, S., & Arcidiacono, A. (2020). Which urban design parameters provide climate-proof cities? An application of the Urban Cooling InVEST model in the city of Milan comparing historical planning morphologies. *Sustainable Cities and Society*, 63, Article e102459. <https://doi.org/10.1016/j.scs.2020.102459>



- Rosenfeld, A. H., Akbari, H., Room, J. J., & Pomerantz, M. (1998). Cool communities: Strategies for heat island mitigation and smog reduction. *Energy and Buildings*, 28(1), 51-62.
[https://doi.org/10.1016/S0378-7788\(97\)00063-7](https://doi.org/10.1016/S0378-7788(97)00063-7)
- Santamouris, M., Cartalis, C., Synnefa, A., & Kolokotsa, D. (2015). On the impact of urban heat island and global warming on the power demand and electricity consumption of buildings—A review. *Energy and Buildings*, 98, 119-124.
<https://doi.org/10.1016/j.enbuild.2014.09.052>
- Schwalm, C. R., Glendon, S., & Duffy, P. B. (2020). RCP8.5 tracks cumulative CO₂ emissions. *Proceedings of the National Academy of Sciences*, 117(33), 19656-19657.
<https://doi.org/10.1073/pnas.2007117117>
- Schwarz, N., Schlink, U., Franck, U., & Großmann, K. (2012). Relationship of land surface and air temperatures and its implications for quantifying urban heat island indicators—An application for the city of Leipzig (Germany). *Ecological Indicators*, 18, 693-704.
<https://doi.org/10.1016/j.ecolind.2012.01.001>
- Seltenrich, N. (2023). No reprieve: Extreme heat at night contributes to heat wave mortality. *Environmental Health Perspectives*, 131(7), Article e074003.
<https://doi.org/10.1289/EHP13206>
- Semenzato, P., & Bortolini, L. (2023). Urban heat island mitigation and urban green spaces: Testing a model in the city of Padova (Italy). *Land*, 12(2), 476.
<https://doi.org/10.3390/land12020476>
- Shu, C., Gaur, A., Lacasse, M., & Wang, L. (2022). Interaction between the urban heat island effect and the occurrence of heatwaves: Comparison of days with and without heatwaves. In Wang, L. L., Ge, H., Zhai, Z. J., Qi, D., Ouf, M., Sun, C., & Wang, D. (Eds.), *Proceedings of the 5th International Conference on Building Energy and Environment* (pp. 3019-3028). Springer. https://doi.org/10.1007/978-981-19-9822-5_322
- Sinha, P., Coville, R. C., Hirabayashi, S., Lim, B., Endreny, T. A., & Nowak, D. J. (2022). Variation in estimates of heat-related mortality reduction due to tree cover in U.S. cities. *Journal of Environmental Management*, 301, Article e113751.
<https://doi.org/10.1016/j.jenvman.2021.113751>
- Sinha, P., Coville, R. C., Hirabayashi, S., Lim, B., Endreny, T. A., & Nowak, D. J. (2021). Modeling lives saved from extreme heat by urban tree cover. *Ecological Modelling*, 449, Article e109553. <https://doi.org/10.1016/j.ecolmodel.2021.109553>
- Skelhorn, C., Lindley, S., & Levermore, G. (2014). The impact of vegetation types on air and surface temperatures in a temperate city: A fine scale assessment in Manchester, UK. *Landscape and Urban Planning*, 121, 129-140.
<https://doi.org/10.1016/j.landurbplan.2013.09.012>



- Statistics Canada. (2022). *Canada's fastest growing and decreasing municipalities from 2016 to 2021* (No. 98-200-X). <https://www12.statcan.gc.ca/census-recensement/2021/as-sa/98-200-x/2021001/98-200-x2021001-eng.cfm>
- Statistics Canada. (2019). *Table 1 Profile of energy use by commercial and institutional buildings, all provinces, 2019* [Data table]. <https://www150.statcan.gc.ca/n1/daily-quotidien/220805/t001c-eng.htm>
- Stewart, I. D., & Oke, T. R. (2012). Local climate zones for urban temperature studies. *Bulletin of the American Meteorological Society*, 93(12), 1879-1900. <https://doi.org/10.1175/BAMS-D-11-00019.1>
- Stone, B., Jr, Vargo, J., Liu, P., Habeeb, D., DeLucia, A., Trail, M., Hu, Y., & Russell, A. (2014). Avoided heat-related mortality through climate adaptation strategies in three US cities. *PLOS One*, 9(6), Article e100852. <https://doi.org/10.1371/journal.pone.0100852>
- Tam, B., Bonsal, B., Zhang, X., Zhang, Q., & Rong, R. (2023). Assessing potential evapotranspiration methods in future drought projections across Canada. *Atmosphere-Ocean*, 62(3), 193-205. <https://doi.org/10.1080/07055900.2023.2288632>
- Timmins, T., & Sawka, M. (2022). *2021 York Region canopy cover assessment technical report*. Toronto and Region Conservation Authority.
- Town of East Gwillimbury. (2022, February 9). *East Gwillimbury tops Canada's growing municipalities list* [Press release]. <https://www.eastgwillimbury.ca/en/news/east-gwillimbury-tops-canada-s-growing-municipalities-list.aspx>
- Town of East Gwillimbury. (n.d.). *About East Gwillimbury*. <https://www.eastgwillimbury.ca/en/living-in-eg/about-east-gwillimbury.aspx?mid=80069>
- Turner, M. G., & Gardner, R. H. (2015). *Landscape ecology in theory and practice* (2nd ed.). Springer New York. <https://doi.org/10.1007/978-1-4939-2794-4>
- United Nations Department of Economic and Social Affairs [UN DESA]. (2018). *World urbanization prospects: The 2018 revision*. United Nations. <https://population.un.org/wup/Publications/Files/WUP2018-Report.pdf>
- Vurro, G., & Carlucci, S. (2024). Contrasting the features and functionalities of urban microclimate simulation tools. *Energy and Buildings*, 311, Article e114042. <https://doi.org/10.1016/j.enbuild.2024.114042>
- Wang, C., Ren, Z., Chang, X., Wang, G., Hong, X., Dong, Y., Guo, Y., Zhang, P., Ma, Z., & Wang, W. (2023). Understanding the cooling capacity and its potential drivers in urban forests at



- the single tree and cluster scales. *Sustainable Cities and Society*, 93, Article e104531. <https://doi.org/10.1016/j.scs.2023.104531>
- Wang, C., Wang, Z.-H., & Yang, J. (2018). Cooling effect of urban trees on the built environment of contiguous United States. *Earth's Future*, 6, 1066-1081. <https://doi.org/10.1029/2018EF000891>
- Wang, T., Hamann, A., Spittlehouse, D., & Carroll, C. (2016a). Locally downscaled and spatially customizable climate data for historical and future periods for North America. *PLoS ONE*, 11(6), Article e0156720. <https://doi.org/10.1371/journal.pone.0156720>
- Wang, Y., Berardi, U., Akbari, H. (2016b). Comparing the effects of urban heat island mitigation strategies for Toronto, Canada. *Energy and Buildings*, 114, 2-19. <https://doi.org/10.1016/j.enbuild.2015.06.046>
- Warren, F. J. (2004). *Climate change impacts and adaptation: A Canadian perspective*. Natural Resources Canada. <https://atrium.lib.uoguelph.ca/server/api/core/bitstreams/108f4aef-e91c-4999-a68e-7cebef9611ab/content>
- Wong, N. H., Tan, C. L., Kolokotsa, D. D., & Takebayashi, H. (2021). Greenery as a mitigation and adaptation strategy to urban heat. *Nature Reviews Earth & Environment*, 2, 166-181. <https://doi.org/10.1038/s43017-020-00129-5>
- Yadav, N., Rajendra, K., Awasthi, A., Singh, C., & Bhushan, B. (2023). Systematic exploration of heat wave impact on mortality and urban heat island: A review from 2000 to 2022. *Urban Climate*, 51, Article e101622. <https://doi.org/10.1016/j.uclim.2023.101622>
- Yang, Q., Huang, X., Tong, X., Xiao, C., Yang, J., Liu, Y., & Cao, Y. (2022). Global assessment of urban trees' cooling efficiency based on satellite observations. *Environmental Research Letters*, 17(3), Article e034029. <https://doi.org/10.1088/1748-9326/ac4c1c>
- Yang, Y., Endreny, T. A., & Nowak, D. J. (2013). A physically based analytical spatial air temperature and humidity model. *Journal of Geophysical Research: Atmospheres*, 118(18), 10449-10463. <https://doi.org/10.1002/jgrd.50803>
- Yenneti, K., Ding, L., Prasad, D., Ulpiani, G., Paolini, R., Haddad, S., & Santamouris, M. (2020). Urban overheating and cooling potential in Australia: An evidence-based review. *Climate*, 8(11), 126. <https://doi.org/10.3390/cli8110126>
- Zawadzka, J. E., Harris, J. A., & Corstanje, R. (2021). Assessment of heat mitigation capacity of urban greenspaces with the use of InVEST urban cooling model, verified with day-time land surface temperature data. *Landscape and Urban Planning*, 214, Article e104163. <https://doi.org/10.1016/j.landurbplan.2021.104163>



- Zhang, B., Xie, G., Gao, J., & Yang, Y. (2014). The cooling effect of urban green spaces as a contribution to energy-saving and emission-reduction: A case study in Beijing, China. *Building and Environment*, 76, 37-43. <https://doi.org/10.1016/j.buildenv.2014.03.003>
- Zhao, Q., Wentz, E. A., & Murray, A. T. (2017). Tree shade coverage optimization in an urban residential environment. *Building and Environment*, 115, 269-280. <https://doi.org/10.1016/j.buildenv.2017.01.036>
- Zhou, W., Cao, F., & Wang, G. (2019). Effects of spatial pattern of forest vegetation on urban cooling in a compact megacity. *Forests*, 10(3), 282. <https://doi.org/10.3390/f10030282>
- Ziter, C. D., Pederson, E. J., Kucharik, C. J., & Turner, M. G. (2019). Scale-dependent interactions between tree canopy cover and impervious surfaces reduce daytime urban heat during summer. *Proceedings of the National Academy of Sciences*, 116(15), 7575-7580. <https://doi.org/10.1073/pnas.1817561116>